Manuscript prepared for Atmos. Chem. Phys.
with version 5.0 of the LaTeX class copernicus.cls.
Date: 27 January 2016

Towards a regional-ocean model for the behaviour of Mediterranean Outflow Water

R.C. Warmer (3379809)

Utrecht University, Faculty of Geosciences, The Netherlands

r.c.warmer@students.uu.nl

Abstract.

To improve our physics-based understanding of the Mediterranean Outflow Water (MOW) a general ocean model has been built in the Princeton Ocean Model (POM) framework. The model has been tested and compared to observations and appears to function correctly. Several of the parameters (bathymetry smoothing, sill depth, Mediterranean source water, and Atlantic water) that control the development of the MOW have been tested for their sensitivity. The results are in agreement with the general consensus that there is a clear link between the MOW and global ocean circulation. And show that there is a strong relationship between MOW development, local bathymetry and the (turbulent) mixing between the MOW and the surrounding waters.

1 Introduction

The Mediterranean Outflow Water (MOW) is the body of water that enters the Atlantic Ocean from the Mediterranean Sea through the Strait of Gibraltar. Presently the Strait of Gibraltar is defined by a two-way flow with a horizontal interface (Baringer and Price, 1999). The upper flow consists of turbulent, cool and eastward flowing Atlantic water, known as the Atlantic Inflow. The bottom flow is the body of water known as the Mediterranean Outflow Water and is the main focus of this study. The MOW consists of warm and saline water from the Mediterranean Sea flowing westwards into the Atlantic Ocean at the Gulf of Cádiz (Hernández-Molina et al., 2006, 2013).

Apart from the MOW there are four other regional water masses identified in the Gulf of Cádiz: Surface Atlantic Water (SAW), Eastern North Atlantic Central Water (ENACW), modified Antarctic Intermediate Water (AAIW) and the North Atlantic Deep Water (NADW) as seen in figure 1 (Hernández-Molina et al., 2013). The Atlantic Inflow is included in the Surface Atlantic Water. Except for the MOW all the water masses have well defined boundaries regarding temperature, salinity and depth. The MOW begins at a depth of 40m in the Eastern Strait of Gibraltar with a high salinity of >38.5 psu and a relative high temperature of 13.5 °C. As the water flows westwards it mixes with the various other water masses until it reaches a depth of 1400m, a salinity of 36.4 psu and a temperature of 13 °C (Table1).

Table 1. Values of the different water masses in the Gulf of Cádiz. Based on Gascard and Richez (1985), Pérez et al. (1995), Macias et al. (2006) and Alves et al. (2011).

	MOW	**SAW**	**NACW**	**AAIW**	**NADW**
Tmax (°C)	13.5	20	16	7	4
Tmin (°C)	13	19	12.5	3	2.5
Smax (psu)	38.5	36.4	36.25	34.5	35.0
Smin (psu)	36.4	36.2	35.5	33.8	34.8
Min depth (m)	40	0	100	500	1500
Max depth (m)	1400	100	600	1500	bottom

The MOW thus starts at a depth below 40m in the Eastern part of the Strait of Gibraltar. The consensus is that the MOW obtains its water from two Mediterranean water masses: the Levantine Intermediate Water (LIW) and the Western Mediterranean Deep Water (WMDW) (Borenäs et al., 2002; Hernández-Molina et al., 2012; Rogerson et al., 2012). Both form in winter as favourable winds and colder temperatures increase overturning in the Mediterranean Sea (Voelker et al., 2006). Two other water masses may also contribute periodically to the MOW: Winter Intermediate Water (WIW) and Tyrrhenian Dense Water (TDW). Above the MOW the Atlantic Inflow is also present as it flows in the opposite direction. The depth of the interface between the two flows increases to 500m as the MOW enters the Gulf of Cádiz. Inside the Strait of Gibraltar limited mixing with the Atlantic Inflow has already occurred (Gascard and Richez, 1985) (Baringer and Price, 1997). The total flux of the MOW as it enters the Gulf of Cádiz is 1.78 Sv with a velocity of 1.4 m s^{-1}. It

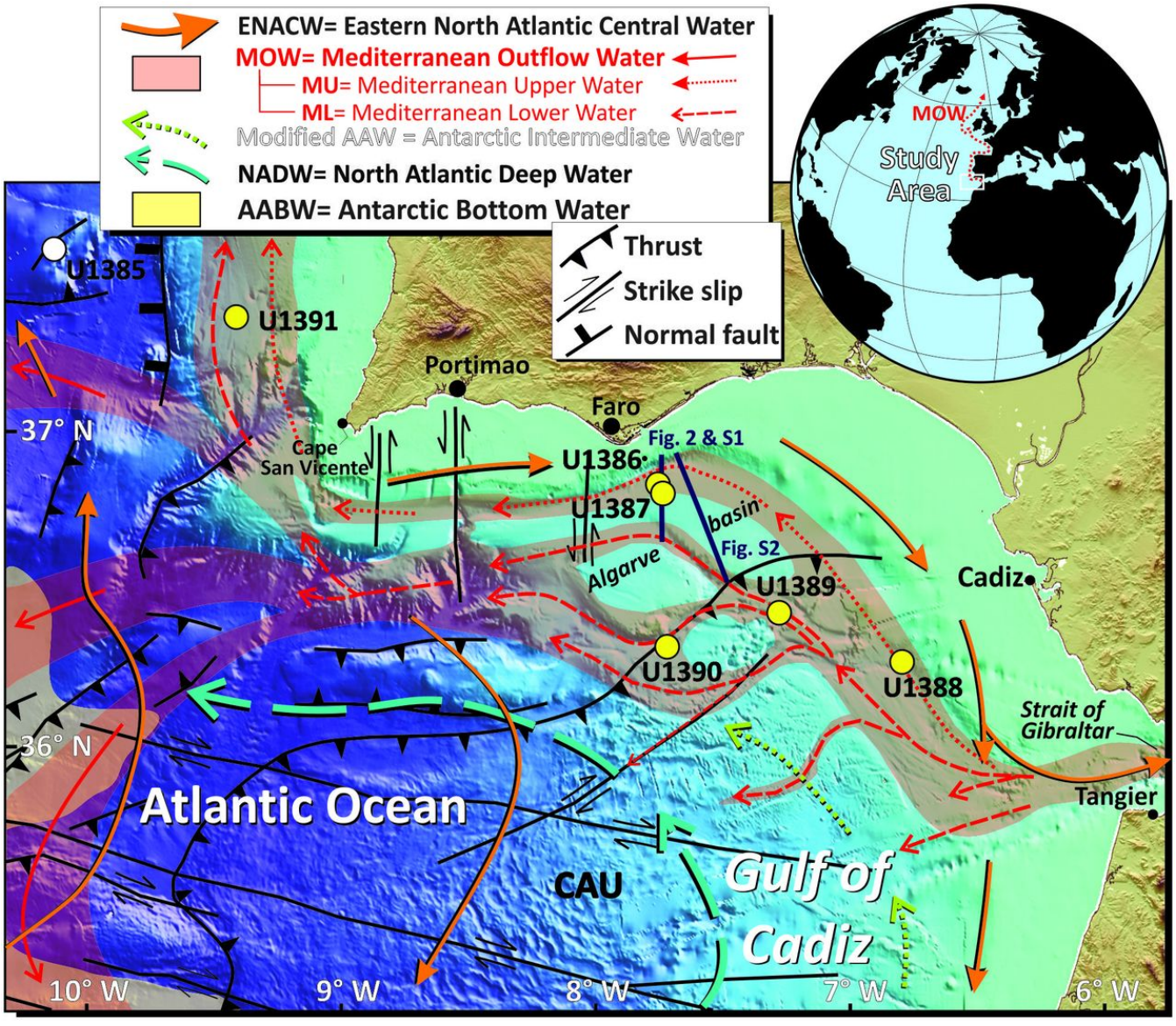

Fig. 1. Regional water masses, major tectonic features, and Gulf of Cádiz CDS site locations sampled during IODP Expedition 339. Taken from Hernández-Molina et al. (2014).

also starts mixing turbulently with the surrounding water due to the large differences in salinity and temperature (Baringer and Price, 1999; Hernández-Molina et al., 2013).

The mixing continues as the MOW moves through the Gulf of Cádiz. Initially the MOW is forced northwards along the Spanish coast by the Coriolis force. It quickly settles as a geostrophic flow that follows the local bathymetry and moves parallel to the coast. The MOW is also forced downwards as it has a higher density than the surrounding water masses because of its high salinity and temperature. As the MOW moves towards the Portuguese coast it is split in two separate cores by the bathymetry. The most northern core flows over the ocean floor at a depth of 500m to 800m below sealevel and is known as the Mediterranean Upper Water (MU). The southern core is known as the Mediterranean Lower Water (ML) and flows over the ocean floor at a depth of 800m to 1400m below sealevel 1. Still split, the MOW reaches Cape St. Vincent with a reduced velocity of 80 cm s^{-1}. Here the MOW flows into the Atlantic Ocean as it becomes neutrally buoyant at a depth between 800m and 1300m (Ambar and Howe, 1979; Baringer and Price, 1997; Hernández-Molina et al., 2006, 2012, 2013, 2014).

After leaving the Gulf of Cádiz the MOW splits into three branches spreading over the Atlantic Ocean (figure 2). The main branch flows northwards at a depth of 500m to 1500m along the European Shelf and reaches as far as the Norwegian

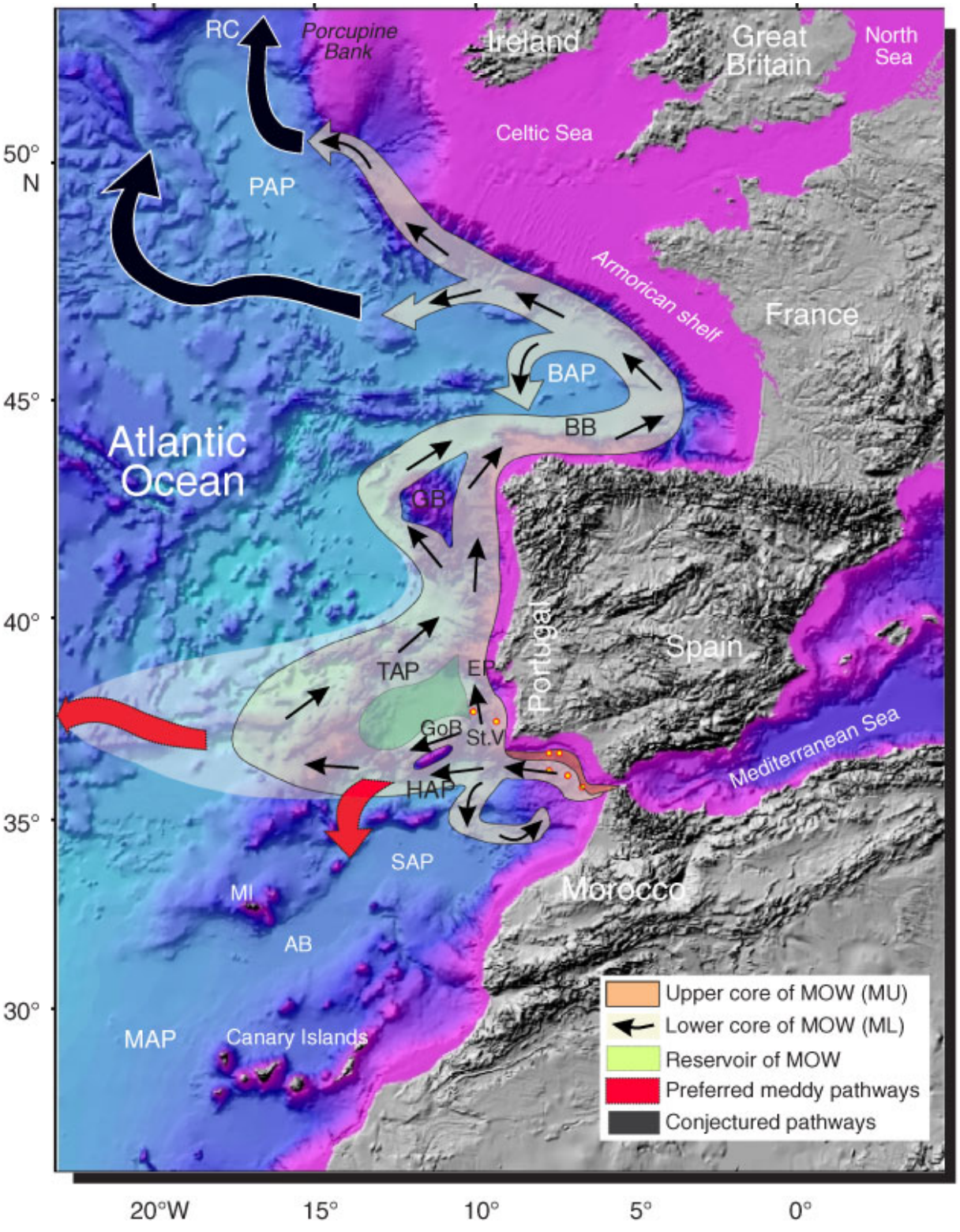

Fig. 2. General circulation pattern of the Mediterranean Outflow Water (MOW) pathway in the North Atlantic (modified from Iorga and Lozier, 1999). AB = Agadir Basin, BAP = Biscay Abyssal Plain, BB = Bay of Biscay, EP = Extremadura Promontory, GaB = Galicia Bank, GoB = Gorringe Bank, HAP = Horseshoe Abyssal Plain, MAP = Madeira Abyssal Plain, MI = Madeira Island, PAP = Porcupine Abyssal Plain, RC = Rockall Channel, SAP = Seine Abyssal Plain, St.V = Cape São Vicente, TAP = Tagus Abyssal Plain. Figure taken from Hernández-Molina et al. (2012), who modified it from (Iorga and Lozier, 1999b).

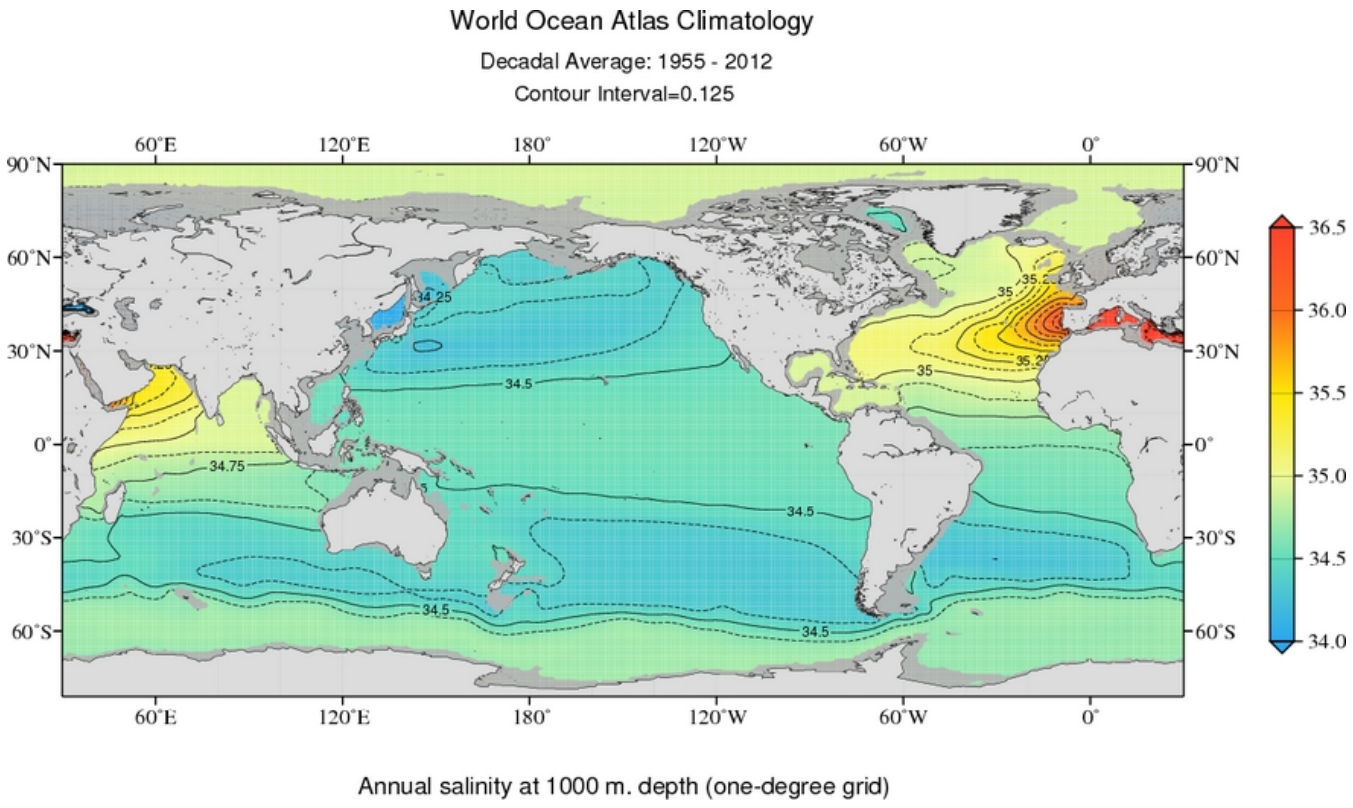

Fig. 3. Map of salinity values at 1000m depth showing the influence of the MOW on the salinity values in the North Atlantic. Based on World Ocean Atlas 2013 data.

and Greenland Seas (Reid, 1979; Iorga and Lozier, 1999b). The other branches flow westwards and southwards. The westward branch slowly descends into the Atlantic Ocean while the southern branch partly flows back towards the Strait of Gibraltar in an anti-clockwise manner (Ambar and Howe, 1979; Hernández-Molina et al., 2012).

1.1 MOW and global climate

The exact influence of the MOW on the North Atlantic, the global ocean circulation and climate is not yet well understood. But it is generally accepted that the MOW affects overturning in the North Atlantic (Bartoli et al., 2005; Rogerson et al., 2012; Hernández-Molina et al., 2014). A model study by Price and Yang (1998) suggested that closure of the Strait of Gibraltar reduces the current rate of overturning by 15%. Measurements from the World Ocean Database 2013 as well, indicate that relatively high salinity and temperature water originating from the Mediterranean is spread over the whole North Atlantic Ocean 3 4.

There is mounting evidence that the composition and strength of the MOW can be directly linked to stadials and interstadials in the past. It is commonly accepted that the strength of the MOW increases during cold periods. Multiple proxies for both the hydrographic conditions of the water column and the strength of the MOW show a clear correlation with each other (Rahmstorf, 1998; Hernández-Molina et al., 2006; Voelker et al., 2006; Rogerson et al., 2006, 2010).

A colder northern hemisphere climate would simultaneously reduce evaporation (reducing MOW density), increase temperature loss of Mediterranean Water (Increasing MOW density), and increase deep water formation in the Mediterranean (Increasing MOW density) (Rahmstorf, 1998; Cacho et al., 2000; Voelker et al., 2006). However the exact consequences are ambiguous and they do not appear to strongly affect MOW properties (Rogerson et al., 2010).

The expression of the stadial Heinrich events (Heinrich, 1988) shows a very strong stratification in both the Atlantic Ocean and the Strait of GibraltarVoelker et al. (2006); Rogerson et al. (2010), which is thought to be the result of a stop in North Atlantic overturning because of iceberg release (Hemming, 2004; Rogerson et al., 2010). The lack of mixing means that that the MOW will retain its initial Mediterranean properties and not affect the inflow of Atlantic water. Rogerson et al. (2010) showed that this will strongly increase transport through the Strait of Gibraltar. Thus an alternative spot of deep water formation is found in the Mediterranean at times of reduced overturning in the North Atlantic. This provides a negative feedback to the reduction of Atlantic overturning that is potentially critical to the reactivation of

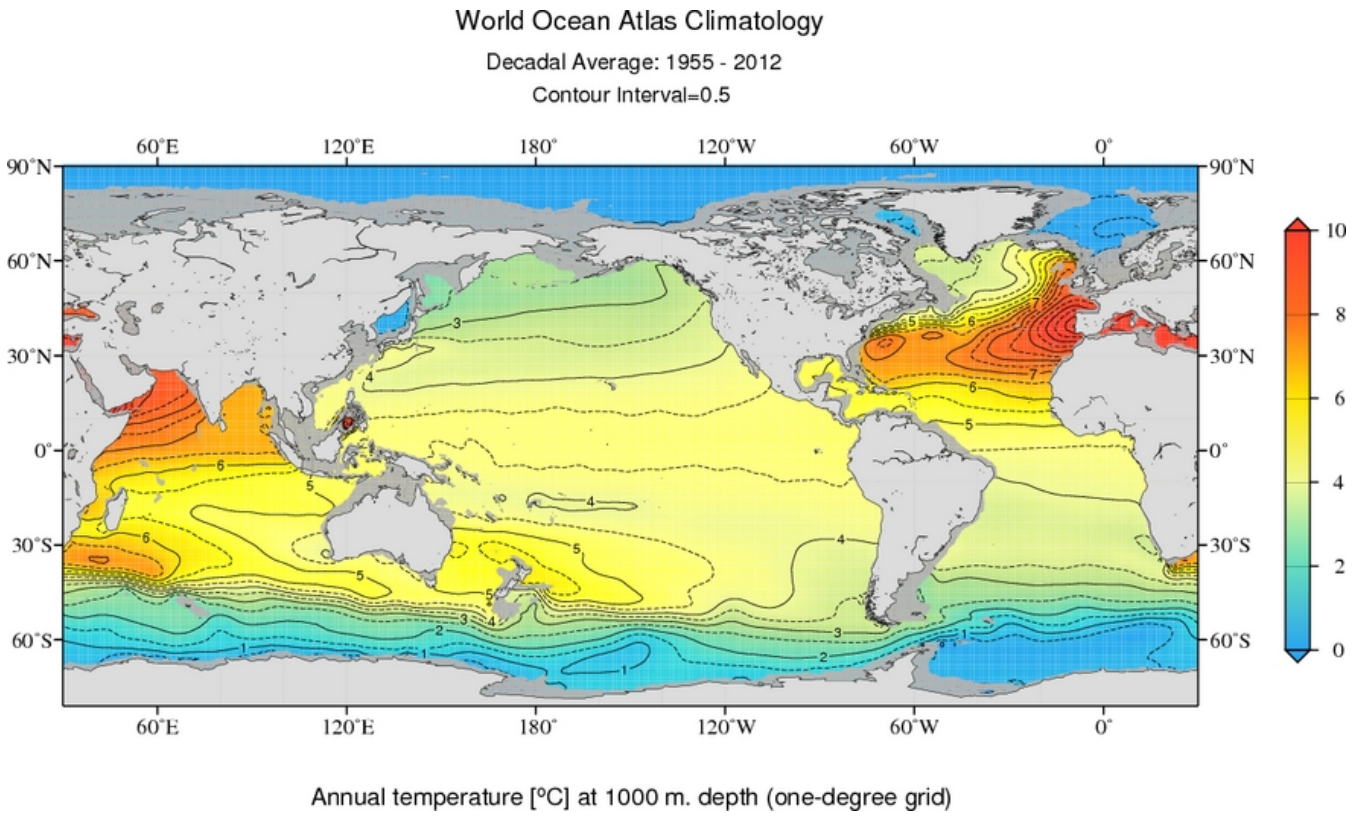

Fig. 4. Map of temperature values at 1000m depth showing the influence of the MOW on the salinity values in the North Atlantic. Based on World Ocean Atlas 2013 data.

Atlantic overturning (Rahmstorf, 1998; Bigg and Wadley, 2001; Rogerson et al., 2010, 2012).

Strengthening of the MOW during stadials through processes on the Mediterranean side was suggested by Rahmstorf (1998); Cacho et al. (2000); Voelker et al. (2006). An increase in wind speeds and colder winter temperatures would increase overturning in the Northern Mediterranean. More high salinity water is thus brought to the LIW and the WMDW. Similar to the input of freshwater in the Atlantic this increases the density contrast between the two sides of the Strait of Gibraltar. Both theories are not mutually exclusive but they do have the same result of bringing an early end to a stadial by providing a negative feedback to reduced overturning in the North Atlantic.

Bethoux et al. (1999) suggested that the MOW does not only influences stadials and interstadials, it also influences the occurrence of sapropels in the Mediterranean Sea. A decrease in MOW strength lowers the need for vertical movement inside the Mediterranean basin. Since the vital component for sapropel formation is stratification, this means that sapropels would form more readily at times of decreased MOW strength.

1.2 Aim

In this study an outline of a new model of the MOW is presented. The aim is to explore the possibilities of a model to analyse the connection between the Mediterranean, the MOW and the Atlantic Ocean. The model is built in the framework of the Princeton Ocean Model (POM) (Mellor, 1998). The new model should be more flexible than the model by Jungclaus and Mellor (2000) in order to simulate the different climatic and tectonic conditions of the past(Rogerson et al., 2006; Hernández-Molina et al., 2014). With the Integrated Ocean Drilling Program (IODP) Expedition 339 (Hernández-Molina et al., 2012) the available data on the MOW and its evolution has significantly increased (see section 2 below). However the theoretical knowledge of the large scale processes involving the MOW is lagging behind. Only several papers by Rogerson et al. (2004, 2005, 2006, 2010, 2012) deal with the theoretical constrains of the MOW. In section 5 several experiments have been done to test the sensitivity of the parameters controlling the development of the MOW. The hope is that the model presented here can contribute to the understanding of the climatic and tectonic conditions necessary to produce the changes the recorded outflow changes as well as the processes that involve the MOW.

2 Geological Setting/MOW evolution

As with any other margin the evolution of the Iberian margin is mainly the result of the interaction of several variables; e.g. sea level changes and climate, sediment supply and local tectonic activities (Hernández-Molina et al., 2014). The consensus is that one of the main factors in MOW evolution is neotectonic activity affecting the local bathymetry (Borenäs et al., 2002; Hernández-Molina et al., 2012, 2013; Brackenridge et al., 2013; Filippelli, 2014).

The objective of IODP Expedition 339 was to study the Contourite Depositional System (CDS in the Gulf of Cádiz to reconstruct a high resolution record of MOW evolution in accordance with the theories described in Hernández-Molina et al. (2006). The Gulf of Cádiz CDS is located along the whole Iberian coastline. Here the contourites are formed by bottom currents induced by the density gradients resulting from the high salinity of the MOW. The composition, shape and location of the CDS are all proxies of MOW properties (Faugèers et al., 1984; Nelson et al., 1993; Llave et al., 2006; Hernández-Molina et al., 2006; Toucanne et al., 2007). This means that a general history of the MOW can be obtained from the CDS (Llave et al., 2006; Toucanne et al., 2007; Hernández-Molina et al., 2012, 2014). Preliminary results from the expedition suggest that the history of the MOW can be divided in to six phases (Hernández-Molina et al., 2012, 2014; Filippelli, 2014):

5.33 to 4.2 Ma: The first phase starts at the opening of the Strait of Gibraltar after the Messinian Salinity Crisis (Roveri et al., 2014). In this phase only limited deposition of contourites occurred while the MOW was still limited in strength.

4.5 to 3.2 Ma: At the start of the second phase the presence of contourites has become a permanent feature in the Gulf of Cádiz (Hernández-Molina et al., 2014). Though Rogerson et al. (2012) suggested that the interaction of the MOW with Atlantic water was still very limited in the early stages of MOW evolution.

3.2 to 3.0 Ma: The third phase coincides with the mid-Pliocene warm period and the closure of the Central American Seaway (Bartoli et al., 2005). It consists of a major hiatus in contourite deposition (Brackenridge et al., 2013). The contourites have mainly been replaced by dolostones(Hernández-Molina et al., 2014). Filippelli (2014) suggested that the enhanced production of warm and salty MOW initiated the general North Atlantic circulation pattern as seen today.

3.0 to 2.4 Ma: The fourth phase consists of enhanced MOW strength (relative to present day) with stable contourite deposition.

2.4 to 2.1 Ma: The fifth phase is another period of a major hiatus in contourite deposition with increased MOW strength Brackenridge et al. (2013); Hernández-Molina et al. (2014). Similar to the hiatus in the mid-Pliocene warm period this phase also occurs during a period of climatic upheaval. Around 2.15 Ma a major glaciation event occurs as the result of the interference of the MOW in the Atlantic Meridional Overturning Circulation (AMOC) (Filippelli, 2014).

2.1 Ma to present: The last phase is still ongoing and is defined by the establishment of present-day North Atlantic circulation and a stable MOW. The CDS are deposited continuously except for a hiatus around the mid-Pleistocene transition at 0.9 Ma (Rogerson et al., 2012). Again the hiatus is associated with an increase in MOW strength (Filippelli, 2014). The total extent of the hiatus is unclear as not all samples taken by IODP339 show an unconformity (Hernández-Molina et al., 2014).

The hiatuses are generally considered to be the result of an increase in overturning in the North Atlantic associated with a decreased pole-to-equator temperature gradient. A denser and stronger MOW would contribute to this in two ways: More and denser water would fuel the formation of deep water in the North Atlantic and at the same time increase the temperature of North Atlantic surface waters (Rogerson et al., 2012).

At the time of the hiatuses there are widespread changes in sedimentation in other margins and basins as well. The changes in MOW can thus be correlated with Atlantic or even global events (Bartoli et al., 2005; Hernández-Molina et al., 2014). It appears that the Strait of Gibraltar is one of the seaway openings that has significantly affected the circulation in the North Atlantic and as a result global climate as well (Hernández-Molina et al., 2014).

3 Previous model studies

The various processes regarding Strait Transport in Gibraltar, MOW evolution, MOW flow direction, and MOW impact (Price and Yang, 1998; Rahmstorf, 1998; Bigg and Wadley, 2001; Rogerson et al., 2012) have all been modeled before. The main reference model used is the Jungclaus and Mellor (2000) model.

Jungclaus and Mellor (2000) used the Princeton Ocean Model, the same model that is used in this study. Their aim was to simulate the entrainment and intrusion of the MOW into the Gulf of Cádiz in an already stratified ocean. They used a limited sized grid of the Gulf of Cádiz with a resolution of approximately 5km. At the eastern border inside the Strait of Gibraltar an in- and outflow was set to simulate the transport through the strait. The whole basin was filled with initial conditions for salinity and temperature.

The results of Jungclaus and Mellor (2000) were in agreement with several other studies (Price and Baringer, 1994; Rahmstorf, 1998; Rogerson et al., 2006, 2010). They all concluded that in a present-day environment the input conditions at Gibraltar do not significantly affect the properties of the MOW around Cape St. Vincent. They managed to reproduce the splitting of the two MOW cores. Their model was limited to following the initial development of MOW in a non-moving ocean for two years.

The aim of Price and Yang (1998) was to make a general assessment of the influence of marginal seas (such as the Mediterranean) on deep ocean circulation of Atlantic-sized basins. They used an Oceanic General Circulation Model (OGCM) with marginal seas in- and outflows as boundary conditions. They concluded that a Mediterranean-like marginal sea in- and outflow would enhance deep water formation with 15%.

Bigg and Wadley (2001) used a global OGCM with regionally varying resolution to incorporate the Mediterranean. In contrast to Price and Yang (1998) their results indicated that for present-day conditions the impact of the MOW on the North Atlantic and thus global climate is very limited. A simulation of a Heinrich event (Heinrich, 1988) however showed that the input of freshwater in the North Atlantic would result in a sixfold increase in MOW strength. This ultimately would lead to a reactivation of North Atlantic overturning and a return of MOW strength to present-day values.

The same results regarding to North Atlantic freshwater input were produced by Rahmstorf (1998) and Rogerson et al. (2006, 2010, 2012), reinforcing the importance of the MOW on control of the global climate. Rahmstorf (1998) used an atmosphere-ocean-sea level model a lot simpler than contemporary ocean models. Rogerson et al. (2012) also concluded that the depth of the MOW after leaving the Gulf of Cádiz is dependent on the composition of the Atlantic. Not on the composition of the Mediterranean or the MOW. A simple numerical model by Price and Baringer (1994) also showed the insensitivity of the outflow to variations in its Mediterranean source water. An increase in density of the source water would only result in more entrainment in the initial stages of the MOW and vice versa.

Thorpe and Bigg (2000) simulated the effect of anthropogenic warming on the Mediterranean. They used a Cox-Type model with a resolution of 0.25°to model the predicted increase in temperatures for 2100. The results indicated that global warming would reduce the formation of deep water in the Mediterranean. The transport through the Strait of Gibraltar would be unaffected but the MOW would get less dense and thus become shallower. It suggests that the opposite would occur with decreased temperatures, which would agree with the theory of Cacho et al. (2000); Voelker et al. (2006); Rogerson et al. (2010).

4 Model set-up

The focus of this study was to assess the viability of using POM to model the MOW. The result of this is the reference experiment. In the section below the steps and decisions made to create the reference experiment are explained ending in an comparison of the reference experiment to present-day data. The reference experiment itself is later used to test the sensitivity of the modeled MOW to its own properties.

4.1 Princeton Ocean Model

The Princeton Ocean Model (POM) by Blumberg and Mellor (1987) is in their own words "a simple-to-run yet powerful ocean modelling code". It has been used extensively to successfully model the Mediterranean Sea and the Strait of Gibraltar (Blumberg and Mellor, 1987; Zavatarelli and Mellor, 1995; Jungclaus and Mellor, 2000; Sannino et al., 2002; Ahumada and Cruzado, 2007; Topper and Meijer, 2014; de la Vara et al., 2015), with the Jungclaus and Mellor (2000) study focusing on the Gulf of Cádiz. The success of POM is the use of a primitive equation ocean model code that also incorporates a free-surface to represent the atmosphere and a sigma coordinate grid to properly represent bathymetries with large variations in depth.

POM uses the turbulence closure scheme by Mellor and Yamada (1982) to calculate the vertical mixing coefficients. And the Smagorinski horizontal diffusion formulation by Mellor and Blumberg (1985) to calculate the horizontal diffusion. To reduce errors in the diffusion calculations the Smolarkiewicz iterative upstream scheme is used. The Jungclaus and Mellor (2000) study specifically used POM to study the day by day evolution of an inflow inside the Gulf of Cádiz that originates from the Strait of Gibraltar.

4.2 Bathymetry

The depth data of all the bathymetries tested is derived from the ETOPO1 1-arc minute global relief model (Amante and Eakins, 2009). To obtain the desired resolution the ETOPO1 data was interpolated with a Gaussian scheme. After this interpolation specific values can be assigned to certain grid cells such as the grid cells inside the Strait of Gibraltar. This is done to achieve the correct depth inside the Strait of Gibraltar. An interpolation inside a narrow channel tends do decrease the maximum depth of the channel as it includes the surrounding shallower data points. Since the depth of the Strait of Gibraltar is critical to the Atlantic-Mediterranean exchange it is best to manually set it to the desired depth. In case of the reference experiment the depth is set to 300m, the present-day depth of the Strait of Gibraltar.

In order to create a model which can also accurately model the MOW under different conditions from the present a good understanding of the neotectonic changes in the bathymetry of the Gulf of Cádiz is required (Borenäs et al., 2002;

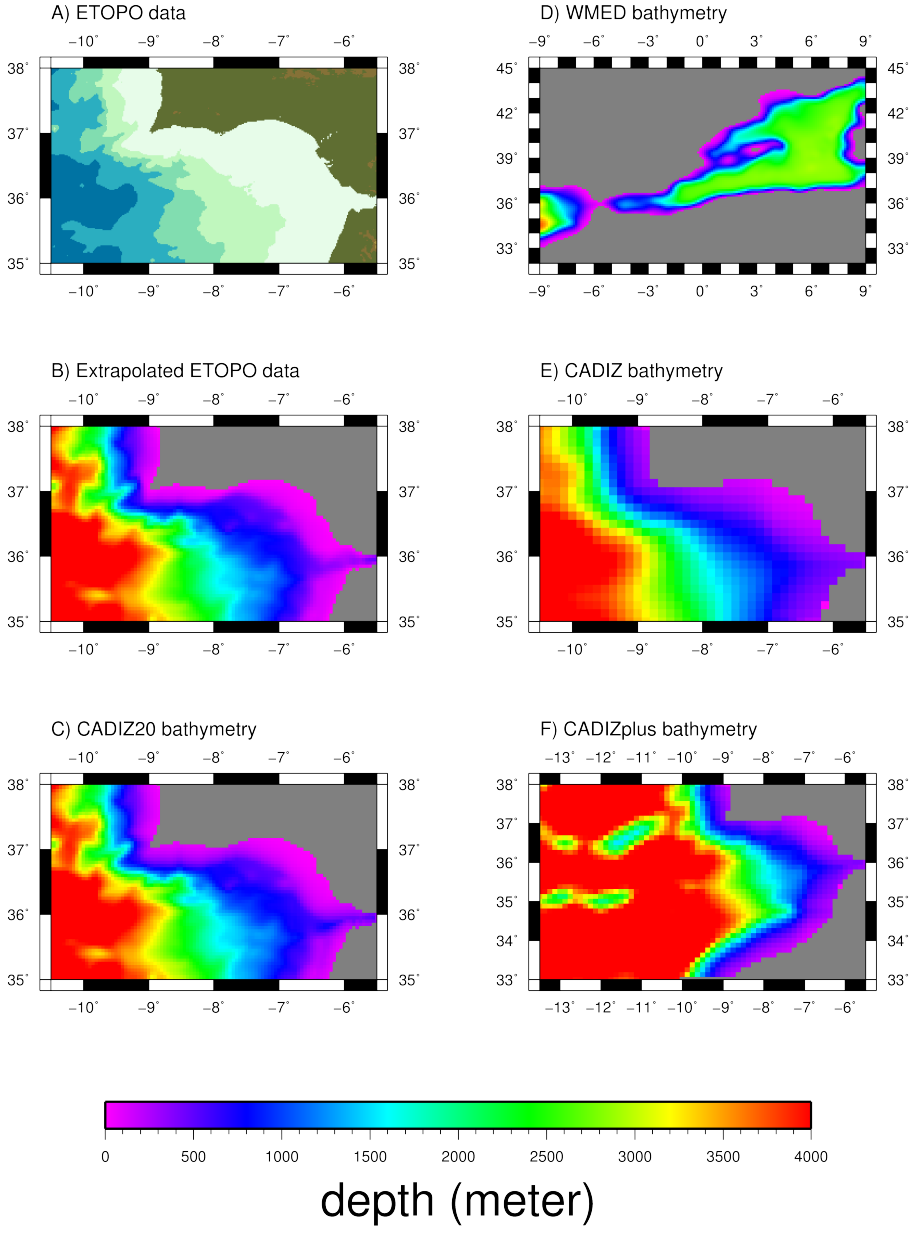

Fig. 5. The different bathymetries used and tested. A) The original ETOPO data. B) The extrapolated and smoothed ETOPO data C) The CADIZ20 bathymetry used in the reference experiment. D) The WMED bathymetry. E) The low resolution CADIZ Bathymetry. F) The expanded CADIZplus bathymetry

Hernández-Molina et al., 2012, 2013; Filippelli, 2014). Since it is expected that even small changes in the local bathymetry could potentially block and/or alter the outflow an incorrect representation of the local bathymetry could result in significant errors (Borenäs et al., 2002; Hernández-Molina et al., 2012, 2013; Brackenridge et al., 2013; Filippelli, 2014).

4.3 Model grid

The size of the MOW is relatively small. So in order to model the MOW it is necessary to have a high resolution. A high resolution however leads to an increase in computation time. In order to find the right balance between these two factors several bathymetries were tested with varying resolutions and varying model domain extents (see table 2). All of the grids tested have a rectangular size with square grid cells.

4.3.1 Horizontal grid

The WMED grid includes the Western Mediterranean Sea (figure 5b) and has a resolution of $1/8$th of a degree in the X and the Y direction, this roughly equals 12.5 square km per grid cell. In theory the most natural simulation of the outflow through the Strait of Gibraltar can be obtained by reproducing the Mediterranean circulation. In this way there is no need to introduce artificial in- and outflow boundary conditions to force the MOW. The Mediterranean side of the WMED model was roughly based on the model by Topper and Meijer (2014). In the WMED model the atmospheric conditions of evaporation, heat flow and wind were imposed. The results looked promising with a produced outflow roughly similar to the MOW. However after a couple of runs it was decided that the WMED model would not be viable for an initial attempt to constrain and test several parameters. The time needed to run the model into equilibrium approached fourteen days, making it very difficult to quickly test parameters.

An attempt was made to improve the calculation time by removing unnecessary sections of the grid with using a curvilinear grid with varying cell sizes instead of a simple rectangular grid. In this way the Mediterranean can be represented with a low resolution while the Gulf of Cádiz has a high resolution to capture the details of the MOW. However the amount of curvature needed to improve the resolution proved impossible to attain in POM.

The CADIZ grid is a small grid that extends from 35°to 38°North and 5.5°to 10.5°West (CADIZ grid, 5c). The resolution is similar to the WMED model with $1/8$th of a degree in the X and the Y direction. The eastern boundary of the model coincides with the Strait of Gibraltar. At this boundary salinity, temperature and velocity are prescribed to simulate the exchange through the Strait of Gibraltar and force the presence of the MOW (section 4.4.1). The CADIZ model has problems with resolving the boundaries that resulted in large disturbances in the average sealevel and kinetic energy. This problem likely arises from outgoing flows that reach the boundary at a dominantly tangential direction (Nycander and Döös, 2003). The artefacts this created affect the whole outflow as the water is partly reflected back into the path of the MOW. Since the composition and movement of the MOW will be affected by the artefacts the CADIZ grid did not allow for accurate modelling.

The CADIZplus grid is an enlarged version of the CADIZ grid. The model domain is extended towards the west and now ranges from 33°to 38°North and 5.5°to 13.5°West (CADIZplus grid, 5d). The resolution remains unchanged with a cell size of $1/8$th of a degree in the X and the Y direction. As in the CADIZ model the eastern boundary coincides with the Strait of Gibraltar where salinity, temperature and velocity are prescribed (section 4.4.1). The problems that the CADIZ model has with correctly resolving the boundaries are much smaller in the CADIZplus model. The western boundary is located further away and the reflections created there do not reach the area of the MOW. The reflections caused by the northern and southern boundaries however still affect the evolution of the MOW.

Instead of further increasing the grid size to reduce the reflections the resolution was increased for the next grid. The previous grids all had a resolution of $1/8$th of degree, roughly 12.5 km per grid cell. The CADIZ20 grid has an increased resolution of $1/20$th of a degree in the X and the Y direction. This translates to a cell size of roughly 5 square km per grid cell (CADIZ20 grid, figure 5e). The increase in resolution removes the boundary problems that occur with the CADIZ model. Likely the reduction of the cell sizes means that the flows reaching the boundaries have to be calculated over a smaller distance with corresponding smaller numbers and thus also smaller absolute errors. The increase in resolution also allows for a more accurate representation of the bathymetry. The CADIZ20 grid performs the best of all the grids tested and was thus chosen for the reference experiment.

4.3.2 Vertical grid

The vertical grid used by POM is a bottom-following, sigma-coordinate system (Mellor, 1998). The sigma-coordinate system defines the depth of a certain level as a fraction of total depth. It allows for a better representation of continuous fields such as salinity and temperature in areas with strong variations in the bathymetry such as the Gulf of Cádiz. Since the MOW strongly follows the coast, an area with a strong variation in bathymetry, this is an important feature to have (Borenäs et al., 2002; Hernández-Molina et al., 2012, 2013, 2014; Brackenridge et al., 2013; Filippelli, 2014). In all experiments the sigma grid used consisted of sixteen sigma levels at the same depth fraction (0.000, -0.003, -0.006, -0.012, -0.025, -0.050, -0.100, -0.200, -0.300, -0.400, -0.500, -0.600, -0.700, -0.800, -0.900, -1.000).

Table 2. The extent and resolution of the different grids.

Grid name	Extent Latitude °N	Extent Longitude °E	Resolution	Comment
WMED	45°- 32°	-9°to 9°	$1/8$ °	Calculation time too long.
CADIZ	35°- 38°	-10.5°to -5.5°	$1/8$ °	Problems with boundary solution
CADIZplus	33°- 38°	-13.5°to -5.5°	$1/8$ °	Good solution
CADIZ20	35°- 38°	-10.5°to -5.5°	$1/20$ °	Good solution, used in reference experiment

4.4 Model boundaries

One of the critical points in any OGCM is the usage of open boundaries in non-landlocked basins. In our reference experiment with the CADIZ20 grid there is not just one open boundary, there are four open boundaries. The eastern boundary inside the Strait of Gibraltar is an inflow condition described in section 4.4.1. At the other three boundaries, radiations conditions were applied to the internal velocity while the external velocity was set to zero in order to avoid any sealevel changes. These boundaries have to absorb the outflowing waters and if necessary compensate the outflowing water with an inflow. This approach reduces the effect that the boundaries have on the model circulation but it also means that the water masses moving through the model area in real life are not present and cannot be easily added.

4.4.1 The eastern boundary: the Strait of Gibraltar

At the eastern boundary salinity, temperature and velocity have to be prescribed. Over the years various measurements and calculations have been done to estimate the total transport through the Strait of Gibraltar. The different estimates vary quite strongly as a result of the extreme variability in the strait flow (Lafuente et al., 2002). The exchange through the strait is affected on the short term by both tidal (Macias et al., 2006) and seasonal (Gomis et al., 2006) variations. The yearly variations in the outflow can be as large as 15 $\%$ (Millot, 2008), though on timescales of more than ten years the effects of these yearly variations can be neglected (Gomis et al., 2006). It is thus possible to take the average of multiple measurements to establish the total in- and outflow transport.

The values used by Jungclaus and Mellor (2000) are taken from Bryden et al. (1994) who estimated an inflow of 0.72 Sv and an outflow of 0.68 Sv. Soto-Navarro et al. (2010) estimate an outflow of 0.78 $\pm$ 0.05 Sv and an inflow of 0.81 $\pm$ 0.06 Sv. Other studies such as Bryden and Kinder (1991) and Tsimplis and Bryden (2000) have a much lower estimate of 0.57 $\pm$ 0.26 Sv for the outflow and 0.66 $\pm$ 0.47 Sv for the inflow. In general the inflow of water into the Mediterranean is ten percent higher than the export of water through the MOW (Jungclaus and Mellor, 2000). The difference compensates the evaporation of water in the Mediterranean Sea that drives the two-way exchange through the Strait of Gibraltar (Bethoux, 1979; Bryden et al., 1994; Millot et al., 2006). The focus of this study is the outflow from the Mediterranean and not the transport through the Strait of Gibraltar. A slightly larger inflow than outflow is not likely to affect the evolution of the MOW. Therefore it was decided to assume for all experiments that the inflow equals the outflow. This allows for much simpler modelling since no water has to be added to the basin to compensate for the smaller outflow.

The velocity profile used in the reference experiment can be seen in figure 6. It is based on the profile used by Jungclaus and Mellor (2000) which has also been adjusted so that the outflow equals the inflow. For our velocity profile the total transport of the inflow and the outflow are set at 0.78 Sv based on the findings of Bryden et al. (1994) and Soto-Navarro et al. (2010). The velocity profile shown in Jungclaus and Mellor (2000) appears to be incorrect. The profile does not have an equal in- and outflow and the total transport values do not add up to 0.78 Sv, the two conditions mentioned in Jungclaus and Mellor (2000). In order to achieve the described value of 0.78 Sv all the values of the velocity profile were adjusted by +0.30 cms^{-1} (inflow is positive). With this adjustment the transport value of 0.78 Sv is obtained if one assumes a minimum depth of 300m and a minimum width of 13 km. Unless stated otherwise the corrected velocity profile was the profile used in all experiments.

Not only the velocity has to be prescribed at the Eastern boundary, the temperature and salinity also have to be prescribed to simulate the source of the MOW. The profiles used in the reference experiment can be seen in figure 6. They have been taken unaltered from Jungclaus and Mellor (2000) and have not been altered.

4.5 Experiment duration

In order to have a adequate model it is important to have a model that can be run in a reasonable amount of time. The time it takes to run the CADIZ20 grid of the reference experiment 20 years is roughly four hours. This is a reasonable amount of time to allow for testing of small changes in parameters. In the reference experiment it takes approximately six years for the MOW to reach the northern boundary of the model. After six years an equilibrium is achieved and only slight changes to the outflow still occur, the result of small changes in mixing. The duration of the experiments are all set to 20 years. This duration was chosen as a compromise between ensuring that an equilibrium is achieved and ensuring that no artefacts significantly affect the outflow.

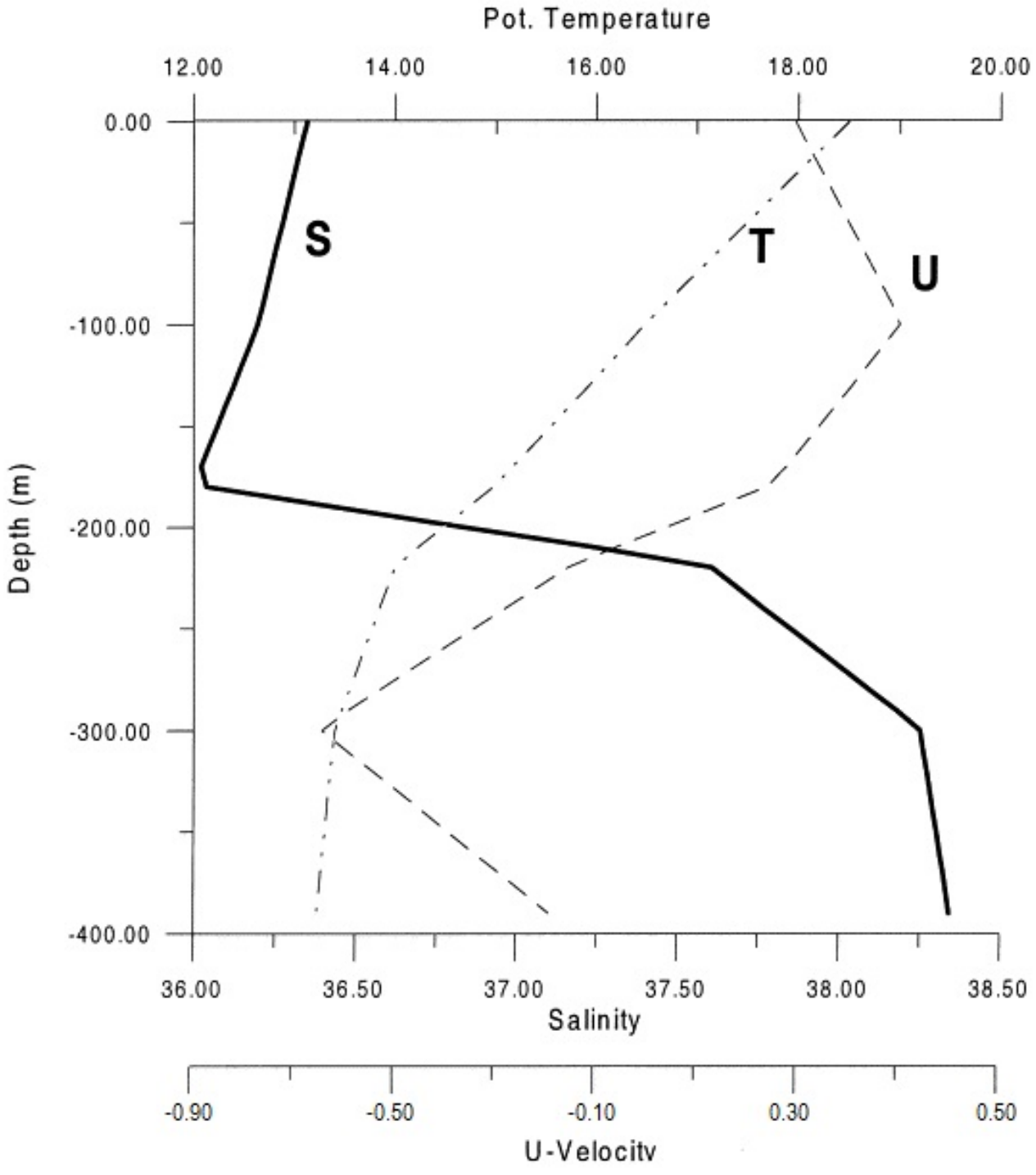

Fig. 6. The salinity, temperature and (corrected) velocity profiles used at the eastern border in the Strait of Gibraltar. Based on and taken from Jungclaus and Mellor (2000).

4.6 Bathymetry smoothing

In addition to the interpolation of the bathymetry extra smoothing is normally done in POM to reduce the so-called 'sigma-coordinate pressure gradient error' first described by Haney (1991) and later examined for POM by Mellor et al. (1994) and Mellor (1998). Sigma-coordinate models often struggle with correctly resolving density and velocity gradients over steep topography. In POM the error is related to the

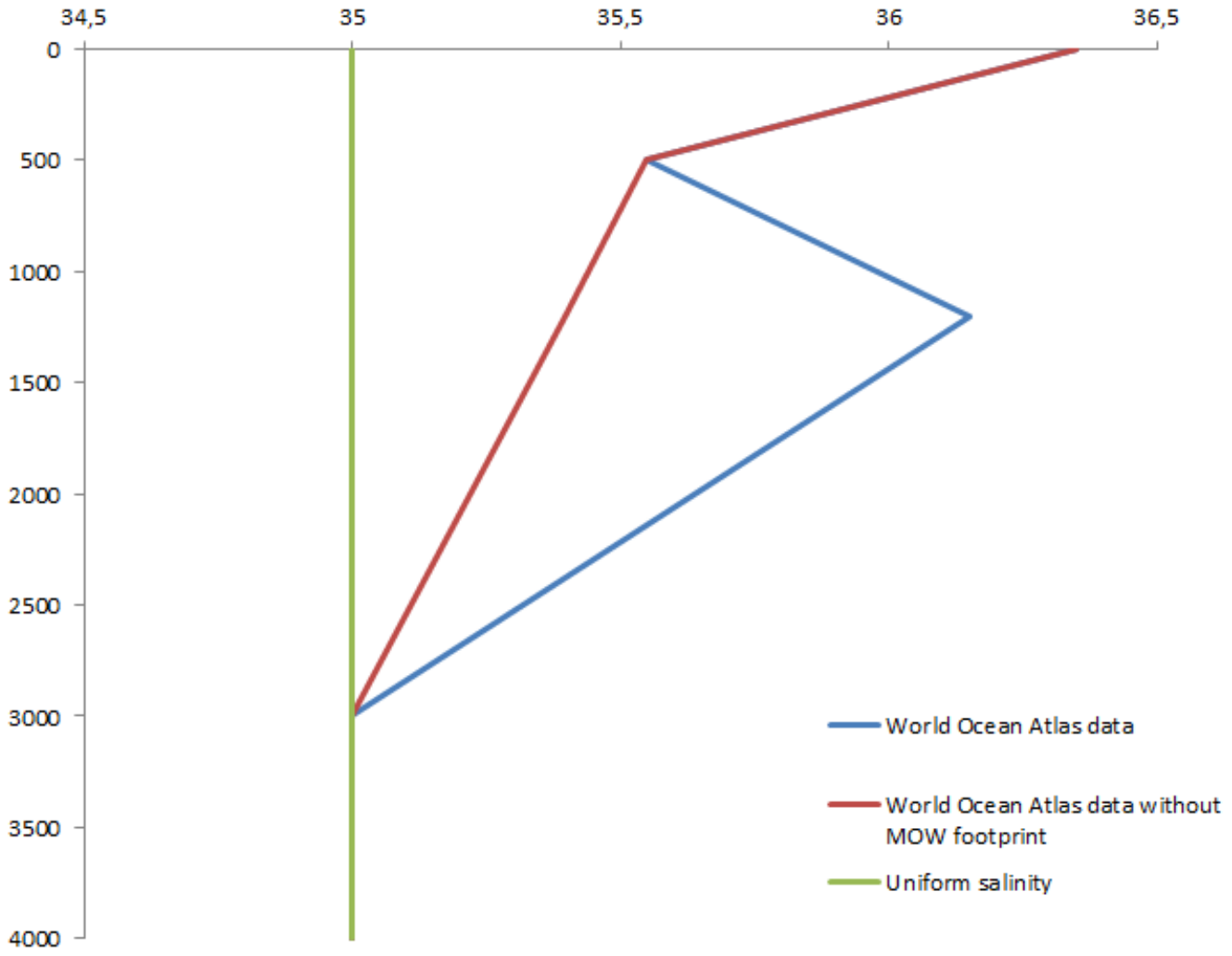

Fig. 7. The three different initial salinity profiles used to test the sensitivity of the model to initial salinity conditions. Green is uniform salinity. Blue is based on actual World Ocean Atlas (Levitus et al., 2013) data from the Gulf of Cádiz. Red is the same World Ocean Atlas data with the footprint of the MOW removed.

square of the cell size (Mellor et al., 1994; Mellor, 1998):

$$Sigma\ coordinate\ pressure\ gradient\ error \propto cellsize^2$$

Mellor (1998) concluded that the error is small though possibly not insignificant. To reduce this error a maximum slope factor was introduced in POM. This factor is the maximum factor with which two adjacent cells can differ in depth and is defined as the ratio between the difference of depths and the sum of depths between two adjacent cells:

$$Slope factor = (\sigma(x+1,z)-\sigma(x,z))/(\sigma(x+1,z)+\sigma(x,z)$$

The slope factor can be set to a value between 0 and 1. With a value of 1 all differences in depth between two adjacent cells are accepted and the bathymetry will not be adjusted. While with 0 no difference in depth between two adjacent cells is accepted at all and the bathymetry will have an equal depth over the whole model domain. In section 6.1 the effect of the smoothness of the bathymetry is tested by adjusting the maximum slope factor. For the reference experiment the slope factor was set to 0.15 as a compromise between smoothing and accurate representation of the bathymetry, similar to the maximum slope factor used by Topper and Meijer (2014)

4.7 Initial salinity conditions in the Atlantic Ocean

Both the mixing speed and the settling depth of the MOW in the Atlantic Ocean are dependent on the density and salinity distribution of the Atlantic waters in the Gulf of Cádiz. To properly represent the water masses in the Gulf of Cádiz present-day of the temperature and the salinity was taken from 'The World Ocean Atlas 2013' (Levitus et al., 2013).

Data from the same area as the model domain was taken from the World Ocean Atlas to construct an initial salinity profile by calculating the average salinity value per depth. To allow for simple input into the the model this profile was further simplified into the profile seen in figure 7 (blue graph).

An unintentional consequence of using present-day Gulf of Cádiz data is the presence of the footprint of the MOW in the initial salinity stratification. To test the consequences of already having the footprint of the MOW present in the model set-up three experiments were performed. The first experiment was done with an initially uniform, basin-wide salinity of 35. The second experiment used the initial salinity profile based on the World Ocean Atlas data. And the third experiment used the World Ocean Atlas data with the footprint of the MOW removed. The different initial salinity profiles are shown in figure 7. The results of the three experiments are shown in Appendix A.

4.7.1 Reference initial salinity profile

To illustrate the effect that the different initial salinity profiles have, the initial evolution of the corresponding experiments are shown in Appendix A1, A2 and A3. Here snapshots of a cross-section at 8°20'W (see figure 8 for actual location) are shown at t=0 days, t=30 days and t=60 days. The snapshots clearly show that initial stratification imposed at the start of the experiment immediately starts to disappear and is already unrecognisable at t=30 days. In the experiments based on the World Ocean Atlas data a small North to South stratification appears. The main features of this stratification along the coastline at the Northern limits of the basin are also present in the experiment with the uniform salinity profile. These features can thus be associated with the development of the MOW in the model and not with the presence of an initial salinity stratification.

The main difference between the salinity profiles at t=60 days is the average salinity of the whole basin. The initial salinity profile with MOW footprint has the highest average salinity and the uniform salinity profile of 35 psu has the lowest average salinity. This simply corresponds to the average salinity of the initial salinity profiles imposed. The main effect of having an initial salinity stratification is thus simply changing the average salinity throughout the whole basin, where as the stratification itself is not maintained.

The increase in average salinity with the salinity profile based on the World Ocean Atlas data with the MOW footprint is roughly 35.75 psu compared to 35.5 psu for the profile without MOW footprint and the uniform profile set at 35 psu (Appendix A13). The effect of this increase is not that significant, it allows the MOW plume to settle at a slightly shallower depth as the surrounding water is denser thus reducing the density difference between the MOW and the surrounding water.

The kinetic energy inside the model evolves oppositely with an uniform or the World Ocean Atlas salinity profile (Appendix A11). The initial kinetic energy is much higher when the World Ocean Atlas data is used ($4.0 * 10^{-2} m^2 s^2$ vs $\approx 0 m^2 s^2$). In contrast the equilibrium level of kinetic energy is higher with an uniform salinity profile ($9.69 * 10^{-3} m^2 s^2$ vs $4.80 * 10^{-3} m^2 s^2$). It is likely that the initial mixing that occurs with a non-uniform salinity profile after t=0 are responsible for the initial spike in kinetic energy. With the lower equilibrium levels the result of the increased average salinity level in the whole basin that reduces flow strength by reducing the density contrast.

For use in the reference experiment the initial salinity profile with the MOW footprint was chosen. The results produced by the different salinity profiles are all very similar. The only thing affected is the average salinity throughout the whole basin while the initial distribution of salinity disappears after the first timestep. The initial salinity profile with the MOW footprint is thought to be the best representation of the present-day situation by at least setting the average salinity values to the actual average present-day values of the Gulf of Cádiz.

5 Reference Experiment

To assess the validity of the model a reference experiment for comparison with present-day data was performed with a run time of 20 years. The choices for the different parameters are given below, with the reasons for these choices found in section 4:

- *Bathymetry:* CADIZ20
- *Boundary Conditions:*
  - *Internal:* Radiation conditions.
  - *External:* Set to 0.
  - *Prescribed flow at Gibraltar:* Corrected inflow based on Jungclaus and Mellor (2000) (figure 6).
- *Conditions source water:* Similar to Jungclaus and Mellor (2000) (figure 6).
- *Initial salinity stratification:* Initial salinity stratification based on World Ocean Atlas data Levitus et al. (2013) with the MOW footprint (figure 7).
- *Initial temperature stratification:* Uniform temperature of 10°C.
- *Bathymetry smoothing factor:* Set to 0.15 (Topper and Meijer (2014)).
- *Evaporation:* None.
- *Wind stress:* None.
- *Surface heat flux:* None.

– *Duration run:* 20 years.

The results of the reference experiment can be found below in figures 9 to 15. After a run of twenty years the change in sealevel in the entire model domain is an insignificant $5.21{*}10^{-3}$m. The average sealevel initially increases slightly until after four years into the model run it starts fluctuating slightly around an average value of $5.21 * 10^{-3}$m 10. The average salinity and temperature reach an equilibrium after seven years after a steady increase from the start of the model as the MOW enters the system (figure 9). The average salinity is increased by approximately 0.96 psu and the average temperature by approximately 0.50°C. The average kinetic energy inside the model reaches equilibrium after seven years of steady decline from t=0 days at a value of approximately $5 * 10^{-3}\ m^2 s^2$. The initial high kinetic energy is likely the result of the mixing that occurs as a result of the initial salinity profile and the entrance of the MOW from the Mediterranean into the system. As after seven years all timeseries have reached an equilibrium this indicates that the whole model has reached an equilibrium state after seven years of running.

Even as equilibrium appears to be achieved after seven years the salinity profiles (figures 11, 12 and 13) and maps (figure 14) are taken at the end of the model run to ensure that total equilibrium has indeed been achieved. In figures 11, 12 and 13 three salinity profiles of the experiment are compared with present-day data provided by Alves et al. (2011), with the location of the profiles shown in figure 8. The comparison with the measured data shows that the model fails to properly represent many of the structures that are present in the present-day data. In the present-day data the upper part of the profiles is dominated by stratified salinity layers that increase in salinity towards the surface. This stratification is mainly the result of local evaporation. However the lack of evaporation in the model means that in the experiment no salinity stratification in the upper layers is present. The present-day data also shows a layer throughout the model domain with an increased salinity of 35.8 psu to 36.4 psu at depths between 800m and 1500m. The main water masses responsible for this layer are Atlantic waters (such as the North Atlantic Central Water (NACW)) and these are not represented in the model as this would make the model needlessly complicated and highly inflexible. Thus this layer of increased salinity is also not present in the experiment.

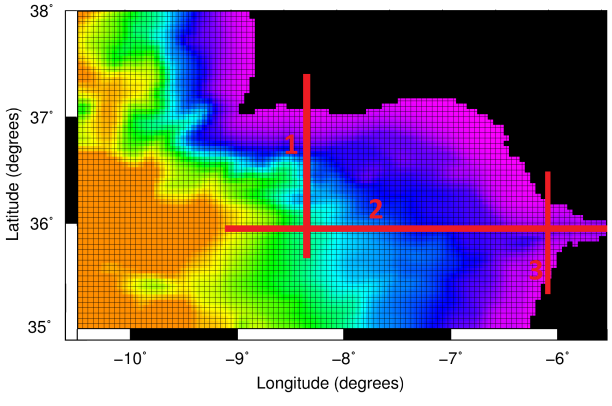

Fig. 8. The locations of the salinity profiles are shown in red. The three profiles are found at (1) 8°20'W, (2) 35°50'N and (3) 6°15'W. All the profiles in this report and the appendix are taken at these three locations.

At the northern side of the basin there is also an area of increased salinity which hugs the Iberian coastline. This is especially apparent in figure 12 where at the northern edge a salinity up to 37.0 psu is reached. This is the main area in which the MOW is focused. Luckily in the model roughly the same is seen, an area of increased salinity along the Iberian coast albeit with lower absolute salinities and at a slightly shallower depth of roughly 200m. The profile taken at the end of the Strait of Gibraltar at 6°15'W (figure 11) is much more different from the present-day data. The modeled MOW hugs the northern side of the strait and is stratified horizontally while the data shows that the MOW tends to be stratified vertically and only have a footprint in the deepest part of the strait. The salinity value of the modeled MOW agrees better with the present-day data with the highest value varying from 37.8 psu in the model to 38.0 psu in the data. Aside from the lack of upper level stratification and the lack of inflowing Atlantic waters the longitudinal model profile at 35°50'N (figure 13) probably shows the largest similarities to its present-day counterpart. At the Eastern edge the MOW footprint follows the ocean floor up to a similar depth of about 800m and the maximum salinity values in both cases are around 37.0 psu. The profiles are in agreement with the salinity maps of the experiment (figure 14). The further the MOW moves westwards the lower its salinity values are as the MOW mixes with the surrounding water, all the while closely hugging the Iberian coastline as it is supposed to do. Figure 15 shows the salinity map at the bottom-sigma layer, e.g. the first resolved layer above the basin floor. The map shows that the MOW strongly follows the basin floor and the local bathymetry. A split between two MOW cores is present though the southern core is not very prominent.

The velocity maps of the experiment cannot be directly compared to a present-day counterpart. Instead they are analysed to determine whether they show a roughly correct pattern. Between 0m and 200m/300m they correctly show a surface current that moves eastward along the Iberian coast through the Strait of Gibraltar. At depths of 200m/300m to 1000m the flow direction is reversed as the MOW itself follows the Iberian bathymetry westwards. At several places the flow is irregular indicating that (turbulent) mixing occurs here as it should.

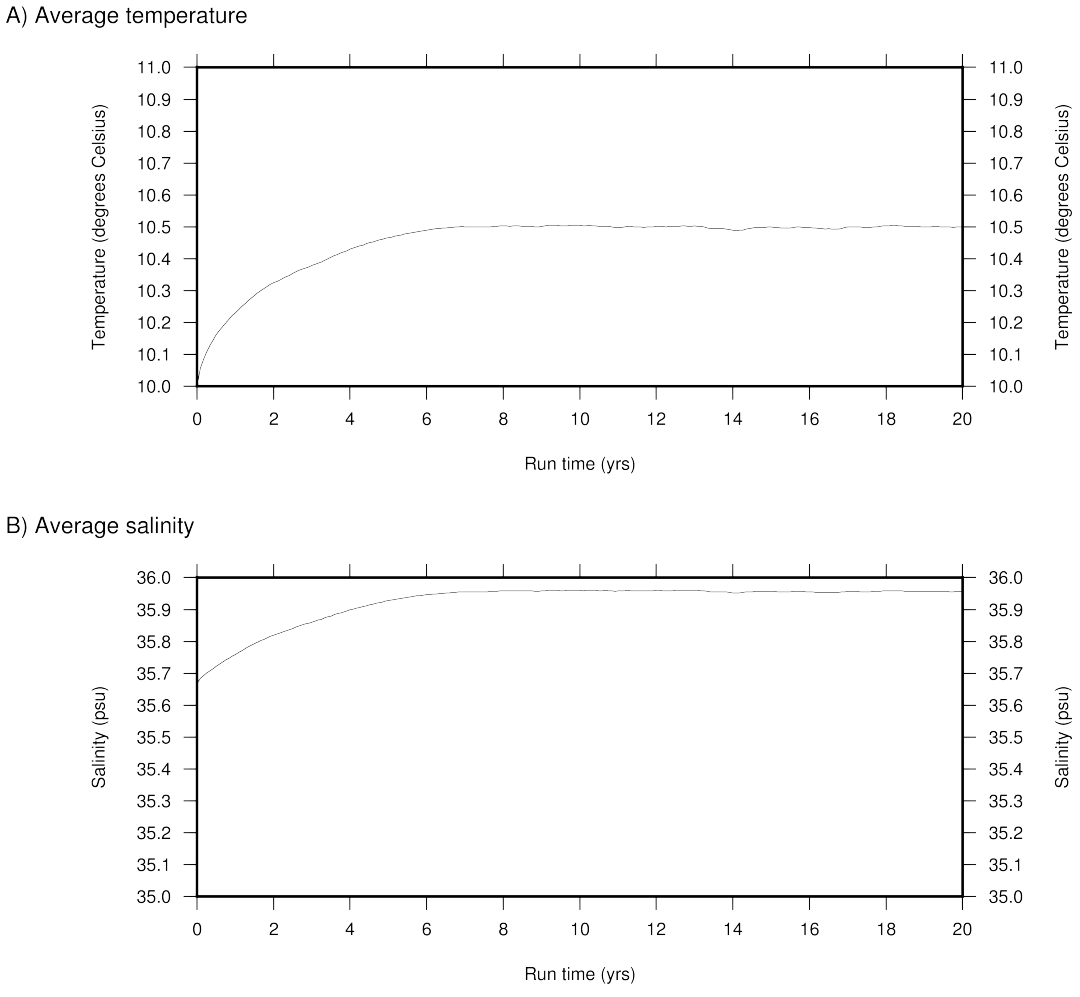

Fig. 9. Reference experiment: A) The change in average temperature throughout the whole model for the run duration. B) The change in average salinity throughout the whole model for the run duration.

5.1 Validity of reference experiment

The observations stated above appear to indicate that the reference experiment does not capture the present-day state quite accurately. Even though this is true one needs to realize that every large scale ocean model is very much a simplification of reality and has even been further simplified in order to reduce computing times. Even with increased computers it remains very hard, if not impossible, to accurately model all the elements affecting an ocean area. Small de

What the model does do is that it produces a roughly accurate MOW in location and strength. Since the object of this study is to analyse the effect that several parameters (e.g. salinity changes, velocity changes, etc.) have on the development of the MOW these are the two most important attributes that need to be modeled. Though smaller details of the MOW such as the split of the MOW in to several cores (Ambar and Howe, 1979; Baringer and Price, 1997; Hernández-Molina et al., 2006, 2012, 2013, 2014) are hard to identify if they are present. I do however believe that together with the model set-up experiments the reference experiment indicates that the model is good enough to analyse the effect of these parameters since the two most important attributes of the MOW are modeled roughly correct.

6 Experiments

After the establishment of the reference experiment several experiments were performed to test the sensitivity of the

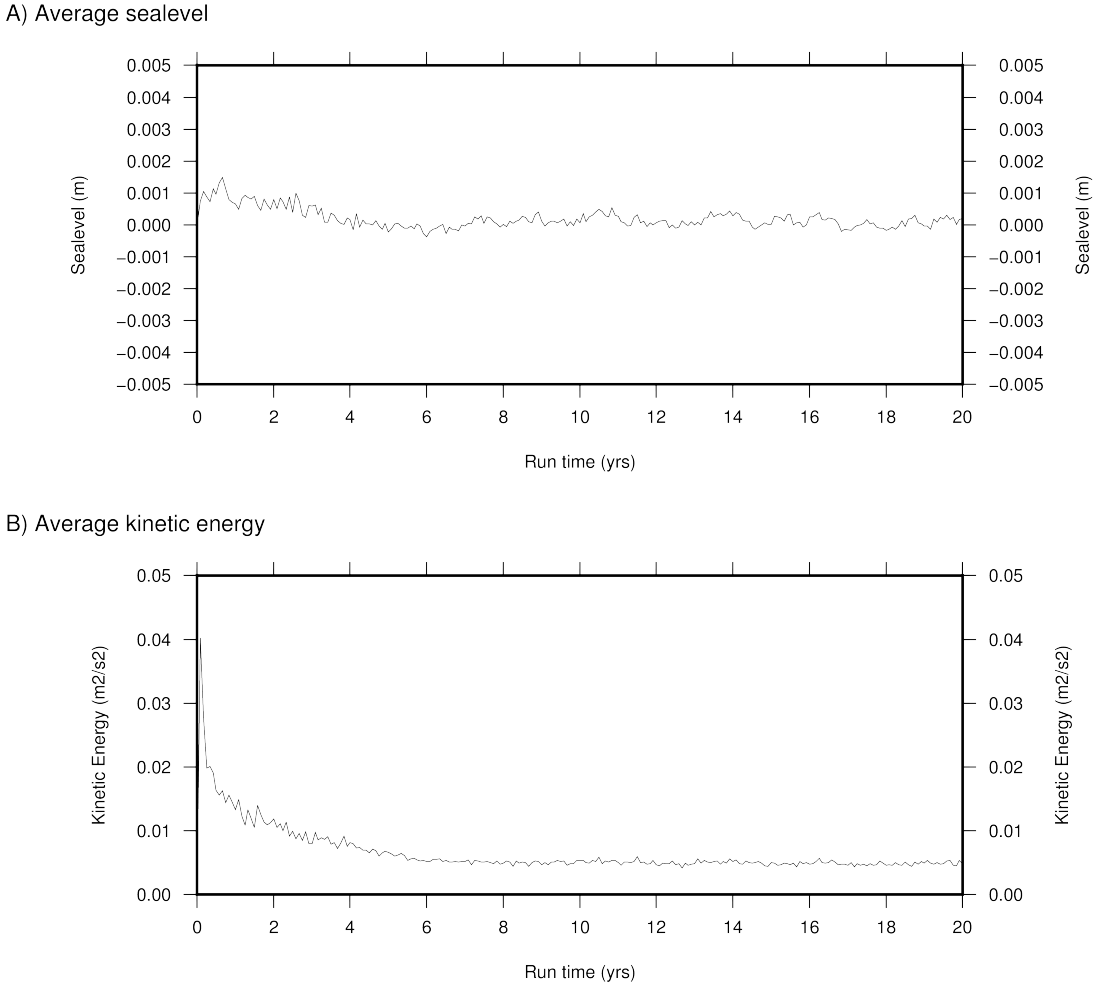

Fig. 10. Reference experiment: A) The change in average sealevel throughout the whole model for the run duration. B) The change in average kinetic energy throughout the whole model for the run duration.

MOW to its own parameters. In most cases the parameter values used to test the sensitivity are quite extreme values that are highly unlikely to have ever occurred in the past or occur in the future.

6.1 Bathymetry smoothing

The first experiment was performed to analyse the effect that changes in the smoothness of the bathymetry have on the development of the MOW. As stated in the introduction it is generally thought that even small changes in the local bathymetry would significantly affect the MOW (Borenäs et al., 2002; Hernández-Molina et al., 2012, 2013; Brackenridge et al., 2013; Filippelli, 2014). To clearly illustrate the influence of the slope factor two runs with extreme slope factors (1.0 = rough bathymetry and 0.01 = smooth bathymetry) were performed and compared to the reference experiment. The results of which can be found in Appendix B.

The effect that the slope factor has on the bathymetry is straightforward. With a slope factor of 1.0, thus without any smoothing of the ETOPO data, the bat bathymetry remains very harsh. The main differences with the reference slope factor of 0.15 are the increased width and depth at the eastern end of the Strait of Gibraltar and the presence of small ridges in the bathymetry. In contrast, a slope factor of 0.01 leads to a nearly equal slope over the whole basin, thus removing all irregularities in the bathymetry.

The salinity distribution maps (Appendix B2 to B5) show that in a smoothed basin the MOW tends to spread out horizontally instead of hugging the Iberian margin. This is es-

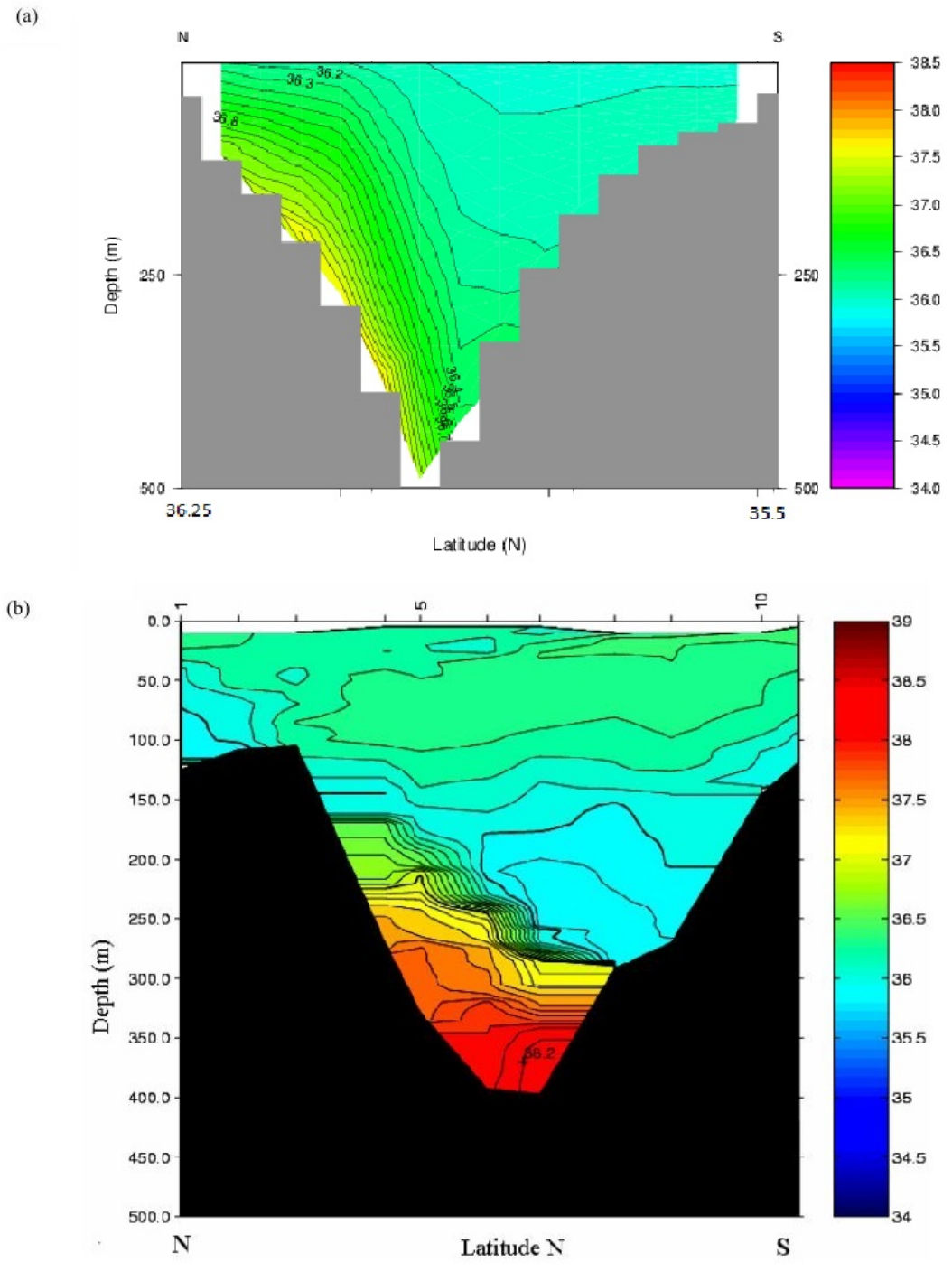

Fig. 11. Reference experiment: North-South salinity profile taken at 6°15'W at t=20 years. A) results from the reference experiments. B) Data from the Gulf of Cádiz Alves et al. (2011).

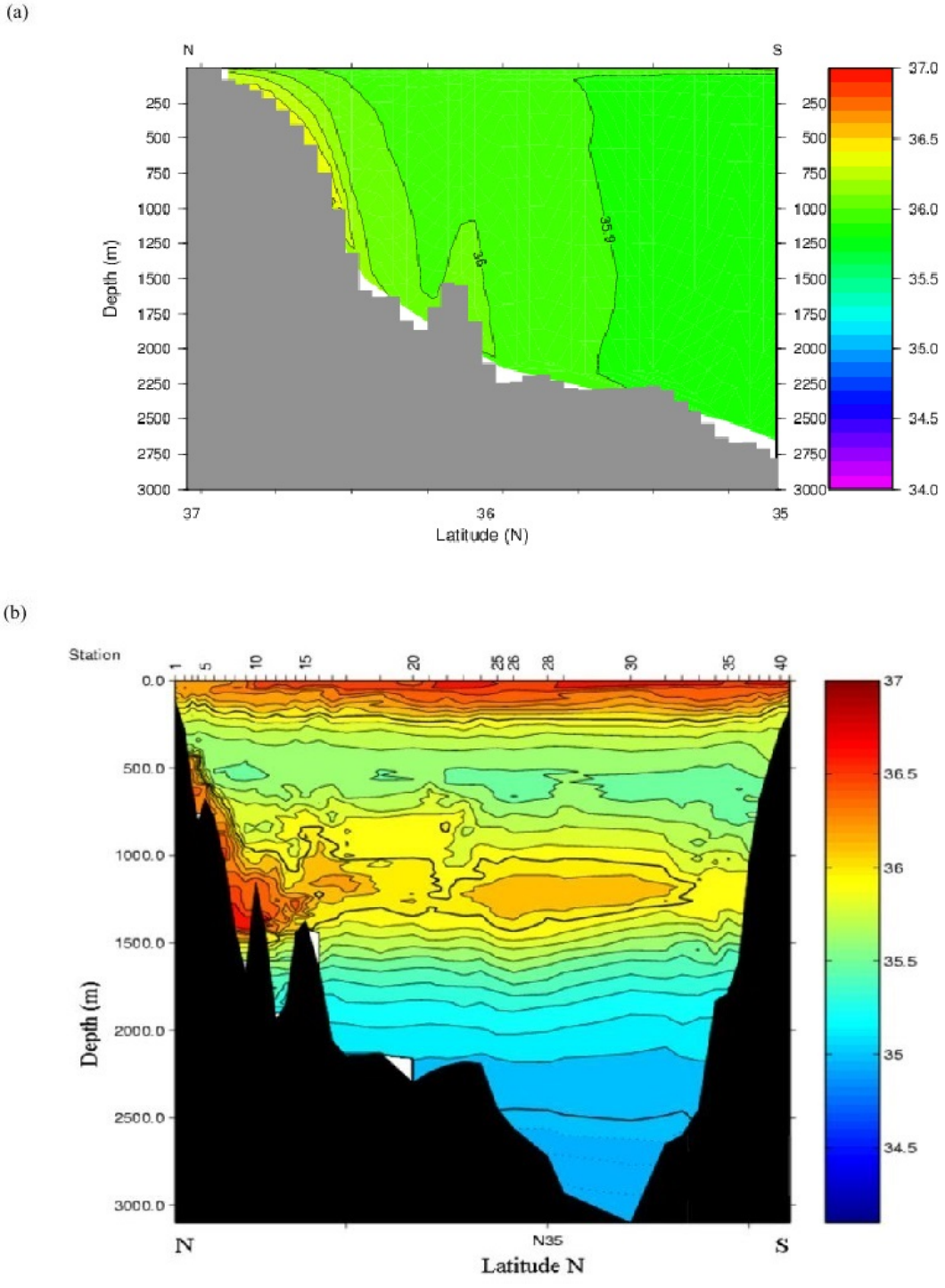

Fig. 12. Reference experiment: North-South salinity profile taken at 8°20'W at t=20 years. A) results from the reference experiments. B) Data from the Gulf of Cádiz Alves et al. (2011). Note the difference in latitudinal scale.

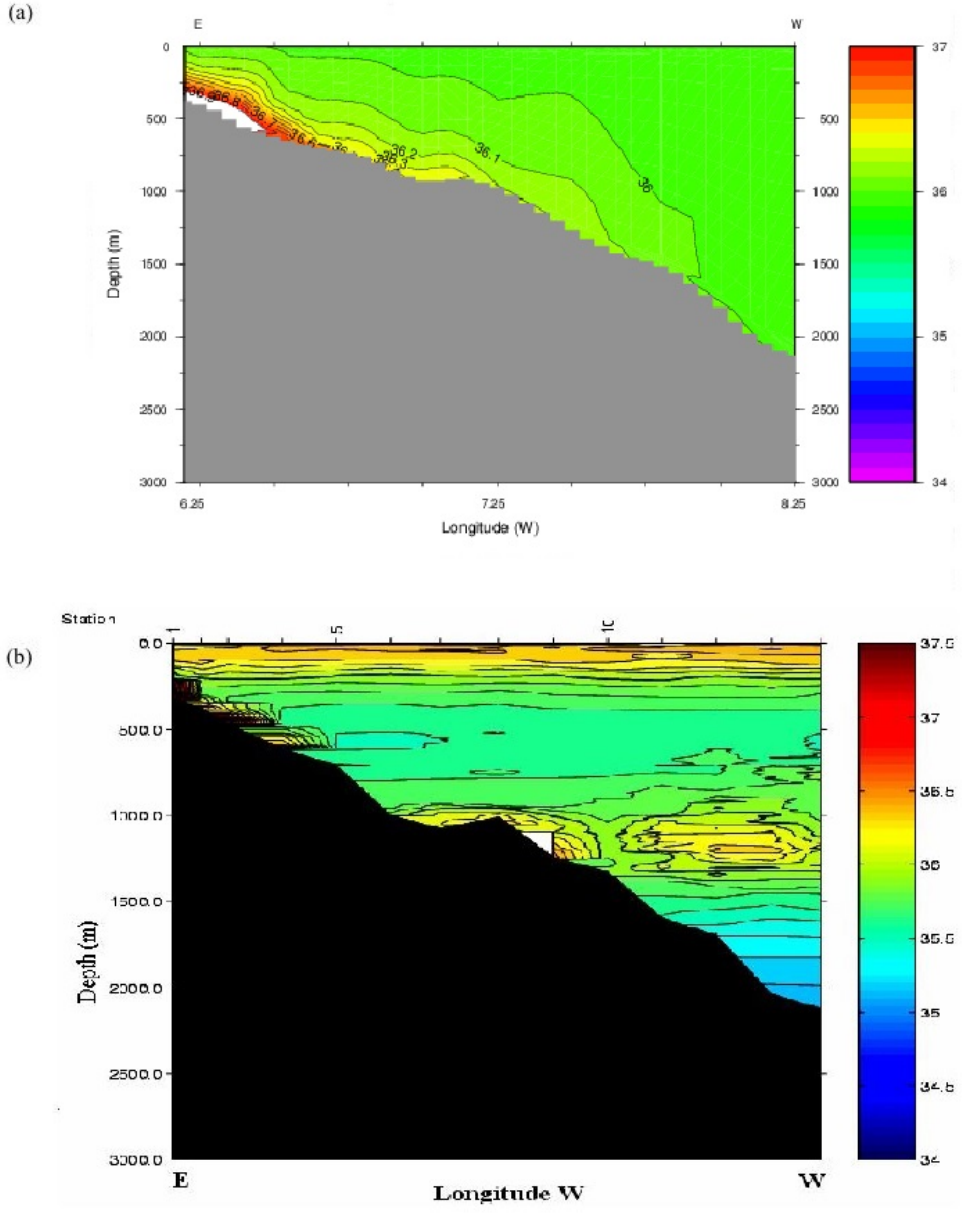

Fig. 13. Reference experiment: West-East salinity profile taken at 35°50'N at t=20 years. A) results from the reference experiments. B) Data from the Gulf of Cádiz Alves et al. (2011). Note the reversed X-axis

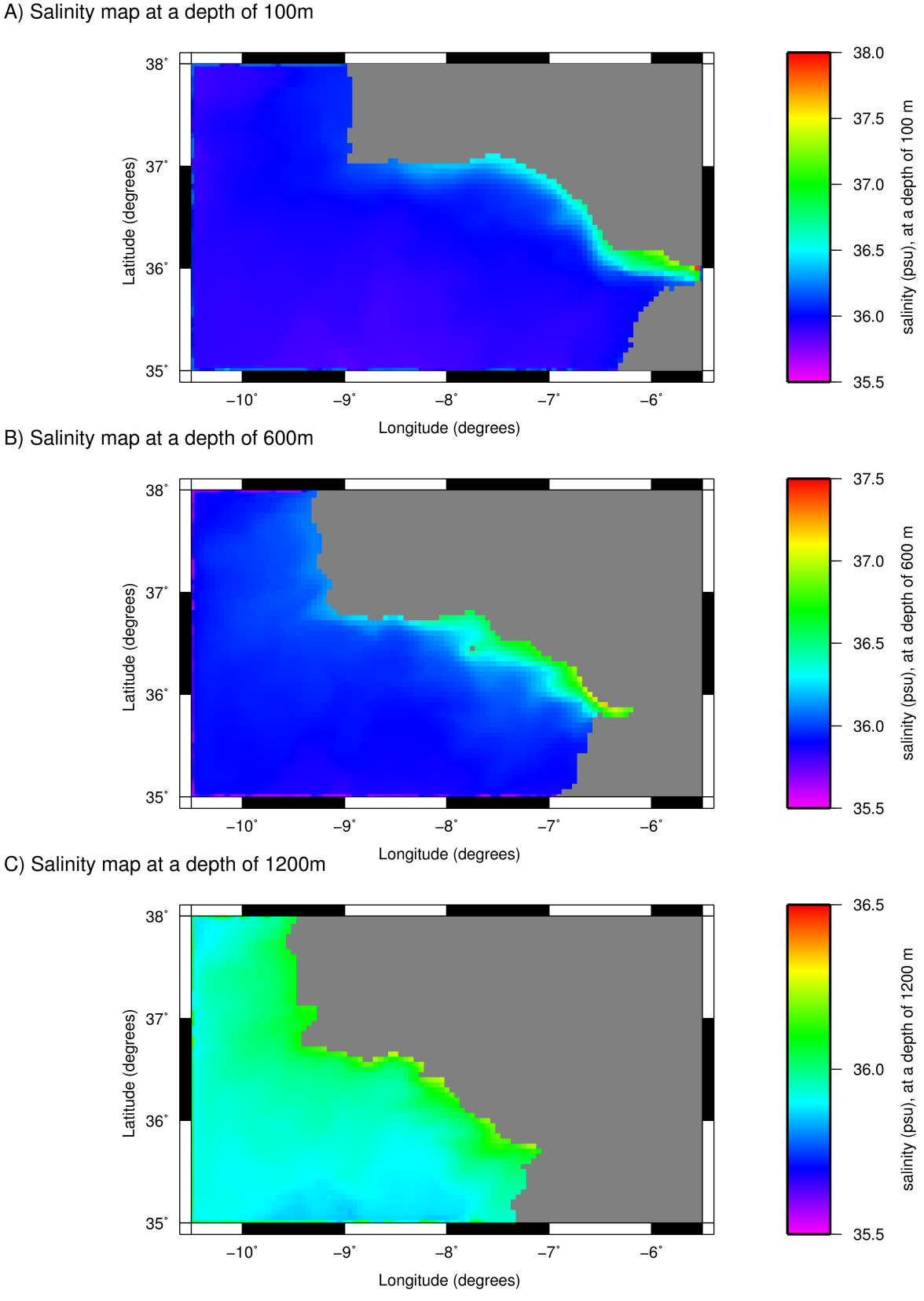

Fig. 14. Reference experiment: The resulting salinity maps of the reference experiment. A) Salinity map at a depth of 100m. B) Salinity map at a depth of 600m. C) Salinity map at a depth of 1200m. Maps taken at t=20 years.

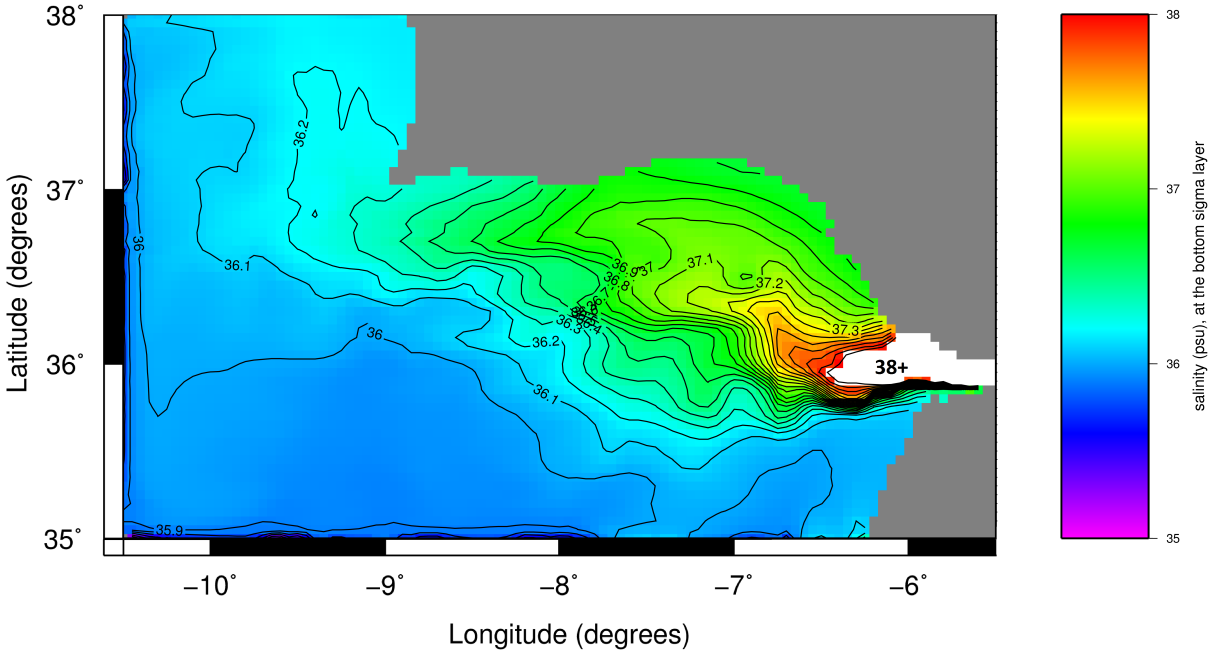

Fig. 15. Reference experiment: The resulting bottom sigma-layer salinity map of the reference experiment. Map taken at t=20 years.

pecially apparent inside the Strait of Gibraltar where a lot more mixing occurs. The high salinity water of the MOW is thus distributed more equally throughout the basin. The density of the MOW plume is thus relatively low and consequently the MOW does not sink as deep as in the reference experiment. The bottom sigma-layer salinity map B5 shows that the distribution of the MOW is very different inside a very rough basin as compared to the smooth basin. With a very rough bathymetry the MOW is concentrated along the Iberian margin and the contour lines of the salinity distribution are strongly irregular. A smooth basin leads to a weaker concentration of the MOW and straight contour lines of the salinity distribution. Inside the Strait of Gibraltar much less mixing occurs and the MOW plume retains a higher density and thus sinks deeper. The exiting depth at Cape St. Vincent though is roughly similar to the reference experiment.

The effect that the slope factor has on the evolution of the average kinetic energy, average sealevel and the average temperature and salinity is not that pronounced (Appendix B9 to B12) . The average kinetic energy in the model is only slightly lower in a smooth basin, while the same can be said about the average temperature and salinity. Interestingly the evolution of the average salinity and temperature suggests, rather counterintuitively, that slightly more high salinity water leaves the model domain in a smooth bathymetry with a spread out MOW than in a rough bathymetry with a concentrated MOW.

The evolution of the average sealevel is more affected by the slope factor. The amplitude of the variation in average sealevel after twenty years is ten times smaller in a smooth basin compared to a rough basin. The smooth basin approaches a low-amplitude equilibrium after ten years where as a rough basin still retains the initial amplitude after twenty years. The reference experiment with a slope factor of 0.15 behaves as would be expected somewhere in between the rough and smooth basins.

Table 3. Average velocities throughout the whole basin at depths of 100m, 600m, and 1200m at t=20 years.

Depth	Factor 0.01	Factor 0.15	Factor 1.0
100m	$-2.60 * 10^{-5}$	$-1.69 * 10^{-4}$	$-2.12 * 10^{-4}$
600m	$-1.05 * 10^{-5}$	$-2.14 * 10^{-5}$	$-2.14 * 10^{-5}$
1200m	$-1.04 * 10^{-5}$	$-1.71 * 10^{-8}$	$1.65 * 10^{-7}$

The average velocities of the whole basin at the depths of 100m, 600m, and 1200m can be found in table 3. The average velocities obtained with a smooth bathymetry are much lower than those with a rough bathymetry. A smooth bathymetry makes the MOW spread out more and not stay as concentrated along the Iberian coast the MOW is not as concentrated and spread more evenly. The resulting differ-

ences in density between the water masses is lower and the resulting velocities thus lower. Together with the velocity maps it shows that turbulent mixing is much more likely to occur with the higher velocities associated with a rough bathymetry.

The experiments seem to confirm the hypothesis that the bathymetry inside the Gulf of Cádiz has a strong impact on the evolution of the POM (Borenäs et al., 2002; Hernández-Molina et al., 2012, 2013; Brackenridge et al., 2013; Filippelli, 2014). The rougher the bathymetry the more concentrated the MOW remains as it leaves the model domain and the more likely it is to affect other water masses and potentially global ocean circulation (Bartoli et al., 2005; Rogerson et al., 2012; Hernández-Molina et al., 2014).

6.2 Sealevel changes

In order to study the effect of sealevel changes two experiments were performed with an altered bathymetry. One experiment with a sealevel drop of 100m and one with a sealevel drop of 250m. Not only the sill depth has been altered but the whole bathymetry has been changed with the set sealevel drop. This means that both the depth and the shape of the basin have been altered as well. The bathymetries can be seen in Appendix C.

In all the experiments the depth at the Eastern border is slightly higher than the sill depth. The inflow at the Eastern border thus needs to be lifted over the sill (Millot, 2009). The strait transport through the Strait of Gibraltar has been adjusted for each experiment based on the results of Topper and Meijer (2014) while retaining the principle of inflow equals outflow. For the sealevel drop of 100m the inflow was set to 0.7 Sv compared to 0.78 Sv in the reference experiment and for the sealevel drop of 250m an inflow of 0.2 Sv was used.

The results C all indicate that a sealevel drop and a corresponding drop in strait transport strongly reduces the strength of the MOW. The evolution of the average kinetic energy, the average sealevel and the average temperature and salinity (Appendix C9 to C12) in both cases are similar compared to the reference experiment. Though the absolute values achieved are lower as less water is being brought into the system.

The salinity maps and profiles shown in Appendix C2 to C8 illustrate that with a sealevel drop of 100m the MOW still has the tendency to move westwards following the bathymetry along the Iberian margin, albeit it does so with a strongly reduced intensity compared to the reference experiment. The overall salinity of the MOW is much lower, allowing for less mixing to occur and reducing the footprint of the the MOW to inside the Gulf of Cádiz. The MOW does not reach as far west or sink as deep is it does in the reference experiment. In the case of a sealevel drop of 250m the intensity of the MOW is even further reduced as the deeper and more saline water struggles to pass over the sill in the Strait of Gibraltar. The MOW plume only remains distinct in the first kilometers after leaving the Strait of Gibraltar. It also does not sink at all and no sign of it is visible at a depth of 600m or 1200m.

A change in sealevel and a corresponding change in sill depth thus has a very strong effect on the development of the MOW. A drop in sealevel reduces the amount of water transport through the Strait of Gibraltar (Topper and Meijer, 2014). As less water enters the Gulf of Cádiz the MOW is more readily absorbed into the surrounding waters. This means that its high salinity and density features are not as well retained and the MOW itself does not penetrate as far east or as deep as it does in the present-day situation.

6.3 Source water conditions

With the Gulf of Cádiz model used in this study it is not possible to test the hypotheses of Price and Baringer (1994) and Thorpe and Bigg (2000) regarding the link between MOW density and strait transport. In the Gulf of Cádiz model strait transport is an assignable variable and can thus not be allowed to move freely as a result of MOW density. It is however possible to analyse the effect of salinity changes on MOW behaviour. Previous models suggested a relative small impact from altering conditions at Gibraltar (Rahmstorf, 1998), though some impact is a robust feature of these models (Bigg et al., 2003). To study the impact of salinity changes on MOW behaviour four experiments were done where the salinity of the inflow at the Eastern border is artificially changed by respectively minus 10, minus 2, plus 2 and plus 10. In all experiments the outflow at the Eastern border remains unaltered, only the inflow is changed.

The results of all four experiments can be found in Appendix D together with the results of the reference experiment. The salinity maps and the profiles (Appendix D1 to D7) show that in the plus 2, plus 10 and the minus 10 a clear outflow forms that hugs the Iberian margin. With the inflow salinity reduced by 10 psu the MOW has a lower salinity than the surrounding waters of the Gulf of Cádiz and as such it remains in the upper 300m of water. The opposite occurs when the inflow salinity is increased. An increase in density causes the MOW to sink deeper and to penetrate further east in a distinct manner. In both the plus 2 and the plus 10 experiments the bottom part of the MOW reaches the ocean floor outside the Gulf of Cádiz (Appendix D5 to D7). The bottom sigma-layer (Appendix D4) shows that the distribution and movement of the MOW in the plus 2, plus 10 and the reference experiment are all similar and all follow the bathymetry, the only difference is the absolute salinity. The minus 2 experiment is different from the other experiments in that a clear outflow fails to form and that the MOW does not penetrate much further than the eastern end of the Strait of Gibraltar. The salinity of the inflow is roughly similar to the water already present in the Gulf of Cádiz. The density contrast between the MOW and the Gulf of Cádiz is thus very

low and aside from the initial velocity applied at the eastern boundary there is no force that wants to propel the MOW.

The absence of a clear, focused MOW in the minus 2 experiment is also apparent in the evolution of the kinetic energy figure D19). It reaches the lowest equilibrium value of all experiments with 0.002 m^2s^2 and the variation over time is also very low indicating that almost nothing happens in the experiment. The other experiments (Appendix D8 and D19) do show an increase in kinetic energy relative to the reference experiment (0.004 m^2s^2). The higher the difference in salinity and density between the MOW and the Gulf of Cádiz the higher the kinetic energy is, thus for plus 2, minus 10 and plus 10 the kinetic energy respectively is 0.08, 0.015 and 0.100 m^2s^2. With the increase in kinetic the variation around the equilibrium value also increases.

The evolution of the average salinity throughout the model run is as expected higher for the experiments with an increased inflow salinity. The differences obtained with the reference experiment are however not that large with an equilibrium value of 36.06 psu, 36.00 psu and 35.96 psu in respectively the plus 10, the plus 2 and the reference experiment (Appendix D10 and D21). When the inflow salinity is reduced the overall salinity has an equilibrium value of 35.70 psu and 35.49 psu respectively for the minus 2 and the minus 10 experiments (Appendix D10 and D21). The increase obtained in overall salinity with an increased inflow salinity is thus smaller than the decrease in overall salinity with a decreased inflow salinity. This suggests that with an increased inflow salinity more MOW leaves the model at the Atlantic boundaries, indicating a stronger MOW.

A problem with both experiments that decrease the inflow salinity is that in essence they are flawed since such a decrease in salinity and corresponding density would very likely alter and possibly reverse the exchange through the Strait of Gibraltar. The results can however be used to analyse the workings of the model. The salinity maps and profiles of both experiments show that the MOW does not follow the Iberian coast at all. Instead the MOW just flows westwards as it spreads and mixes with the surrounding waters until it is assimilated before it even reaches the longitude of the Cape St. Vincent. This makes sense as it is the relation between the density of the waters and the Coriolis force that governs the direction of movement.

6.4 MOW velocity

Another parameter to be tested is the velocity of the MOW coming from the Mediterranean Sea. This is evaluated by altering the velocity of the inflow and outflow at the eastern boundary of the model. Two experiments were performed with the reference speed 6 multiplied by 0.5 and by 1.5. The equilibrium results that have been obtained after a run of twenty years can be found in Appendix 1E to 10E.

The salinity maps and the profiles (Appendix 1E to 6E) show that the differences resulting from a change in initial MOW velocity are small. The MOW still tends to follow the bathymetry along the Iberian margin. With an increased velocity the MOW spreads out slightly more in a horizontal direction as the increased velocity reduces the available time for the denser MOW to sink, while with a decreased velocity the MOW spreads out less in a horizontal direction. A similar effect can be seen by the slightly higher absolute salinity further eastwards in the experiment with an increased velocity and slightly lower absolute salinity in the experiment with a decreased velocity. The evolution of kinetic energy, sealevel, temperature and salinity (Appendix 7E to 10E) are also largely unaffected by the change in initial velocity. They strongly resemble the graphs of the reference experiment. The overall effect of the change in initial velocity is low.

7 Discussion

The aim of this study was to build a model of the MOW to provide insight in the dynamics of the MOW. In section 6 several parameters affecting the MOW were tested. The settling depth and penetration of the MOW are affected by the properties of the Atlantic waters and by the properties of the Mediterranean source water.

The MOW properties at Cape St. Vincent, where the MOW leaves the Gulf of Cádiz, are surprisingly similar in all of the sensitivity experiments performed. The velocity test shows that a change in MOW velocity through the Strait of Gibraltar barely has any effect at all. An increase in speed leads to an increase in mixing near the Strait of Gibraltar but the overall effect at Cape St. Vincent is negligible.

The effect of changing the salinity of the Mediterranean source water at the eastern boundary is also surprisingly low. An increase of 10 psu in the inflow only leads to an increase of ≈ 0.3 psu around Cape St. Vincent. The limited increase in salinity at Cape St. Vincent is the result of an increase in mixing inside the Gulf of Cádiz.

The effect of changing the average salinity of the other side of the Strait of Gibraltar is much more pronounced. A decrease of ≈ 0.75 psu of the salinity of the Atlantic water is matched by a similar decrease of ≈ 0.75 psu of the MOW at Cape St. Vincent. The relative difference in density and salinity is thus not altered and as a result the settling depth of the MOW also remains largely unaltered. Again the extra decrease in salinity is caused by increased mixing inside the Gulf of Cádiz.

Since the flow and stratification of Atlantic waters is not simulated in the model it is unclear how the water masses affected by the differences in mixing behave. This makes it hard to determine the likelihood of the hypothesis that the MOW could function as a feedback system to a reduction in North-Atlantic deep-water formation associated with climate change as suggested by Rahmstorf (1998),Rogerson et al. (2010) and Rogerson et al. (2012). Though the lack of large changes in the MOW at Cape St. Vincent suggests that

the MOW will at least be present under wildly varying conditions. The results do confirm the suggestion by Price and Baringer (1994) and Rogerson et al. (2012) that the settling depth of the MOW is largely insensitive to changes to the Mediterranean source and more affected by changes to the Atlantic waters.

The link between MOW behaviour and the bathymetry in the Gulf of Cádiz is also tested. A reduction in sealevel together with a reduction in strait transport (Topper and Meijer, 2014) strongly reduces the influence the MOW has on the Atlantic waters with very little saline water even reaching as far as Cape St. Vincent. This means that a size-able connection (especially in depth) between the Mediterranean Sea and the Atlantic Ocean is needed for the MOW to impact the global ocean circulation.

Sealevel change is however not the only bathymetry-related factor that affects the development of the MOW. Another critical factor is the smoothness and shape of the bathymetry itself (Borenäs et al., 2002; Hernández-Molina et al., 2012, 2013; Filippelli, 2014). A highly smoothed bathymetry contributes to a more equal latitudinal distribution of the MOW while a rough bathymetry forces the MOW to move along the Iberian Coast with higher velocities. About an equal amount of the MOW leaves the Gulf of Cádiz in both cases but in a rough bathymetry the MOW plume remains much more concentrated. The high density of the MOW is thus retained much further into the Atlantic ocean and will therefore have a larger effect on the water bodies inside the Atlantic. It is clear that the bathymetry of the Gulf of Cádiz is critical in controlling the behaviour of the MOW. The splitting observed in the MOW after leaving the Gulf of Cádiz (Ambar and Howe, 1979; Baringer and Price, 1997; Hernández-Molina et al., 2012) is however not present in detail in the model. The hypotheses of Millot et al. (2006) and Millot (2009) regarding the relation between local bathymetry and the splitting of the MOW cannot be tested.

7.1 Future improvements

It is clear that even though some clear conclusions can be drawn from the results described above the model built here is not perfect. The whole MOW system and the interaction with Atlantic waters is a highly complex system that involves a lot of interaction between a lot of variables. Several simplifications have been made in order to create a model that is quick and easy to alter and test for a varying range of parameters. To obtain an even more accurate model improvements can be made by including or expanding the following components:

- *The flow of Atlantic water through the model:* The lack of movement and input at the Atlantic boundaries means that the MOW only interacts with an initially defined column of water. As the experiment progresses the Atlantic waters slowly get more saturated with the high salinity MOW. Since no new 'fresh' Atlantic water enters the model oversaturation might occur.
- *Mediterranean Sea:* In the experiments performed the Mediterranean Sea was represented by a predefined in- and outflow at the eastern edge of the Strait of Gibraltar. This allows for quick model runs to test parameters. It however does not allow to test the development of the MOW for processes that occur in the Mediterranean Sea. Climate changes that affect the global ocean circulation also affect the evaporation, precipitation and prevailing winds in the Mediterranean Sea. Rahmstorf (1998); Cacho et al. (2000); Voelker et al. (2006) all suggested that these processes in the Mediterranean should affect the development of the MOW. Though previous model studies by Price and Yang (1998) and Thorpe and Bigg (2000) recorded a relatively constant outflow. In order to properly study this the Mediterranean should be included in the model. An attempt was made in this study to include the Western Mediterranean, this however led to computation times of more than fourteen days. A solution would be to use the Stony Brook Parallel Ocean Model (Jordi and Wang, 2012) based on POM to reduce computation time. This is the model used by Topper and Meijer (2014) to model the whole Mediterranean Sea. A model well suited to be expanded by a high resolution Gulf of Cádiz.
- *MOW cores:* The splitting of the MOW into several cores and branches is one of the main features of the MOW (Ambar and Howe, 1979; Iorga and Lozier, 1999a; Millot et al., 2006; Millot, 2009; Hernández-Molina et al., 2012). The split between a lower and a upper core inside the Gulf of Cádiz appears to be present in the model. The split west of Cape St. Vincent is however not clearly present. This is likely the result from the limited size of the model grid and a lack of vertical resolution. It would be useful to increase the amount of sigma-levels in the model to better capture the the split as done by Jungclaus and Mellor (2000).

Aside from these improvements to the model more research should be done into constraining several unclear external factors:

- *Tectonic evolution of the Gulf of Cádiz.* To improve our understanding of the MOW system and the development of the Strait of Gibraltar and the Gulf of Cádiz a more accurate reconstruction of the tectonic development of the region would be very useful. A start is made by Hernández-Molina et al. (2014) but by linking the presence of contourites to sealevel and bathymetry smoothness changes it should be possible to reconstruct a more detailed history of the last 4.5 Ma.
- *Mediterranean deep water formation* The source waters of the MOW are the intermediate to deep Mediterranean

waters. The formation of deep water in the Mediterranean mainly occurs in the winter. It is known that seasonal changes to the total transport through the strait exist however it is not clear whether there are also seasonal changes to the density of the MOW. In order to study this a field study in the Gulf of Cádiz is required.

– *Tidal forces inside the Strait of Gibraltar* The transport through the Strait of Gibraltar can be attributed to tidal and atmospheric forces for 80% (Gomis et al., 2006; Rogerson et al., 2012). The effect of the tidal forces on mixing and density distribution do not appear to be well known.

8 Conclusions

In this study a set-up is provided for a model of the MOW to test the sensitivity of the parameters affecting the MOW. All the parameters can be easily altered in the model. Several experiments have been done to test the sensitivity of the MOW to changes in the bathymetry of the Gulf of Cádiz (e.g. smoothness and sealevel changes), the conditions of the Mediterranean source water, the velocity of the MOW and the conditions of the Atlantic Ocean. The complexity of the MOW system however does not allow for easy modelling and the reliability of the results is therefore uncertain. Even so a lot of useful information and conclusions regarding the behaviour of the MOW is obtained.

The sensitivity experiments show that the most important factors in the behaviour of the MOW are the smoothness and depth of the bathymetry of the Gulf of Cádiz and the conditions of the Atlantic waters. They all influence the amount of mixing inside the Gulf of Cádiz, the penetration of the MOW outside the Gulf of Cádiz and the settling depth of the MOW at Cape St. Vincent. The velocity and the conditions of the Mediterranean source water are far less important. The most surprising conclusion is however that radical changes are needed to any parameter to cause a significant change in MOW behaviour.

Though the model provides a good analysis of the sensitivity of the MOW to certain parameters more research is required before any definite conclusions can be made. Two significant improvements to the model would be to include the flow of Atlantic water through the model domain and to increase the grid resolution (especially the number of sigma-layers). This should allow for a better control on the mixing inside the Gulf of Cádiz and the split of the MOW into multiple cores. New data and research resulting from the IODP expedition 339 (Hernández-Molina et al., 2012) should also lead to a better understanding of the Gulf of Cádiz over the last 5 Ma. Hopefully this can together with models such as this one lead to an improved understanding of the behaviour and function of the MOW in the global climate.

Acknowledgements. I would like to thank the following persons for their contributions to this thesis: Alba de la Vera Fernandez, Anneke Kleppe, Jan van Lopik, Jasper Ploegstra, Luuk Schuurmans, Robin Topper and last but not least Paul Meijer.

References

Ahumada, M. and Cruzado, A.: Modeling of the circulation in the Northwestern Mediterranean Sea with the Princeton Ocean Model, Ocean Science, 3, 77–89, 2007.

Alves, J. M. R., Carton, X., Ambar, I., et al.: Hydrological structure, circulation and water mass transport in the Gulf of Cadiz, International Journal of Geosciences, 2, 432, 2011.

Amante, C. and Eakins, B.: ETOPO1 1 Arc-Minute Global Relief Model: Procedures, Data Sources and Analysis, NOAA Technical Memorandum NESDIS NGDC-24, 2009.

Ambar, I. and Howe, M.: Observations of the Mediterranean outflow—I mixing in the Mediterranean outflow, Deep Sea Research Part A. Oceanographic Research Papers, 26, 535–554, 1979.

Baringer, M. O. and Price, J. F.: Mixing and spreading of the Mediterranean outflow, Journal of Physical Oceanography, 27, 1654–1677, 1997.

Baringer, M. O. and Price, J. F.: A review of the physical oceanography of the Mediterranean outflow, Marine Geology, 155, 63–82, 1999.

Bartoli, G., Sarnthein, M., Weinelt, M., Erlenkeuser, H., Garbe-Schönberg, D., and Lea, D.: Final closure of Panama and the onset of northern hemisphere glaciation, Earth and Planetary Science Letters, 237, 33–44, 2005.

Bethoux, J.: Budgets of the Mediterranean Sea-Their dependance on the local climate and on the characteristics of the Atlantic waters, Oceanologica acta, 2, 157–163, 1979.

Bethoux, J., Gentili, B., Morin, P., Nicolas, E., Pierre, C., and Ruiz-Pino, D.: The Mediterranean Sea: a miniature ocean for climatic and environmental studies and a key for the climatic functioning of the North Atlantic, Progress in Oceanography, 44, 131–146, 1999.

Bigg, G., Jickells, T., Liss, P., and Osborn, T.: The role of the oceans in climate, International Journal of Climatology, 23, 1127–1159, 2003.

Bigg, G. R. and Wadley, M. R.: Millennial-scale variability in the oceans: An ocean modelling view, Journal of Quaternary Science, 16, 309–319, 2001.

Blumberg, A. F. and Mellor, G. L.: A description of a three-dimensional coastal ocean circulation model, Three-dimensional coastal ocean models, pp. 1–16, 1987.

Borenäs, K., Wåhlin, A., Ambar, I., and Serra, N.: The Mediterranean outflow splitting—a comparison between theoretical models and CANIGO data, Deep Sea Research Part II: Topical Studies in Oceanography, 49, 4195–4205, 2002.

Brackenridge, R. E., Hernández-Molina, F., Stow, D., and Llave, E.: A Pliocene mixed contourite–turbidite system offshore the Algarve Margin, Gulf of Cadiz: Seismic response, margin evolution and reservoir implications, Marine and Petroleum Geology, 46, 36–50, 2013.

Bryden, H. L. and Kinder, T. H.: Steady two-layer exchange through the Strait of Gibraltar, Deep Sea Research Part A. Oceanographic Research Papers, 38, S445–S463, 1991.

Bryden, H. L., Candela, J., and Kinder, T. H.: Exchange through the Strait of Gibraltar, Progress in Oceanography, 33, 201–248, 1994.

Cacho, I., Grimalt, J. O., Sierro, F. J., Shackleton, N., and Canals, M.: Evidence for enhanced Mediterranean thermohaline circulation during rapid climatic coolings, Earth and Planetary Science Letters, 183, 417–429, 2000.

de la Vara, A., Topper, R. P., Meijer, P. T., and Kouwenhoven, T. J.: Water exchange through the Betic and Rifian corridors prior to the Messinian Salinity Crisis: A model study, Paleoceanography, 2015.

Faugèers, J.-C., Gonthier, E., and Stow, D. A.: Contourite drift molded by deep Mediterranean outflow, Geology, 12, 296–300, 1984.

Filippelli, G.: A salty start to modern ocean circulation, science, 344, 1228–1229, 2014.

Gascard, J.-C. and Richez, C.: Water masses and circulation in the Western Alboran Sea and in the Straits of Gibraltar, Progress in Oceanography, 15, 157–216, 1985.

Gomis, D., Tsimplis, M., Martín-Míguez, B., Ratsimandresy, A., García-Lafuente, J., and Josey, S. A.: Mediterranean Sea level and barotropic flow through the Strait of Gibraltar for the period 1958–2001 and reconstructed since 1659, Journal of Geophysical Research: Oceans (1978–2012), 111, 2006.

Haney, R. L.: On the pressure gradient force over steep topography in sigma coordinate ocean models, Journal of Physical Oceanography, 21, 610–619, 1991.

Heinrich, H.: Origin and consequences of cyclic ice rafting in the northeast Atlantic Ocean during the past 130,000 years, Quaternary research, 29, 142–152, 1988.

Hemming, S. R.: Heinrich events: Massive late Pleistocene detritus layers of the North Atlantic and their global climate imprint, Reviews of Geophysics, 42, 2004.

Hernández-Molina, F., Stow, D., and Alvarez-Zarikian, C.: IODP Expedition 339 in the Gulf of Cadiz and off West Iberia: decoding the environmental significance of the Mediterranean outflow water and its global influence, Scientific Drilling, 16, 1–11, 2013.

Hernández-Molina, F. J., Llave, E., Stow, D., García, M., Somoza, L., Vázquez, J. T., Lobo, F., Maestro, A., del Río, V. D., León, R., et al.: The contourite depositional system of the Gulf of Cadiz: a sedimentary model related to the bottom current activity of the Mediterranean outflow water and its interaction with the continental margin, Deep Sea Research Part II: Topical Studies in Oceanography, 53, 1420–1463, 2006.

Hernández-Molina, F. J., Stow, D. A., Alvarez-Zarikian, C., Williams, T., Lofi, J., Acton, G. D., Bahr, A., Balestra, B., Ducassou, E., Flood, R. D., et al.: Integrated Ocean Drilling Program Expedition 339 Preliminary Report: Mediterranean Outflow: Environmental significance of the Mediterranean Outflow water and its global implications: 16 November 2011-16 January 2012, 2012.

Hernández-Molina, F. J., Stow, D. A., Alvarez-Zarikian, C. A., Acton, G., Bahr, A., Balestra, B., Ducassou, E., Flood, R., Flores, J.-A., Furota, S., et al.: Onset of Mediterranean outflow into the North Atlantic, Science, 344, 1244–1250, 2014.

Iorga, M. C. and Lozier, M. S.: Signatures of the Mediterranean outflow from a North Atlantic climatology: 2. Diagnostic velocity fields, Journal of Geophysical Research: Oceans (1978–2012), 104, 26 011–26 029, 1999a.

Iorga, M. C. and Lozier, M. S.: Signatures of the Mediterranean outflow from a North Atlantic climatology: 1. Salinity and density fields, Journal of Geophysical Research: Oceans (1978–2012), 104, 25 985–26 009, 1999b.

Jordi, A. and Wang, D.-P.: sbPOM: A parallel implementation of Princenton Ocean Model, Environmental Modelling & Software, 38, 59–61, 2012.

Jungclaus, J. H. and Mellor, G. L.: A three-dimensional model study of the Mediterranean outflow, Journal of Marine Systems, 24, 41–66, 2000.

Lafuente, J. G., Delgado, J., Vargas, J. M., Vargas, M., Plaza, F., and Sarhan, T.: Low-frequency variability of the exchanged flows through the Strait of Gibraltar during CANIGO, Deep Sea Research Part II: Topical Studies in Oceanography, 49, 4051–4067, 2002.

Levitus, S., Antonov, J., Baranova, O., Boyer, T., Coleman, C., Garcia, H., Grodsky, A., Johnson, D., Locarnini, R., Mishonov, A., et al.: The World Ocean Database, Data Science Journal, 12, WDS229–WDS234, 2013.

Llave, E., Schönfeld, J., Hernández-Molina, F., Mulder, T., Somoza, L., Del Rio, V. D., and Sánchez-Almazo, I.: High-resolution stratigraphy of the Mediterranean outflow contourite system in the Gulf of Cadiz during the late Pleistocene: the impact of Heinrich events, Marine Geology, 227, 241–262, 2006.

Macias, D., García, C. M., Navas, F. E., Vázquez-López-Escobar, A., and Mejías, M. B.: Tidal induced variability of mixing processes on Camarinal Sill (Strait of Gibraltar): A pulsating event, Journal of Marine Systems, 60, 177 – 192, 2006.

Mellor, G. L.: Users guide for a three dimensional, primitive equation, numerical ocean model, Program in Atmospheric and Oceanic Sciences, Princeton University Princeton, NJ 08544-0710, 1998.

Mellor, G. L. and Blumberg, A. F.: Modeling vertical and horizontal diffusivities with the sigma coordinate system, Monthly Weather Review, 113, 1379–1383, 1985.

Mellor, G. L. and Yamada, T.: Development of a turbulence closure model for geophysical fluid problems, Reviews of geophysics and space physics, 20, 851–875, 1982.

Mellor, G. L., Ezer, T., and Oey, L.-Y.: The pressure gradient conundrum of sigma coordinate ocean models, Journal of atmospheric and oceanic technology, 11, 1126–1134, 1994.

Millot, C.: Short-term variability of the Mediterranean in-and outflows, Geophysical Research Letters, 35, 2008.

Millot, C.: Another description of the Mediterranean Sea outflow, Progress in Oceanography, 82, 101–124, 2009.

Millot, C., Candela, J., Fuda, J.-L., and Tber, Y.: Large warming and salinification of the Mediterranean outflow due to changes in its composition, Deep Sea Research Part I: Oceanographic Research Papers, 53, 656–666, 2006.

Nelson, C. H., Baraza, J., and Maldonado, A.: Mediterranean undercurrent sandy contourites, Gulf of Cadiz, Spain, Sedimentary Geology, 82, 103–131, 1993.

Nycander, J. and Döös, K.: Open boundary conditions for barotropic waves, Journal of Geophysical Research: Oceans (1978–2012), 108, 2003.

Price, J. F. and Baringer, M. O.: Outflows and deep water production by marginal seas, Progress in Oceanography, 33, 161–200, 1994.

Price, J. F. and Yang, J.: Marginal sea overflows for climate simulations, in: Ocean Modeling and Parameterization, pp. 155–170,

Springer, 1998.

Pérez, F. F., Ríos, A. F., King, B. A., and Pollard, R. T.: Decadal changes of the S relationship of the Eastern North Atlantic Central Water, Deep Sea Research Part I: Oceanographic Research Papers, 42, 1849 – 1864, http://www.sciencedirect.com/science/article/pii/0967063795000917, 1995.

Rahmstorf, S.: Influence of Mediterranean outflow on climate, Eos, Transactions American Geophysical Union, 79, 281–282, 1998.

Reid, J. L.: On the contribution of the Mediterranean Sea outflow to the Norwegian-Greenland Sea, Deep Sea Research Part A. Oceanographic Research Papers, 26, 1199–1223, 1979.

Rogerson, M., Rohling, E., Weaver, P., and Murray, J.: The azores front since the last glacial maximum, Earth and Planetary Science Letters, 222, 779–789, 2004.

Rogerson, M., Rohling, E., Weaver, P., and Murray, J.: Glacial to interglacial changes in the settling depth of the Mediterranean Outflow plume, Paleoceanography, 20, 2005.

Rogerson, M., Rohling, E., and Weaver, P.: Promotion of meridional overturning by Mediterranean-derived salt during the last deglaciation, Paleoceanography, 21, 2006.

Rogerson, M., Colmenero-Hidalgo, E., Levine, R., Rohling, E., Voelker, A., Bigg, G., Schönfeld, J., Cacho, I., Sierro, F., Löwemark, L., et al.: Enhanced Mediterranean-Atlantic exchange during Atlantic freshening phases, Geochemistry, Geophysics, Geosystems, 11, 2010.

Rogerson, M., Rohling, E., Bigg, G., and Ramirez, J.: Paleoceanography of the Atlantic-Mediterranean exchange: Overview and first quantitative assessment of climatic forcing, Reviews of Geophysics, 50, 2012.

Roveri, M., Flecker, R., Krijgsman, W., Lofi, J., Lugli, S., Manzi, V., Sierro, F. J., Bertini, A., Camerlenghi, A., De Lange, G., et al.: The Messinian Salinity Crisis: past and future of a great challenge for marine sciences, Marine Geology, 352, 25–58, 2014.

Sannino, G., Bargagli, A., and Artale, V.: Numerical modeling of the mean exchange through the Strait of Gibraltar, Journal of Geophysical Research: Oceans (1978–2012), 107, 9–1, 2002.

Soto-Navarro, J., Criado-Aldeanueva, F., García-Lafuente, J., and Sánchez-Román, A.: Estimation of the Atlantic inflow through the Strait of Gibraltar from climatological and in situ data, Journal of Geophysical Research: Oceans (1978–2012), 115, 2010.

Thorpe, R. and Bigg, G.: Modelling the sensitivity of Mediterranean Outflow to anthropogenically forced climate change, Climate dynamics, 16, 355–368, 2000.

Topper, R. and Meijer, P.: A high resolution ocean model of restriction of the Mediterranean-Atlantic connection: Changes in Mediterranean circulation and water characteristics, in: EGU General Assembly Conference Abstracts, vol. 16, p. 11148, 2014.

Toucanne, S., Mulder, T., Schönfeld, J., Hanquiez, V., Gonthier, E., Duprat, J., Cremer, M., and Zaragosi, S.: Contourites of the Gulf of Cadiz: a high-resolution record of the paleocirculation of the Mediterranean outflow water during the last 50,000 years, Palaeogeography, Palaeoclimatology, Palaeoecology, 246, 354–366, 2007.

Tsimplis, M. and Bryden, H.: Estimation of the transports through the Strait of Gibraltar, Deep Sea Research Part I: Oceanographic Research Papers, 47, 2219–2242, 2000.

Voelker, A. H., Lebreiro, S., Schönfeld, J., Cacho, I., Erlenkeuser, H., and Abrantes, F.: Mediterranean outflow strengthening during northern hemisphere coolings: a salt source for the glacial Atlantic?, Earth and Planetary Science Letters, 245, 39–55, 2006.

Zavatarelli, M. and Mellor, G. L.: A numerical study of the Mediterranean Sea circulation, Journal of Physical Oceanography, 25, 1384–1414, 1995.

Appendix overview

- Appendix A: Initial stratification experiment results
- Appendix B: Slope factor experiment results
- Appendix C: Sealevel experiment results
- Appendix D: Source water experiment results
- Appendix E: MOW entrance velocity experiment results

Appendix A

Experiment Results: Initial stratification

- Figure A1: Evolution of initial stratification with the World Ocean Atlas data.
- Figure A2: Evolution of initial stratification with the MOW footprint removed from the World Ocean Atlas data.
- Figure A3: Evolution of initial stratification with an uniform salinity of 35 psu.
- Figure A4: Salinity map at a depth of 100m.
- Figure A5: Salinity map at a depth of 600m.
- Figure A6: Salinity map at a depth of 1200m.
- Figure A7: Salinity map at the bottom sigma-layer.
- Figure A8: Salinity profile N-S at 6°15'W.
- Figure A9: Salinity profile N-S at 8°20'W.
- Figure A10: Salinity profile W-E at 35°50'N.
- Figure A11: Graph of evolution of kinetic energy.
- Figure A12: Graph of evolution of sealevel.
- Figure A13: Graph of evolution of salinity.
- Figure A14: Graph of evolution of temperature.

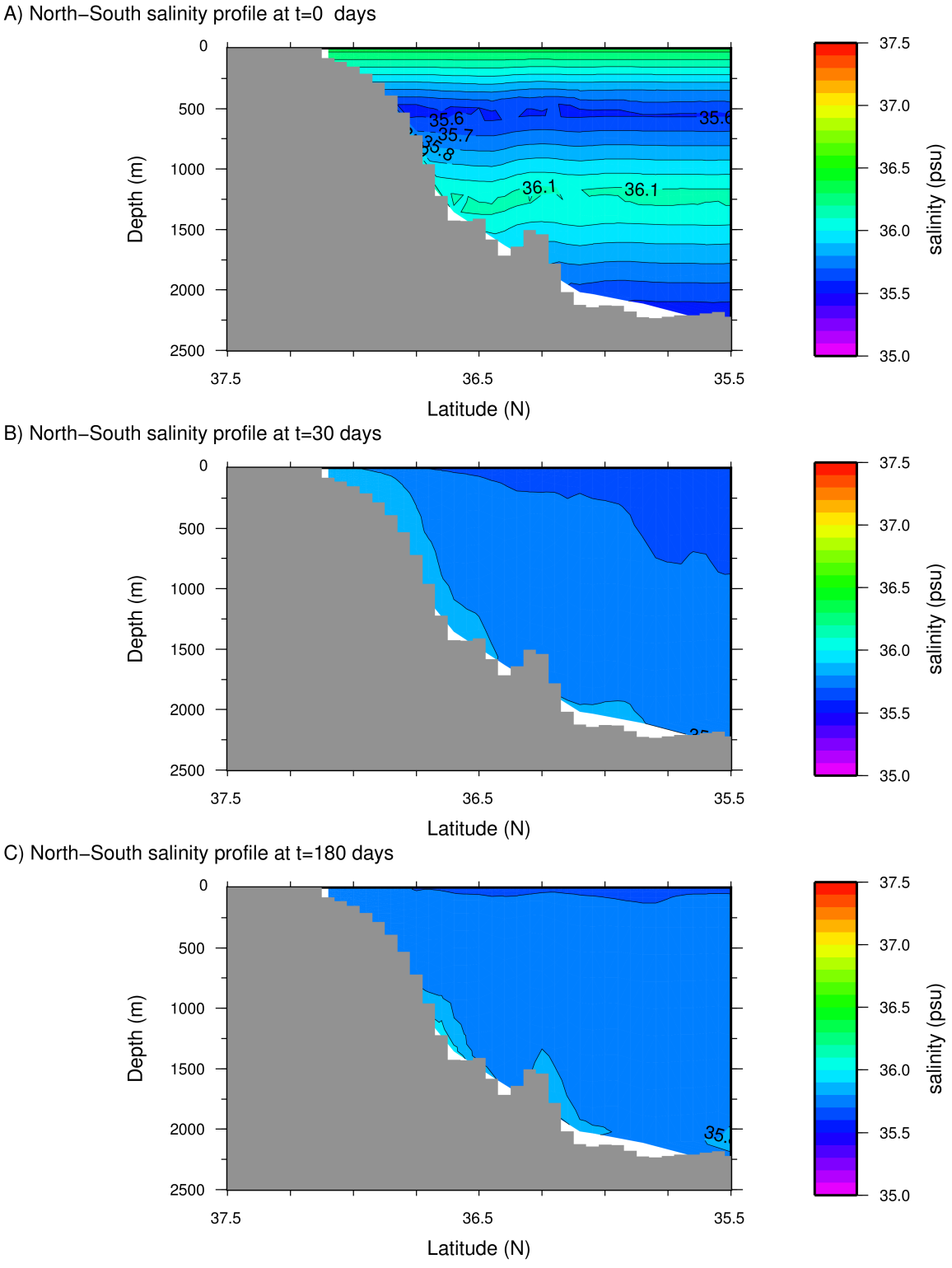

Fig. A1. Evolution of north-south profiles at the start of the experiment taken at 8°20'W. The initial salinity stratification profile shown here is based on the World Ocean Atlas data and is the initial profile used in the reference experiment. A) North-south profile at time=0 days B) North-south profile at time=30 days C) North-south profile at time=60 days. Profiles taken at t=20 years.

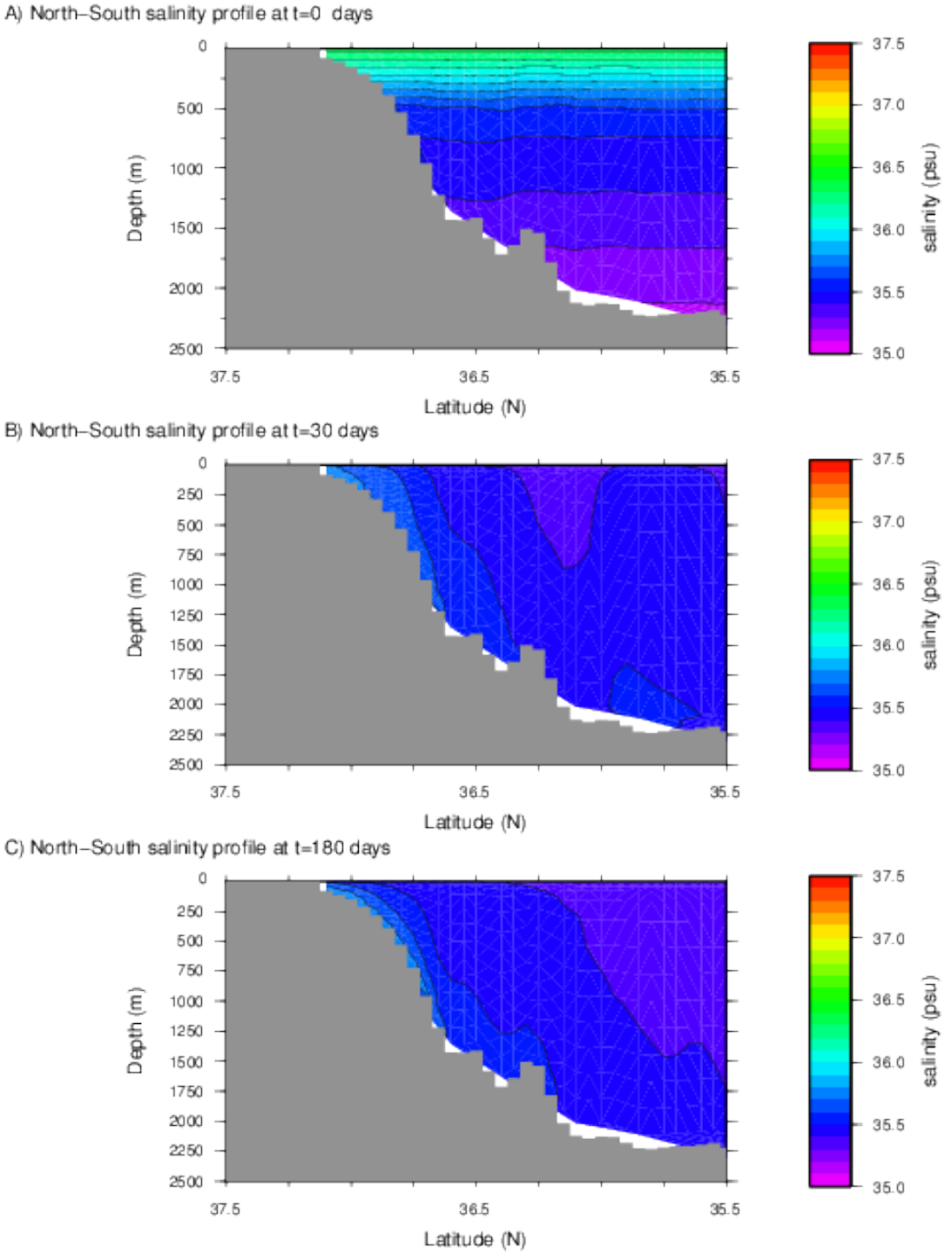

Fig. A2. Evolution of north-south profiles at the start of the experiment taken at 8°20'W. The initial salinity stratification profile shown here is based on the World Ocean Atlas data but with the footprint of the MOW removed. A) North-south profile at time=0 days B) North-south profile at time=30 days C) North-south profile at time=180 days. Profiles taken at t=20 years.

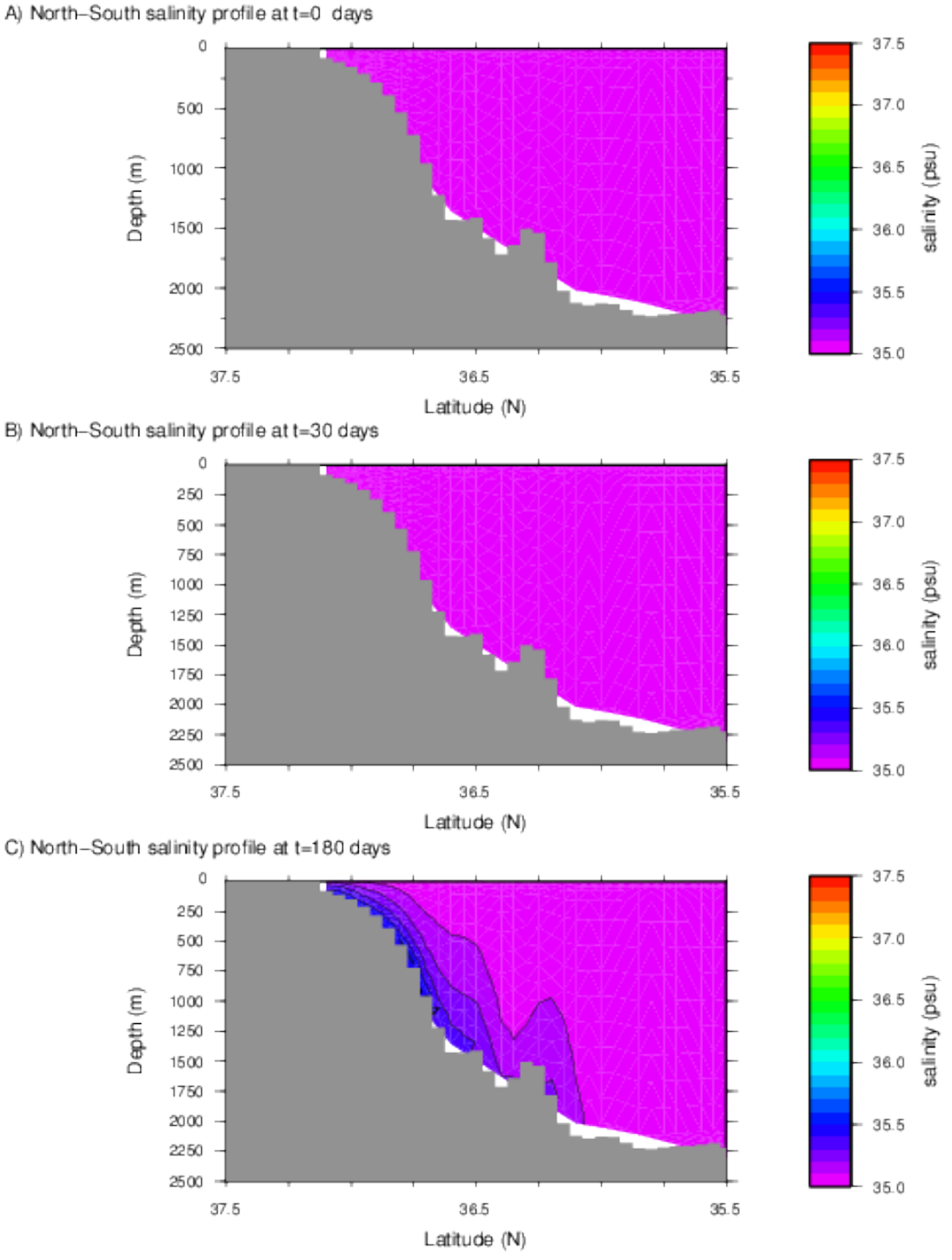

Fig. A3. Evolution of north-south profiles at the start of the experiment taken at 8°20'W. The initial salinity stratification profile shown here is an uniform stratification of 35 psu. A) North-south profile at time=0 days B) North-south profile at time=30 days C) North-south profile at time=180 days. Profiles taken at t=20 years.

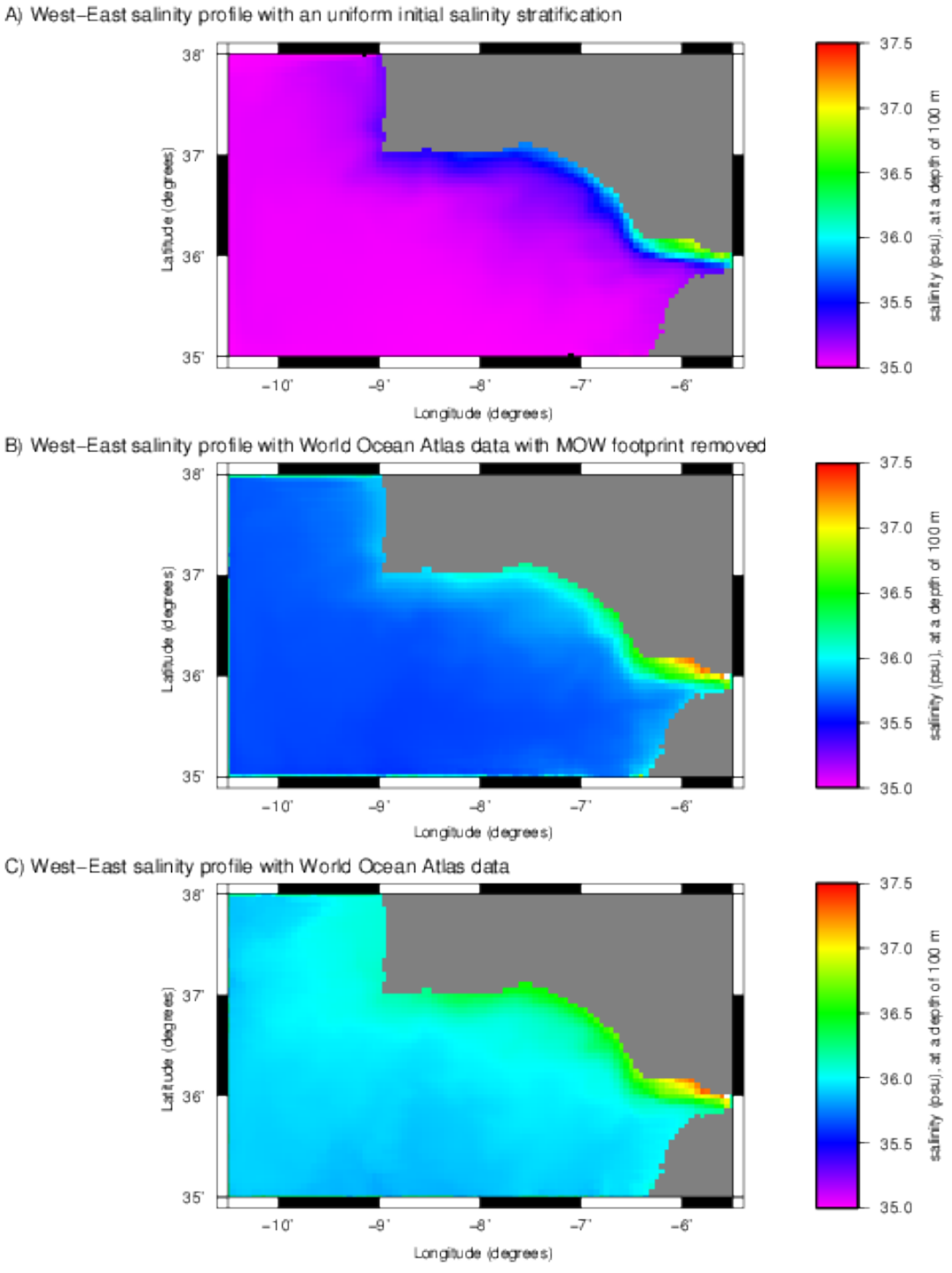

Fig. A4. Salinity maps at a depth of 100m. A) Uniform stratification of 35 psu. B) World Ocean Atlas stratification without MOW footprint. C) World Ocean Atlas data (reference experiment). Maps taken at t=20 years.

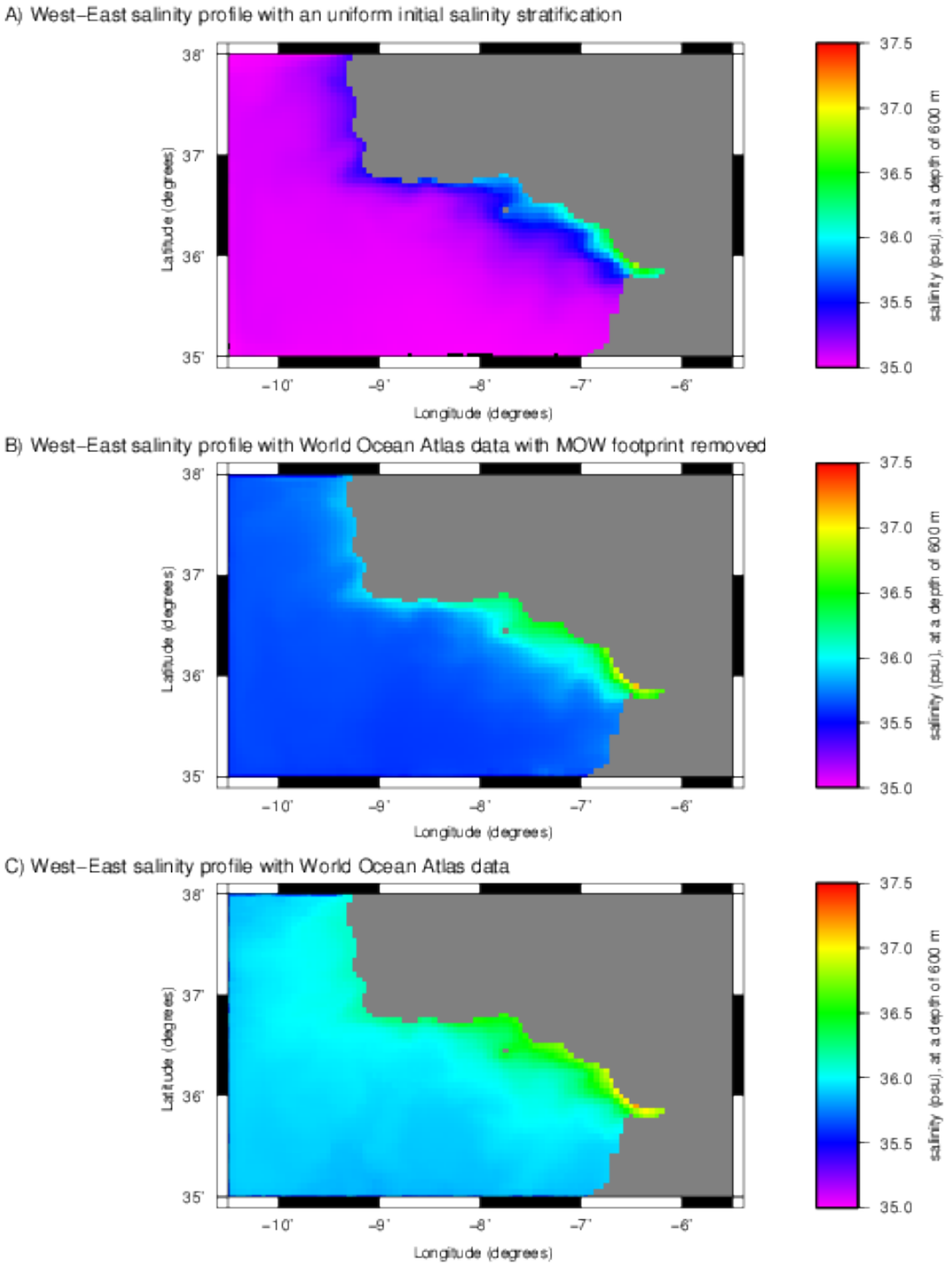

Fig. A5. Salinity maps at a depth of 600m. A) Uniform stratification of 35 psu. B) World Ocean Atlas stratification without MOW footprint. C) World Ocean Atlas data (reference experiment). Maps taken at t=20 years.

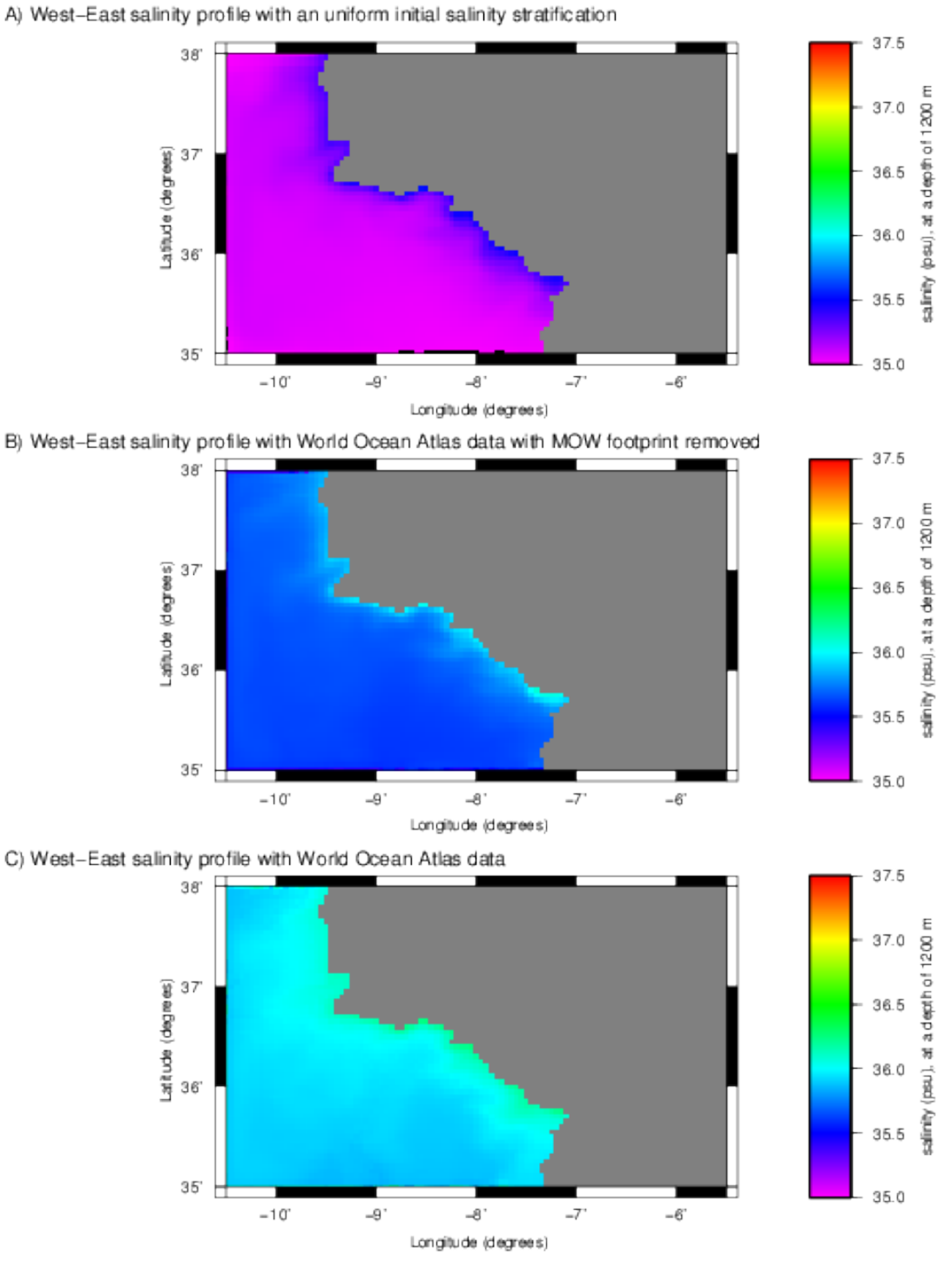

Fig. A6. Salinity maps at a depth of 1200m. A) Uniform stratification of 35 psu. B) World Ocean Atlas stratification without MOW footprint. C) World Ocean Atlas data (reference experiment). Maps taken at t=20 years.

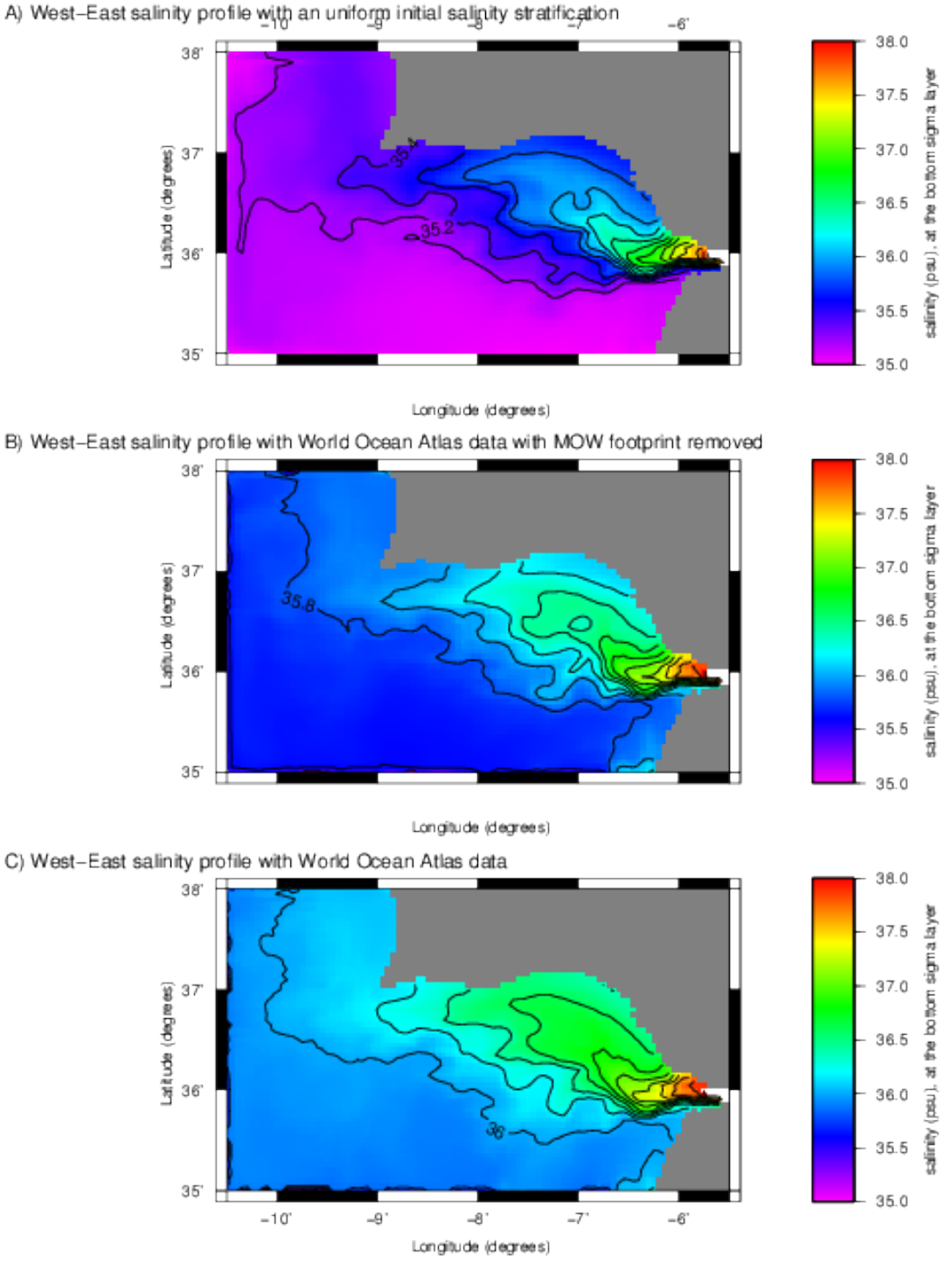

Fig. A7. Salinity map of the bottom sigma-layer in the reference experiment. Map taken at t=20 years.

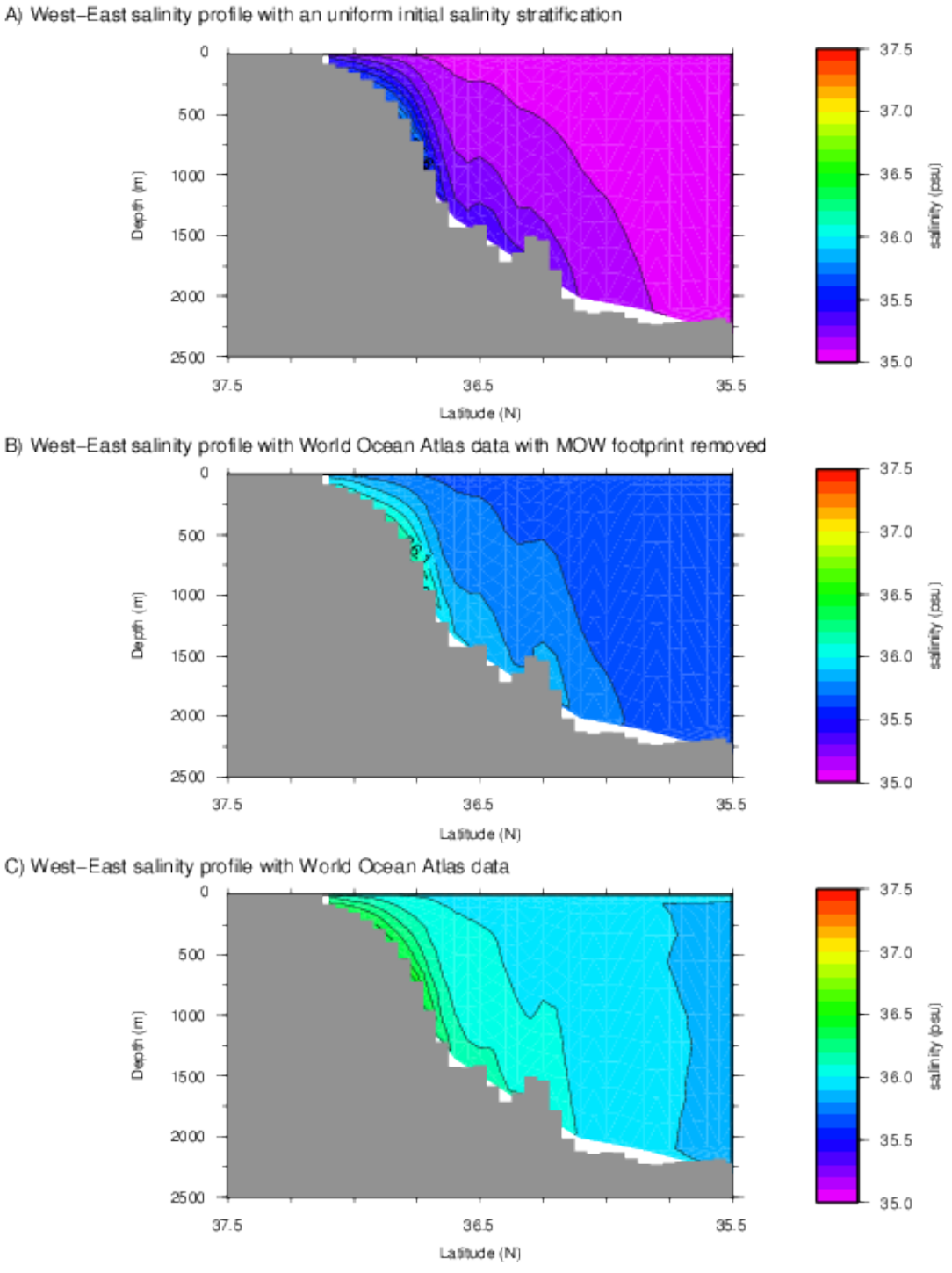

Fig. A8. North-South salinity profiles taken at 6°N 15'W. A) Uniform stratification of 35 psu. B) World Ocean Atlas stratification without MOW footprint. C) World Ocean Atlas data (reference experiment). Profiles taken at t=20 years.

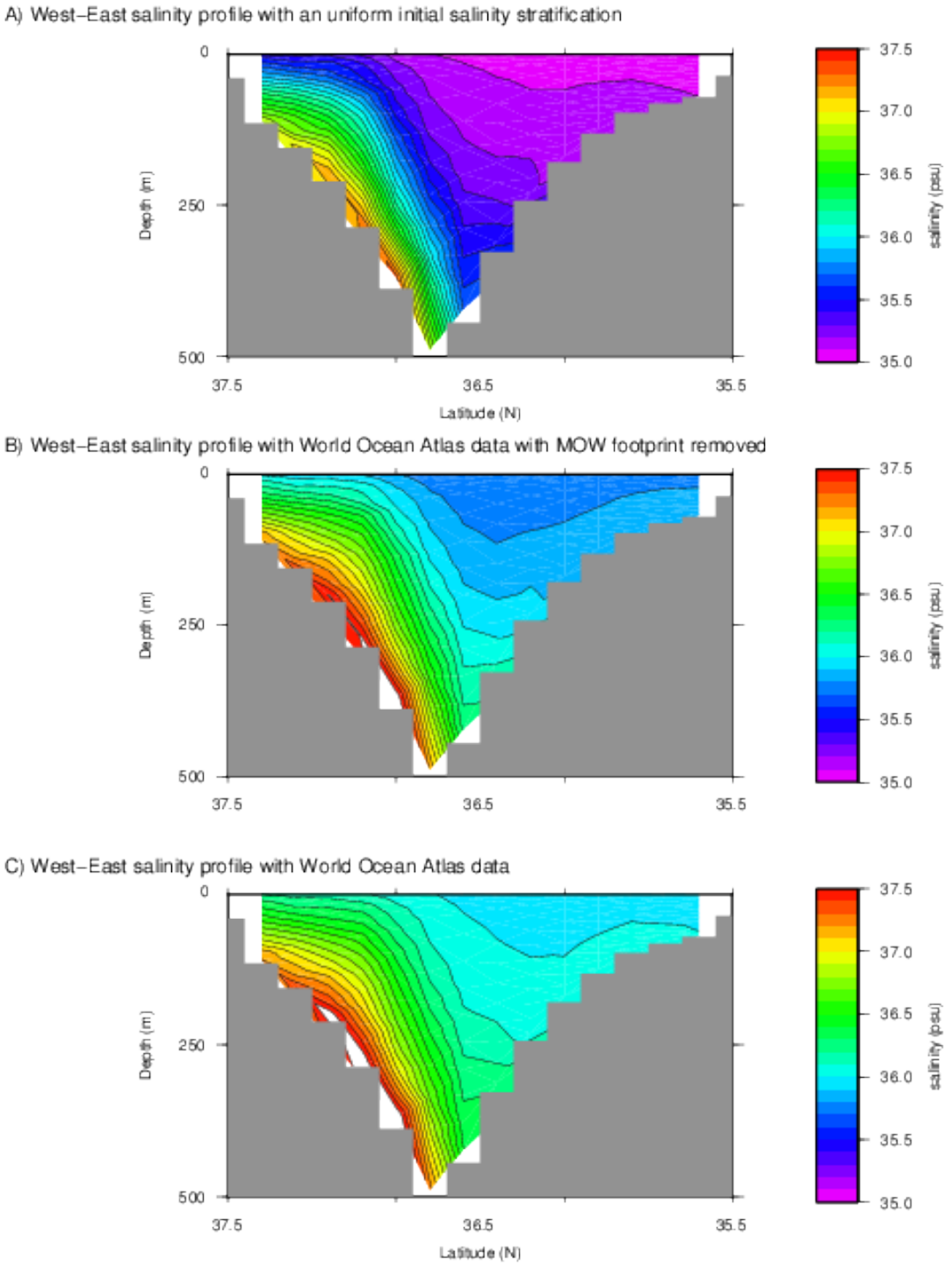

Fig. A9. North-South salinity profiles taken at 8°N 20'W. A) Uniform stratification of 35 psu. B) World Ocean Atlas stratification without MOW footprint. C) World Ocean Atlas data (reference experiment). Profiles taken at t=20 years.

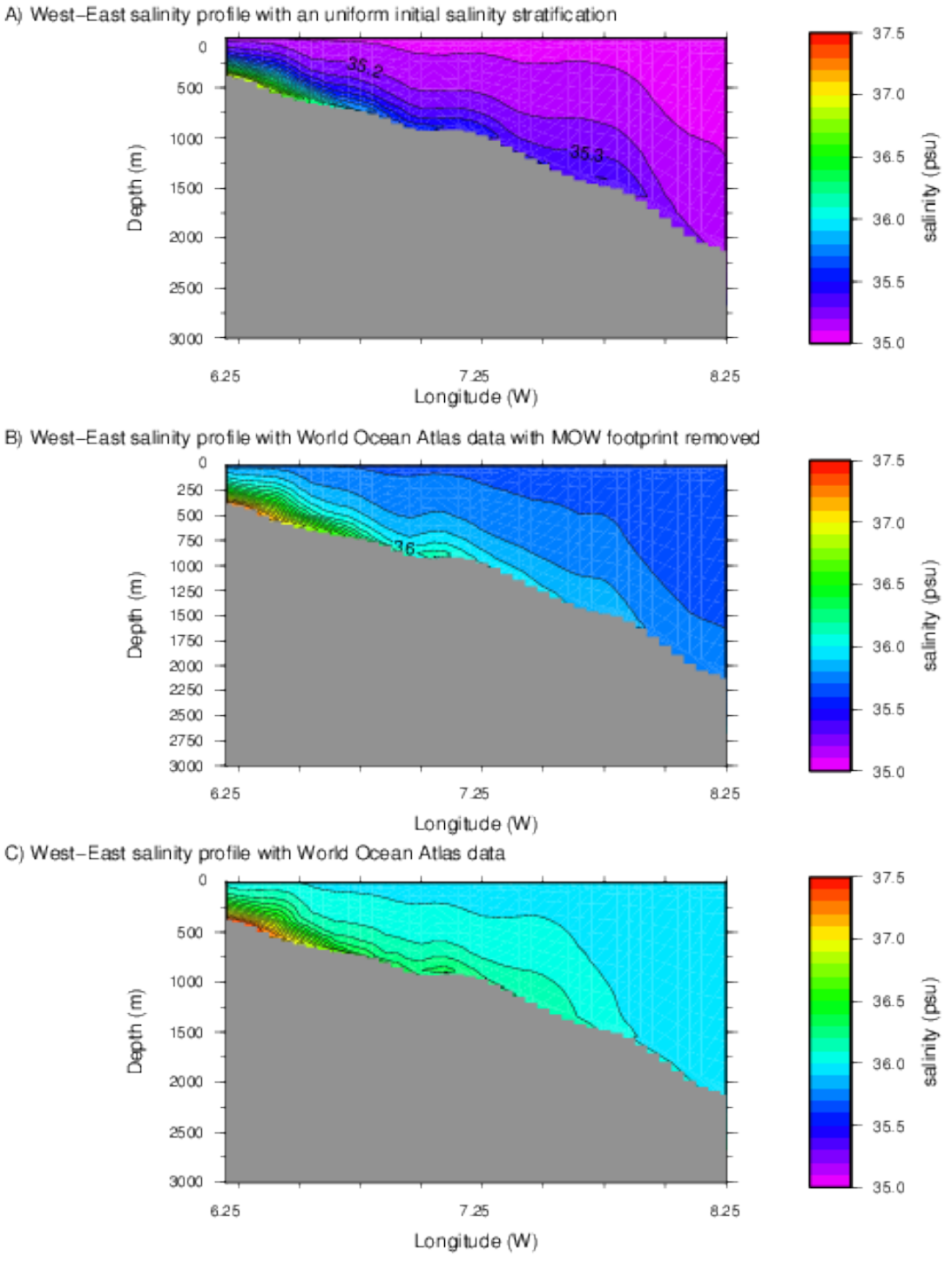

Fig. A10. West-East salinity profiles taken at 35°50'N. A) Uniform stratification of 35 psu. B) World Ocean Atlas stratification without MOW footprint. C) World Ocean Atlas data (reference experiment). Profiles taken at t=20 years.

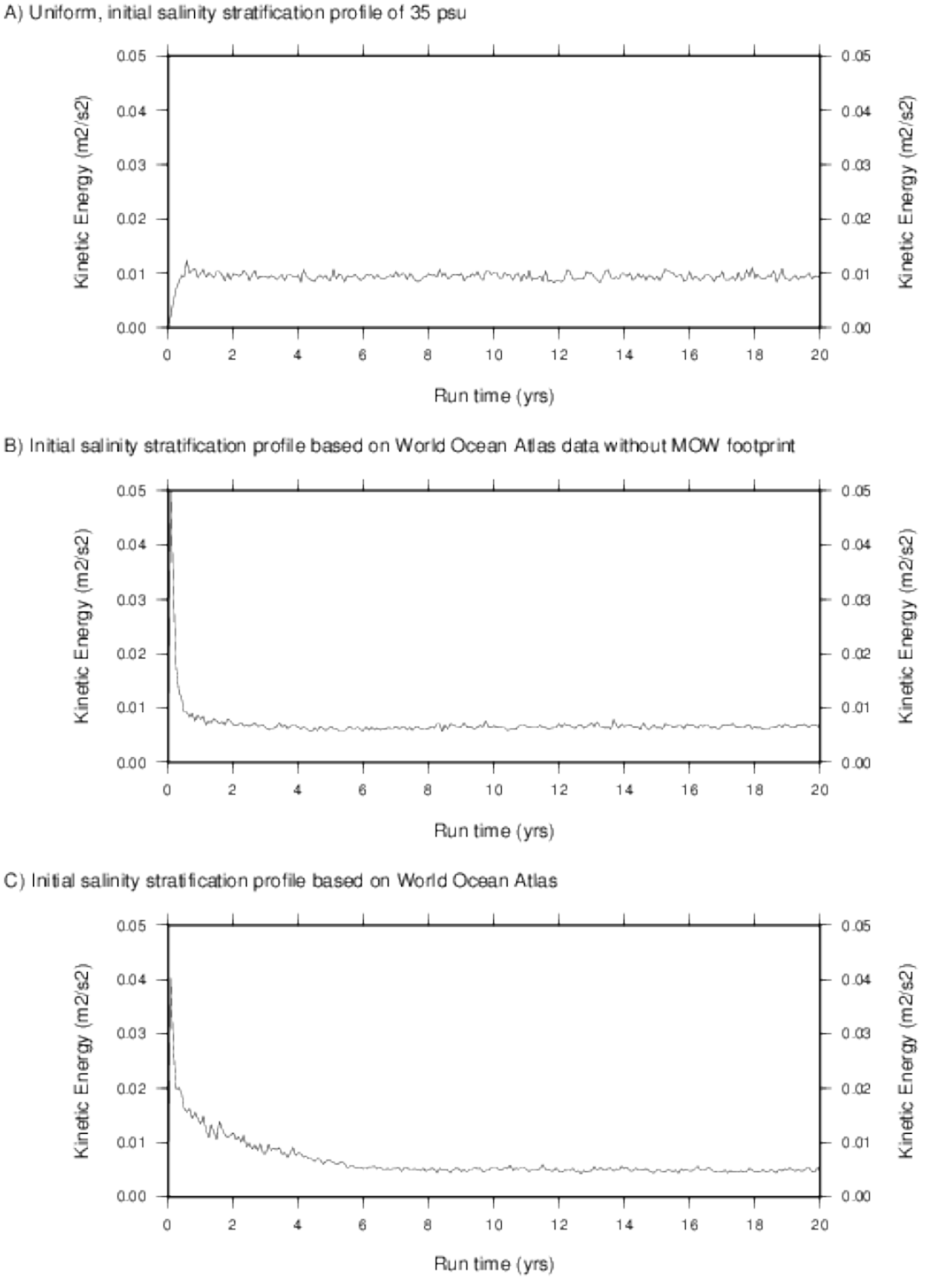

Fig. A11. Evolution of kinetic energy throughout the runs. A) Uniform stratification of 35 psu. B) World Ocean Atlas stratification without MOW footprint. C) World Ocean Atlas data (reference experiment). Profiles taken at t=20 years.

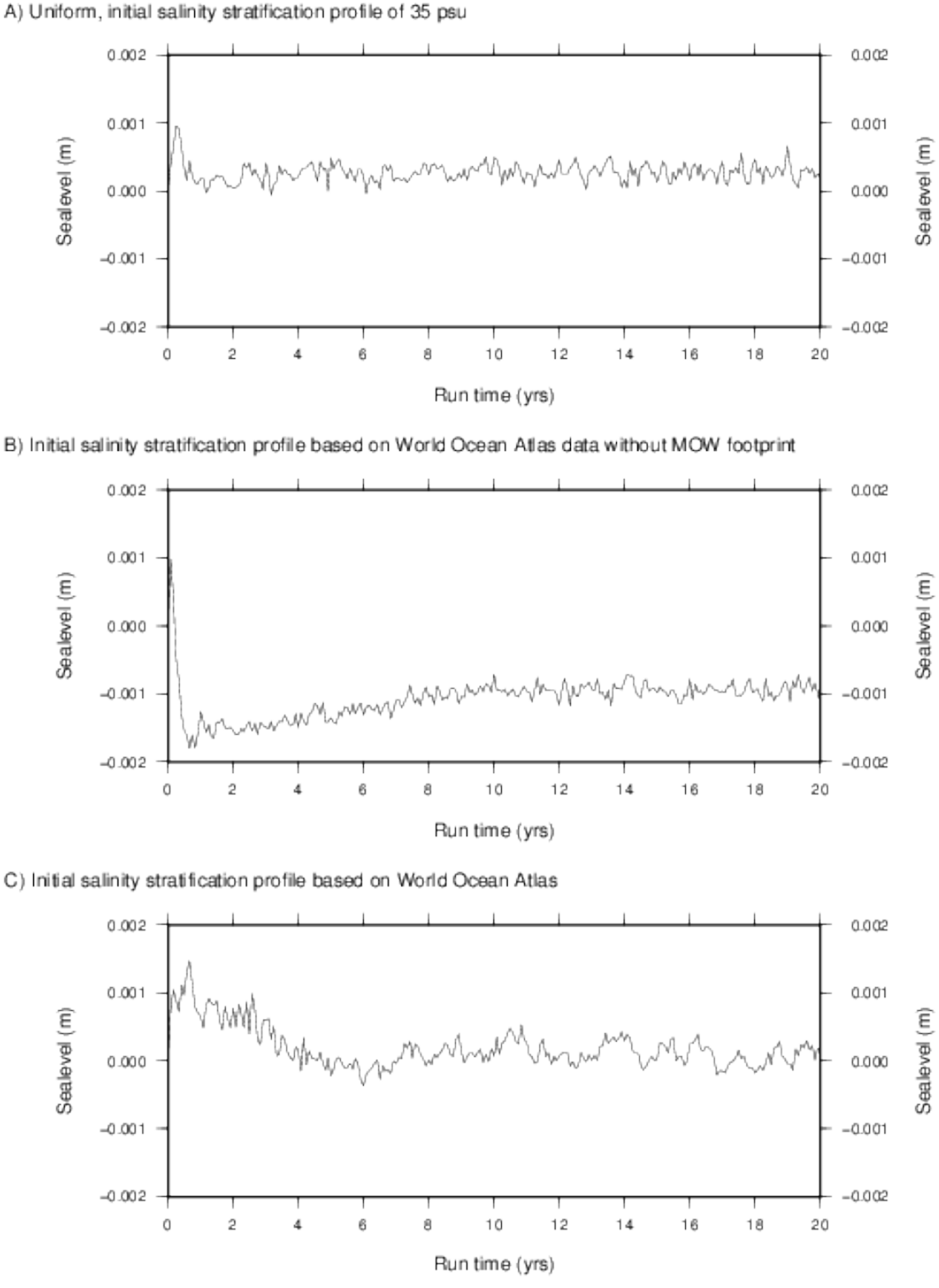

Fig. A12. Evolution of sealevel throughout the runs. A) Uniform stratification of 35 psu. B) World Ocean Atlas stratification without MOW footprint. C) World Ocean Atlas data (reference experiment). Profiles taken at t=20 years.

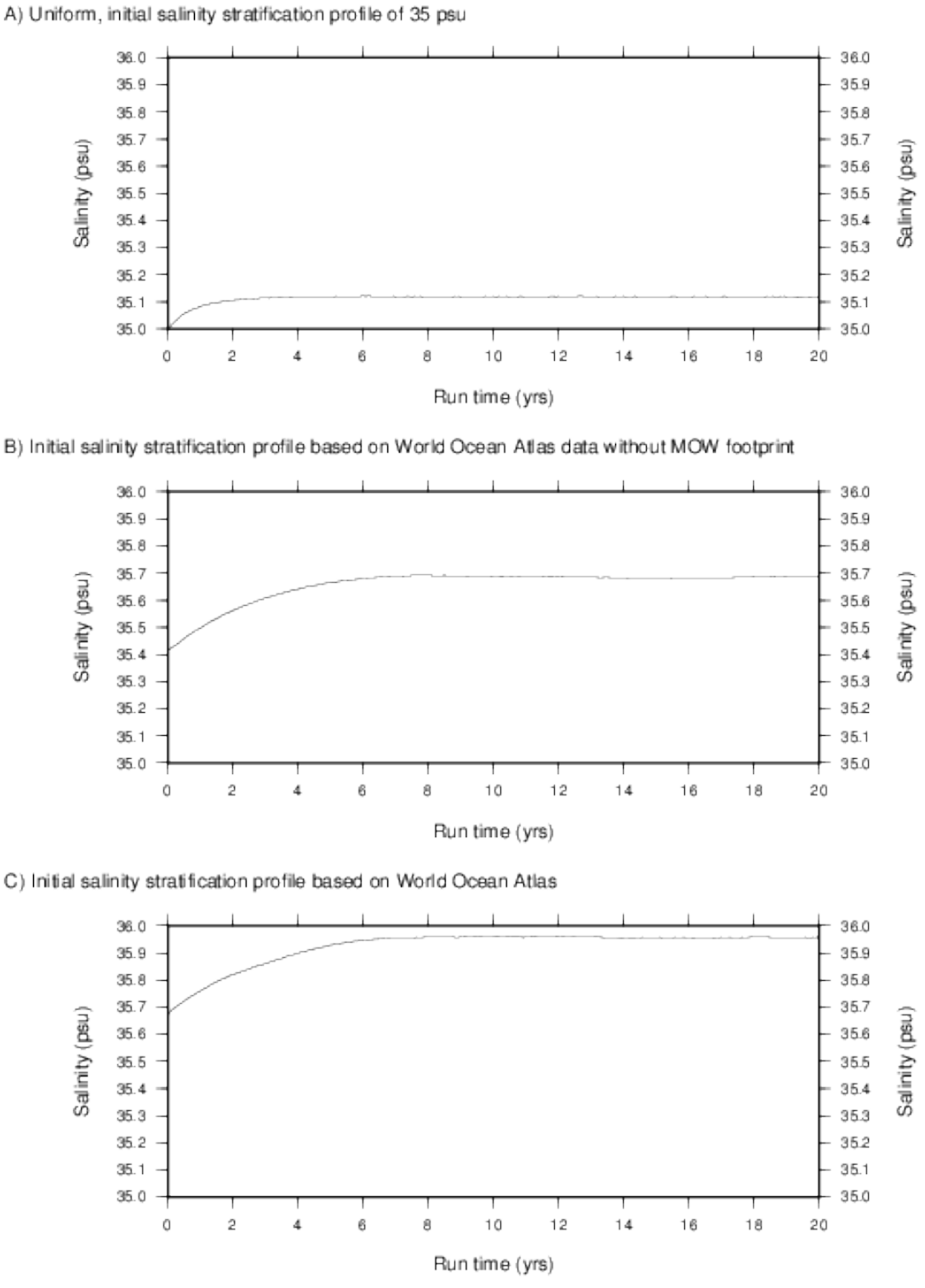

Fig. A13. Evolution of salinity throughout the runs. A) Uniform stratification of 35 psu. B) World Ocean Atlas stratification without MOW footprint. C) World Ocean Atlas data (reference experiment). Profiles taken at t=20 years.

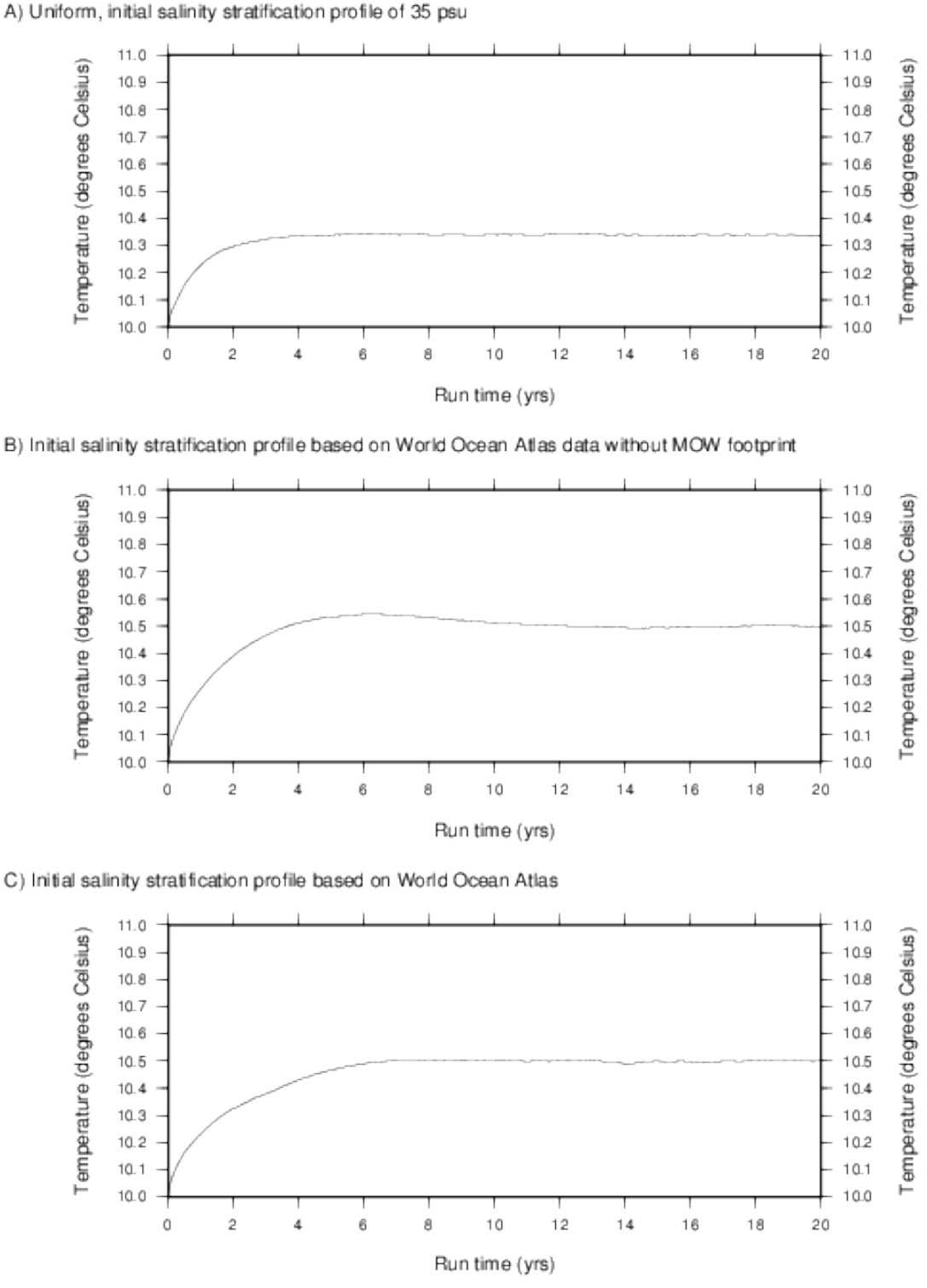

Fig. A14. Evolution of temperature throughout the runs. A) Uniform stratification of 35 psu. B) World Ocean Atlas stratification without MOW footprint. C) World Ocean Atlas data (reference experiment). Profiles taken at t=20 years.

Appendix B

Experiment Results: Slope factor

- Figure B1 Bathymetry.
- Figure B2: Salinity at a depth of 100m.
- Figure B3: Salinity at a depth of 600m.
- Figure B4: Salinity at a depth of 1200m.
- Figure B5: Salinity at the bottom sigma-layer.
- Figure B6: Salinity profile N-S at 6°15'W.
- Figure B7: Salinity profile N-S at 8°20'W.
- Figure B8: Salinity profile E-W at 35°50'N.
- Figure B9: Graph of evolution of kinetic energy.
- Figure B10: Graph of evolution of sealevel.
- Figure B11: Graph of evolution of salinity.
- Figure B12: Graph of evolution of temperature.

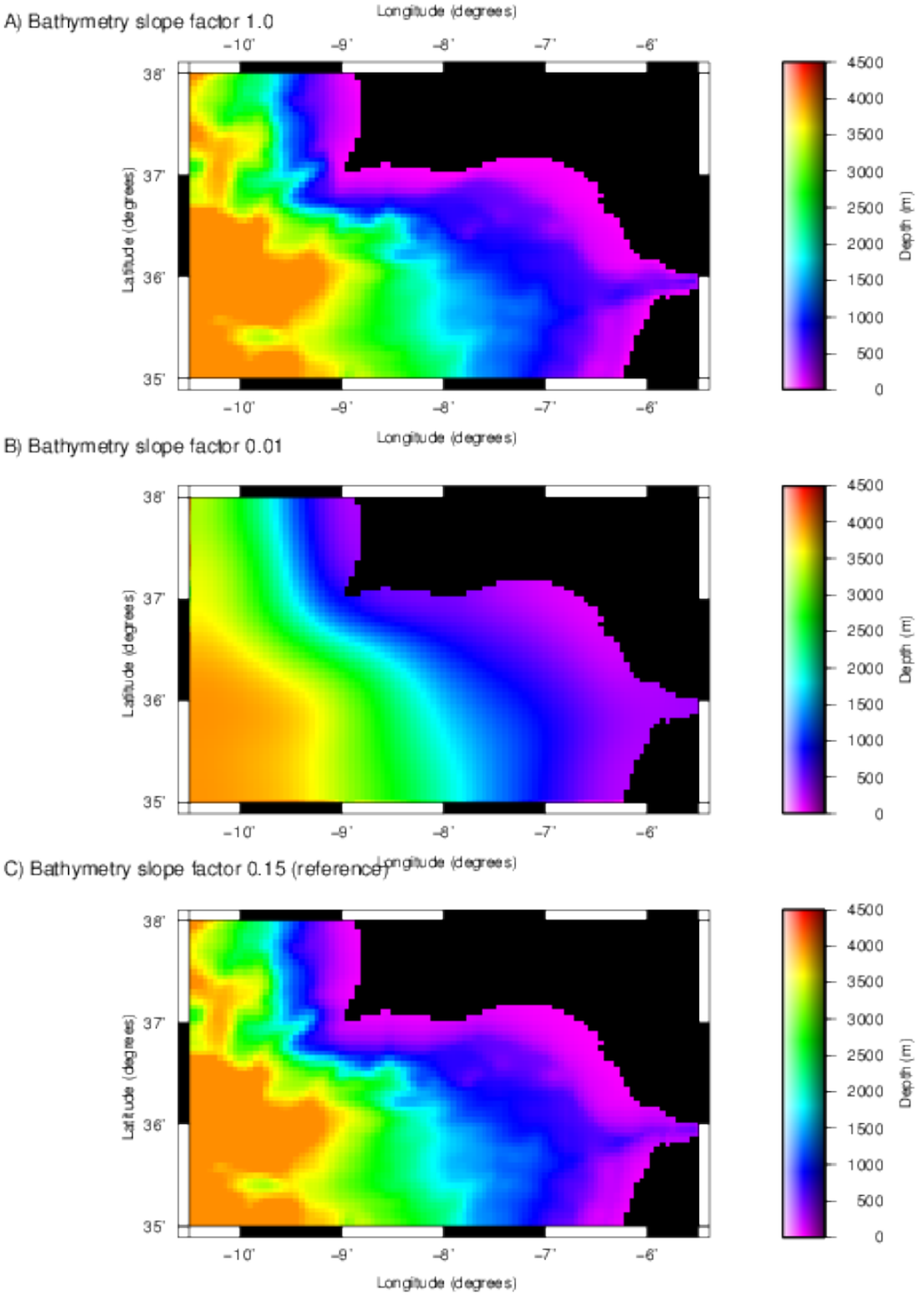

Fig. B1. Bathymetry obtained by using the different slope factors.

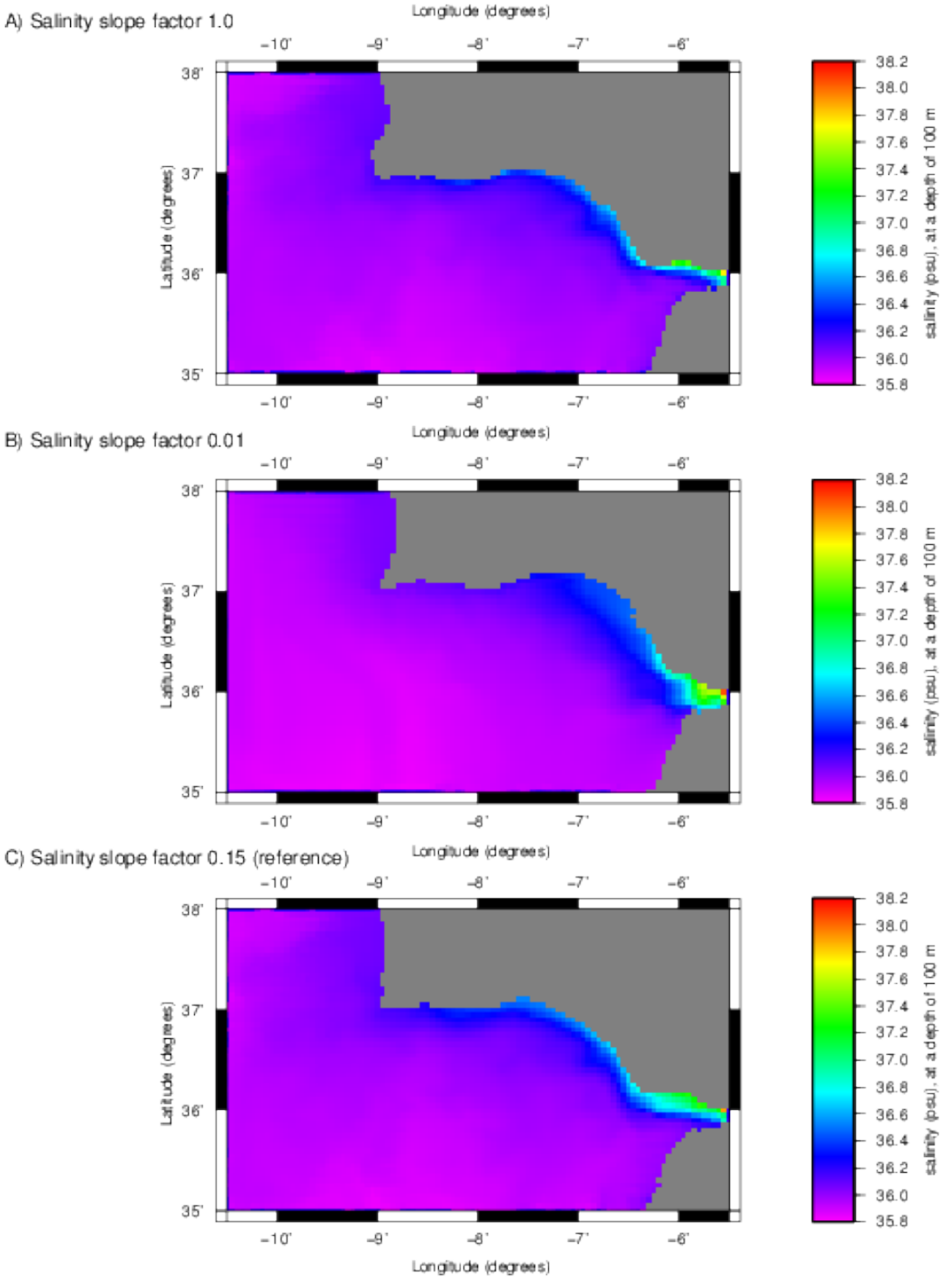

Fig. B2. Salinities at a depth of 100m. Maps taken at t=20 years.

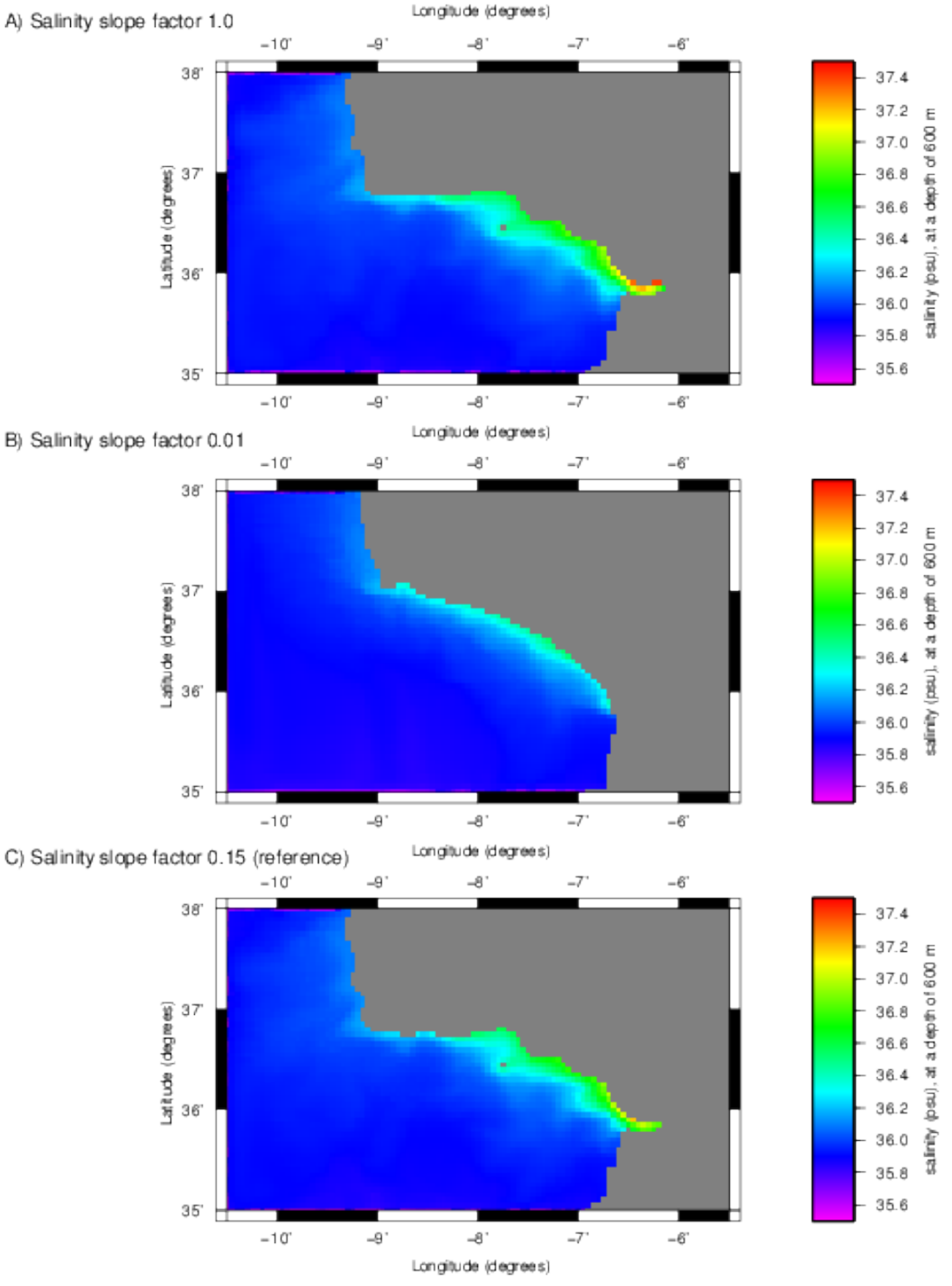

Fig. B3. Salinities at a depth of 600m. Maps taken at t=20 years.

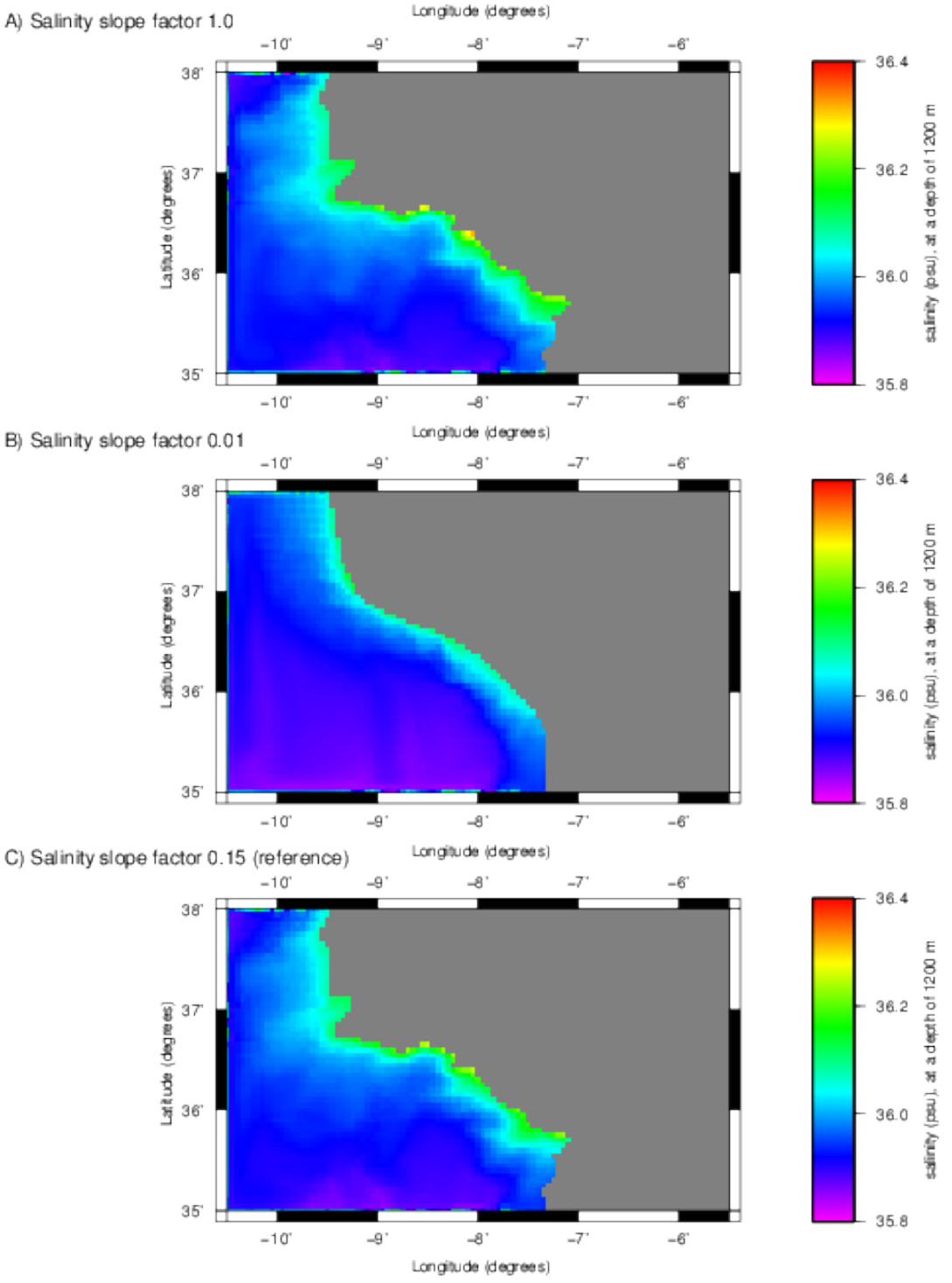

Fig. B4. Salinities at a depth of 1200m. Maps taken at t=20 years.

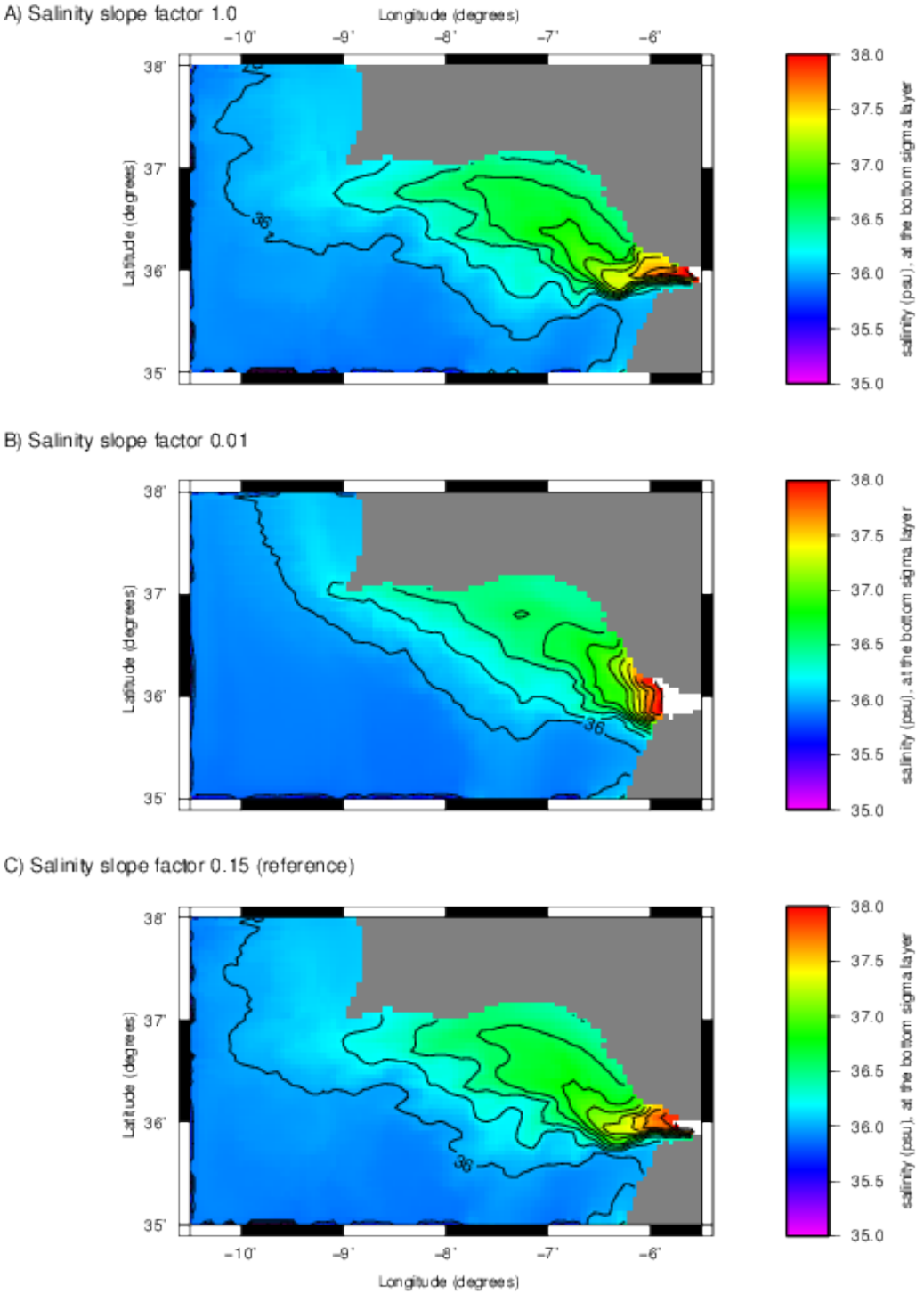

Fig. B5. Salinities at the bottom sigma-layer. Maps taken at t=20 years.

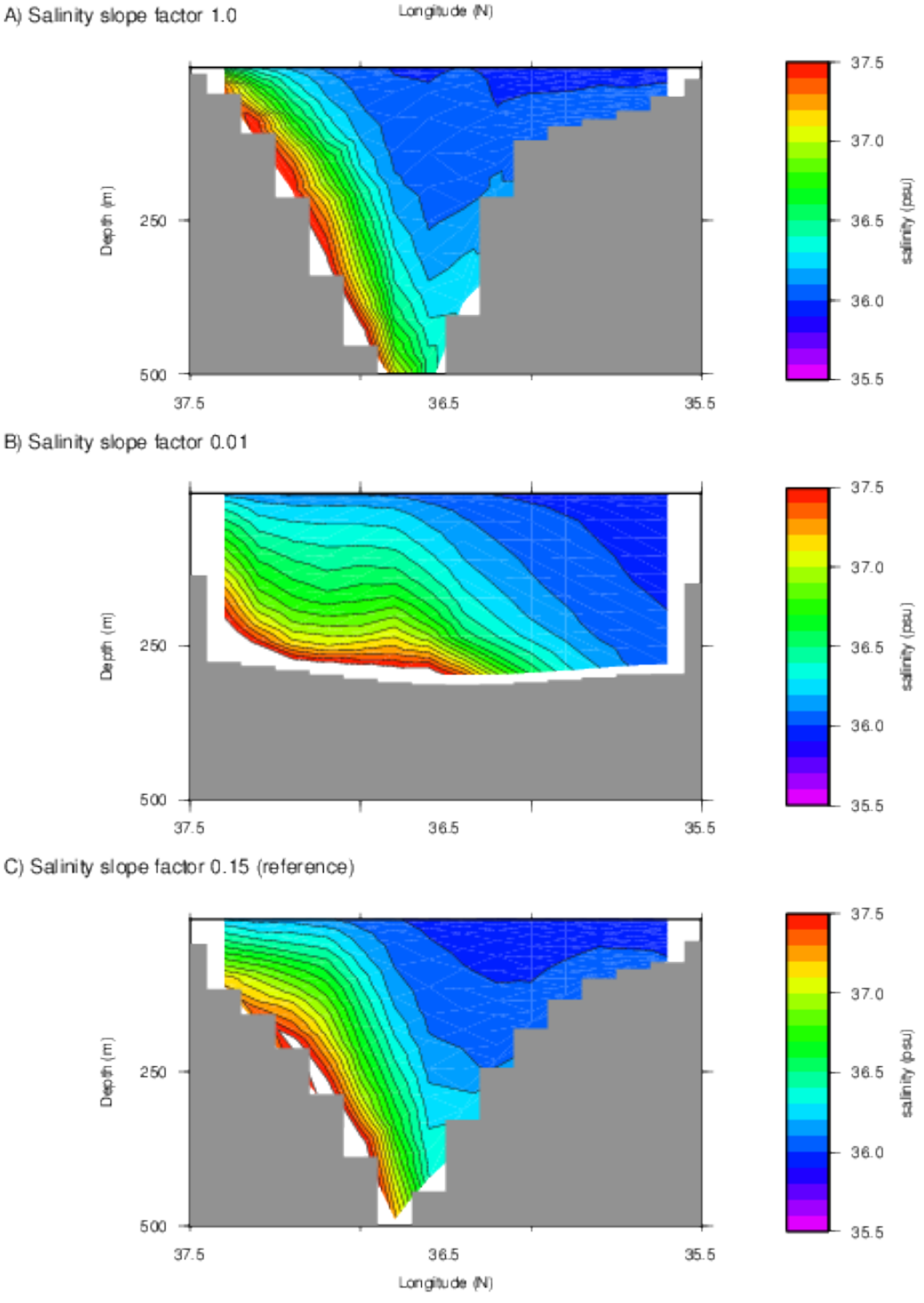

Fig. B6. A north to south salinity profile at 6°15'W. Profiles taken at t=20 years.

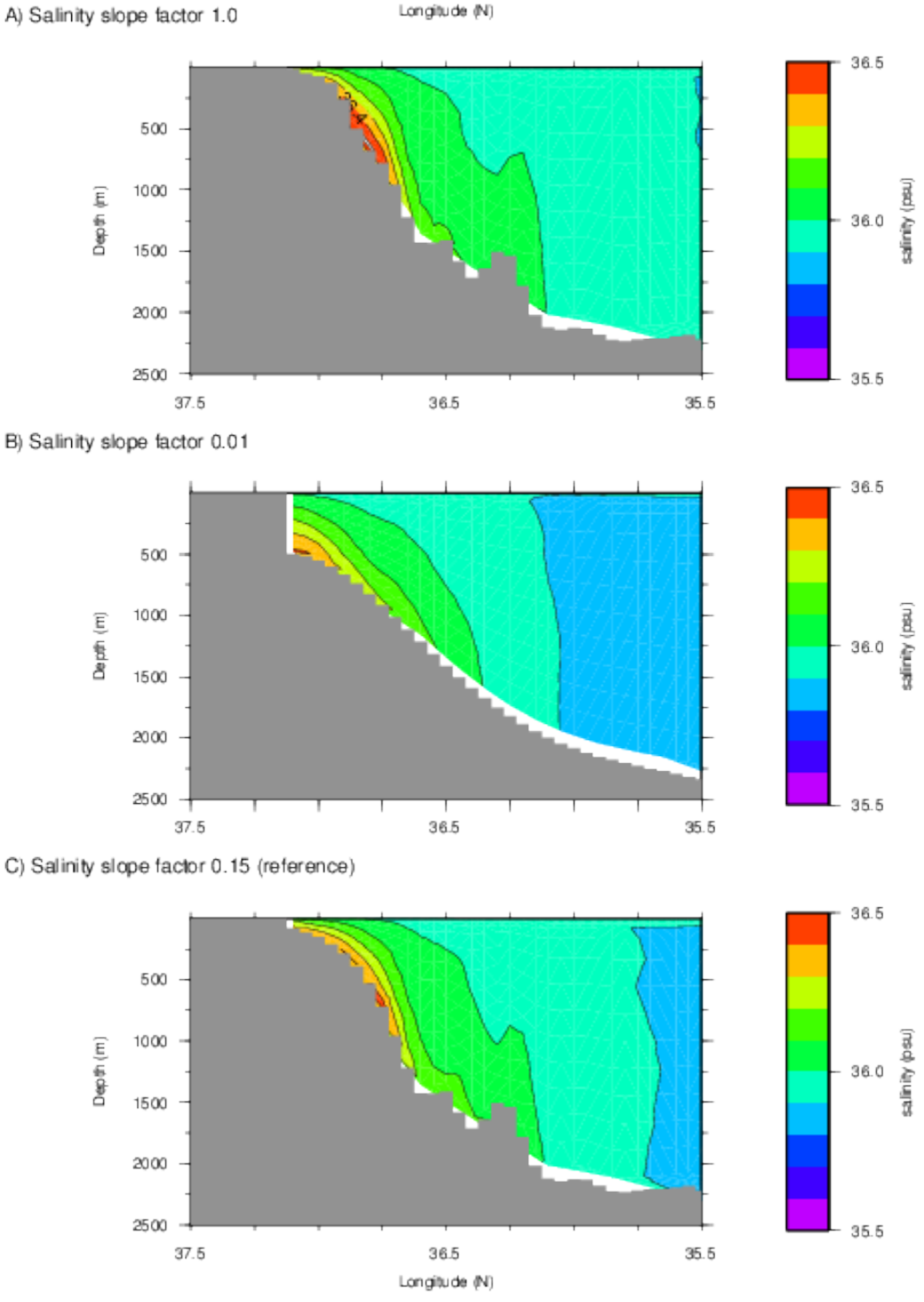

Fig. B7. A north to south salinity profile at 8°20'W. Profiles taken at t=20 years.

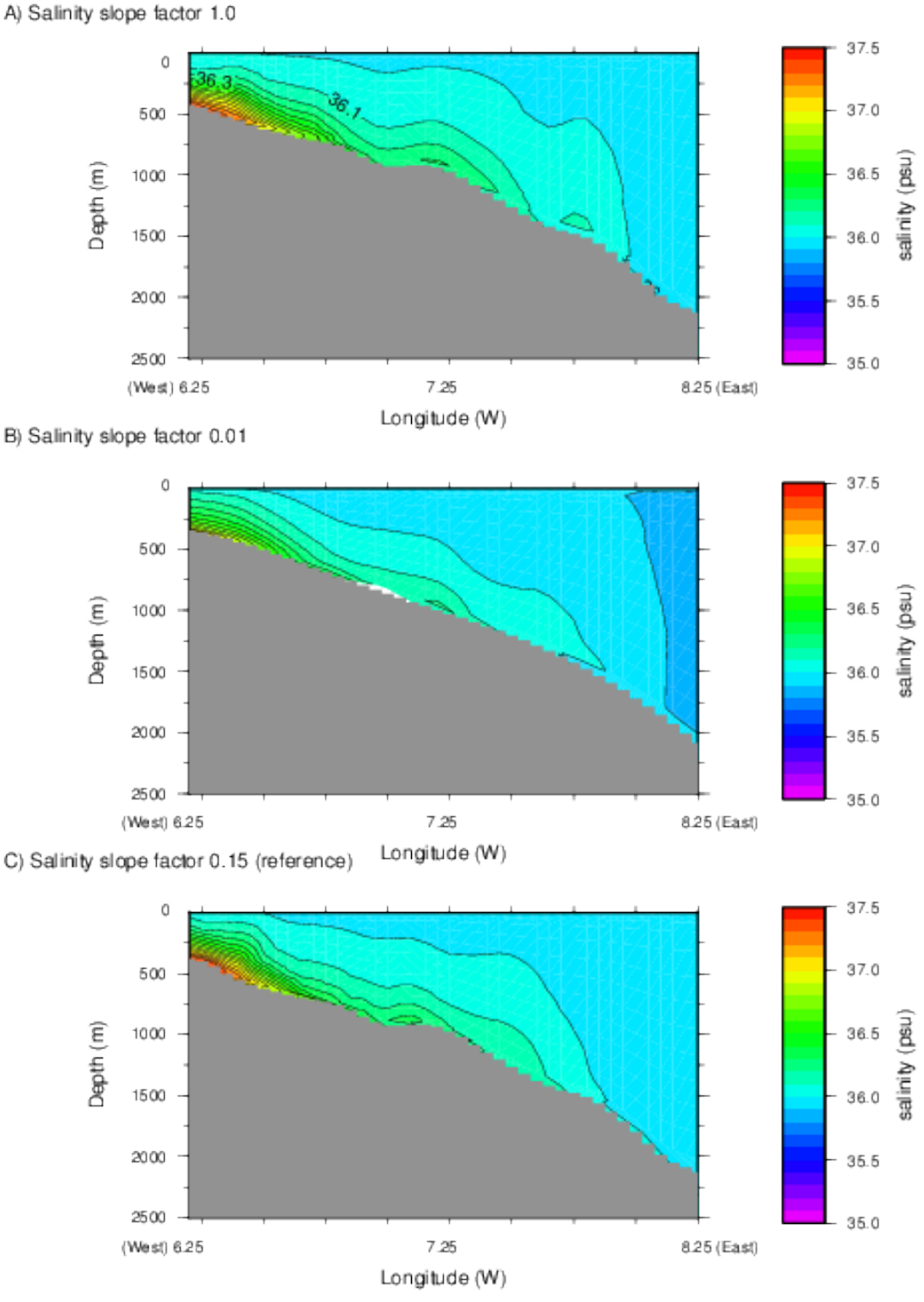

Fig. B8. An east to west salinity profile at 35°50'N, note that east is in the left of the profile. Profiles taken at t=20 years.

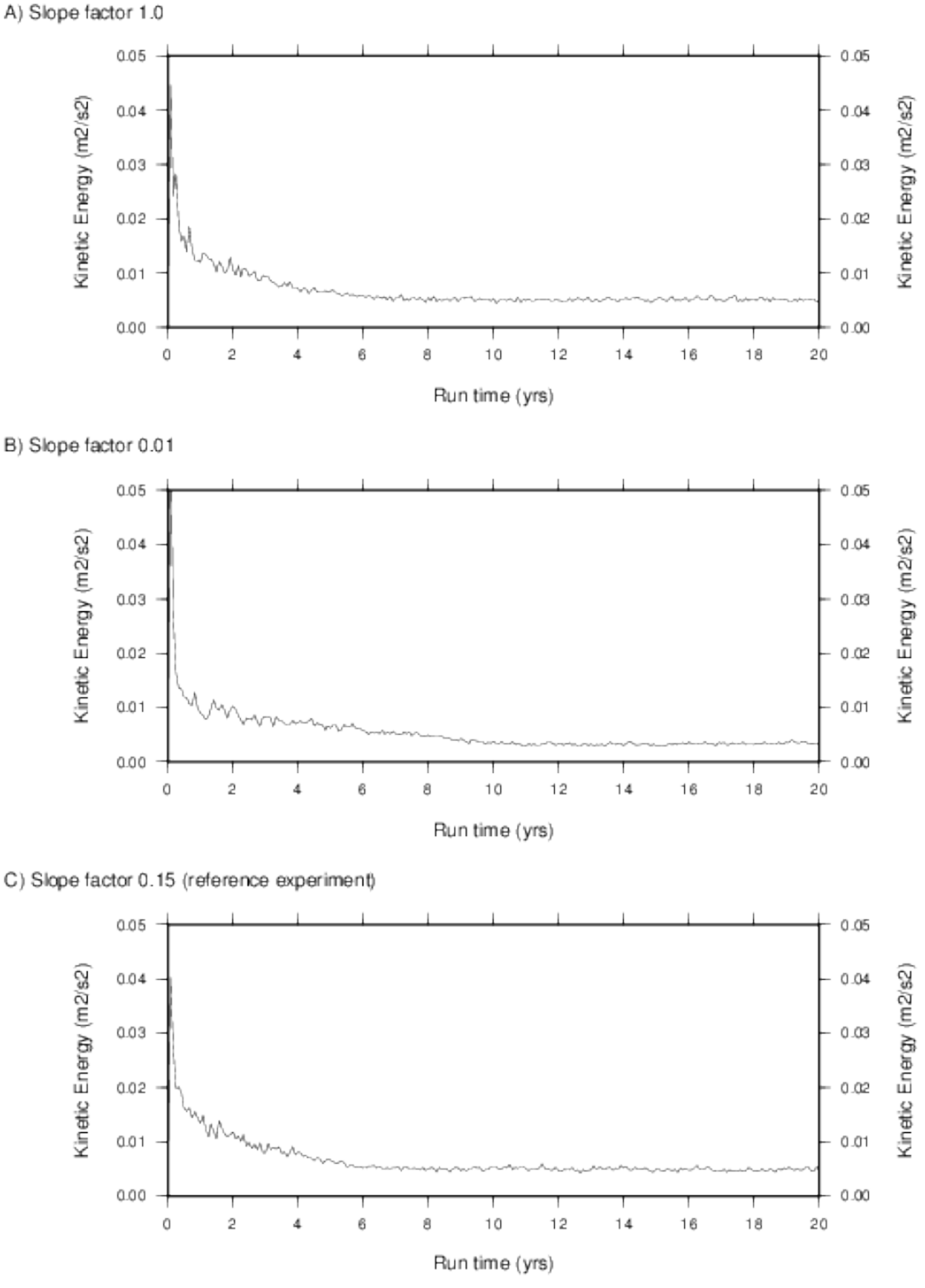

Fig. B9. Evolution of kinetic energy throughout the runs.

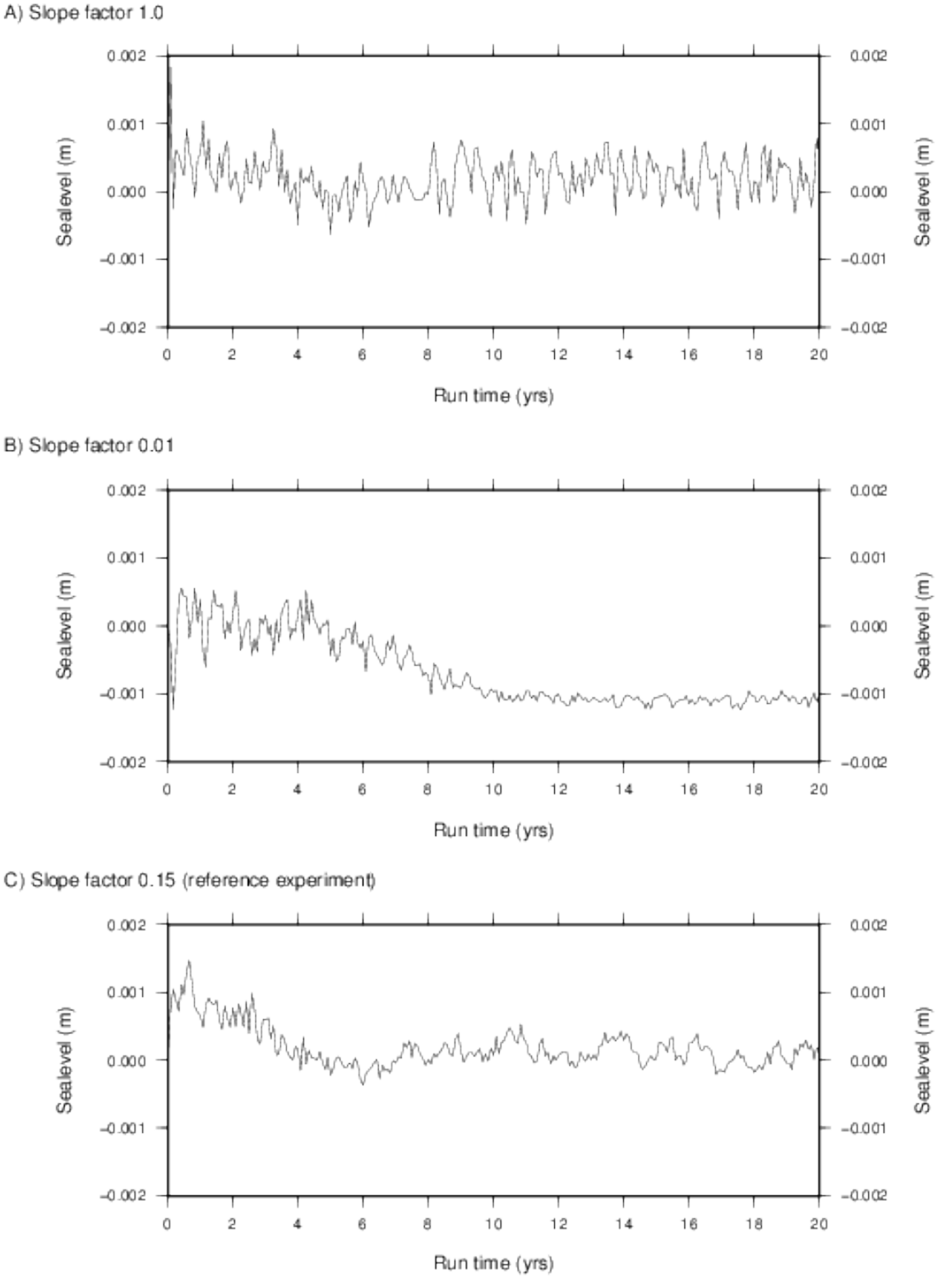

Fig. B10. Evolution of sealevel throughout the runs.

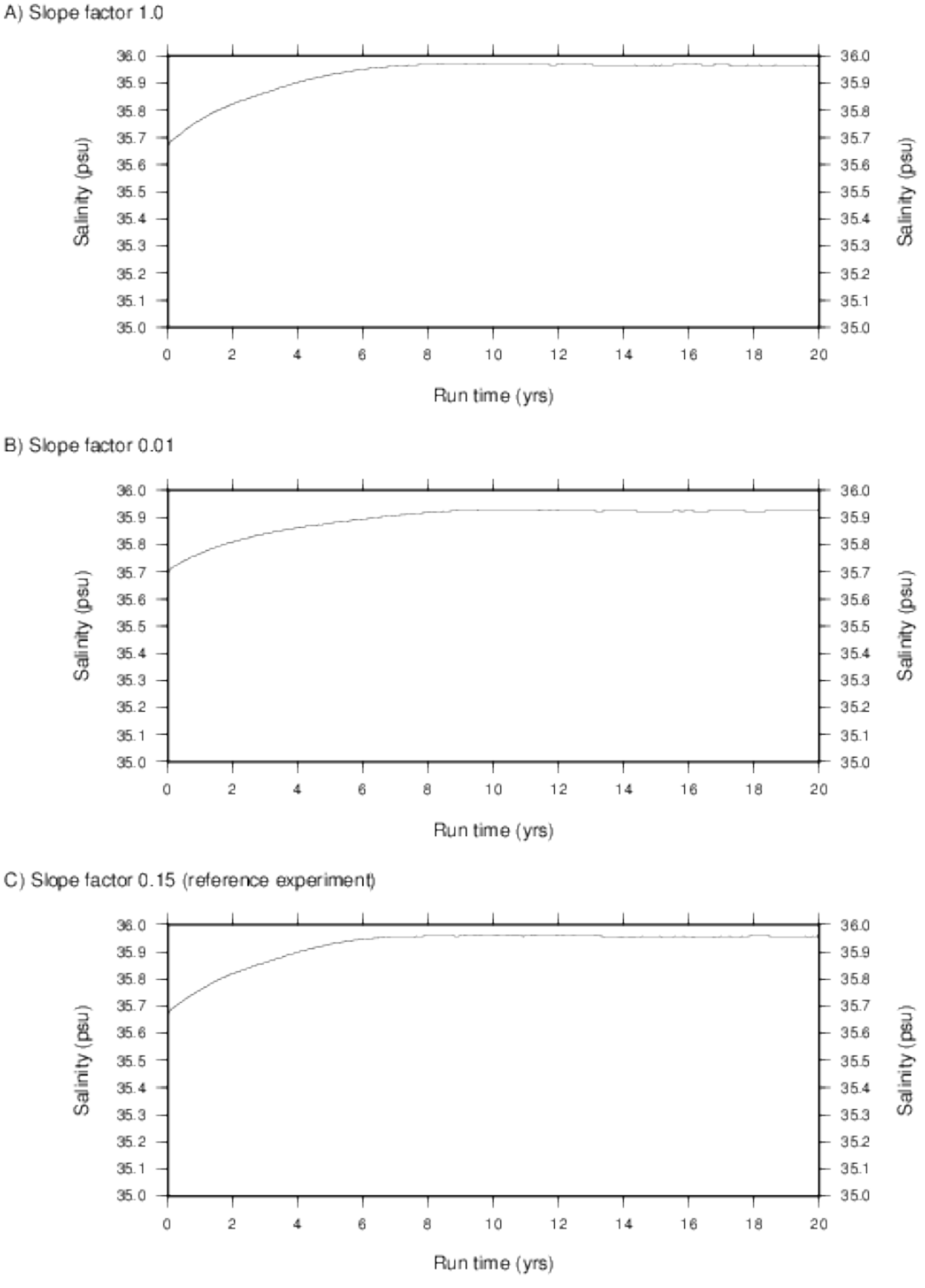

Fig. B11. Evolution of salinity throughout the runs.

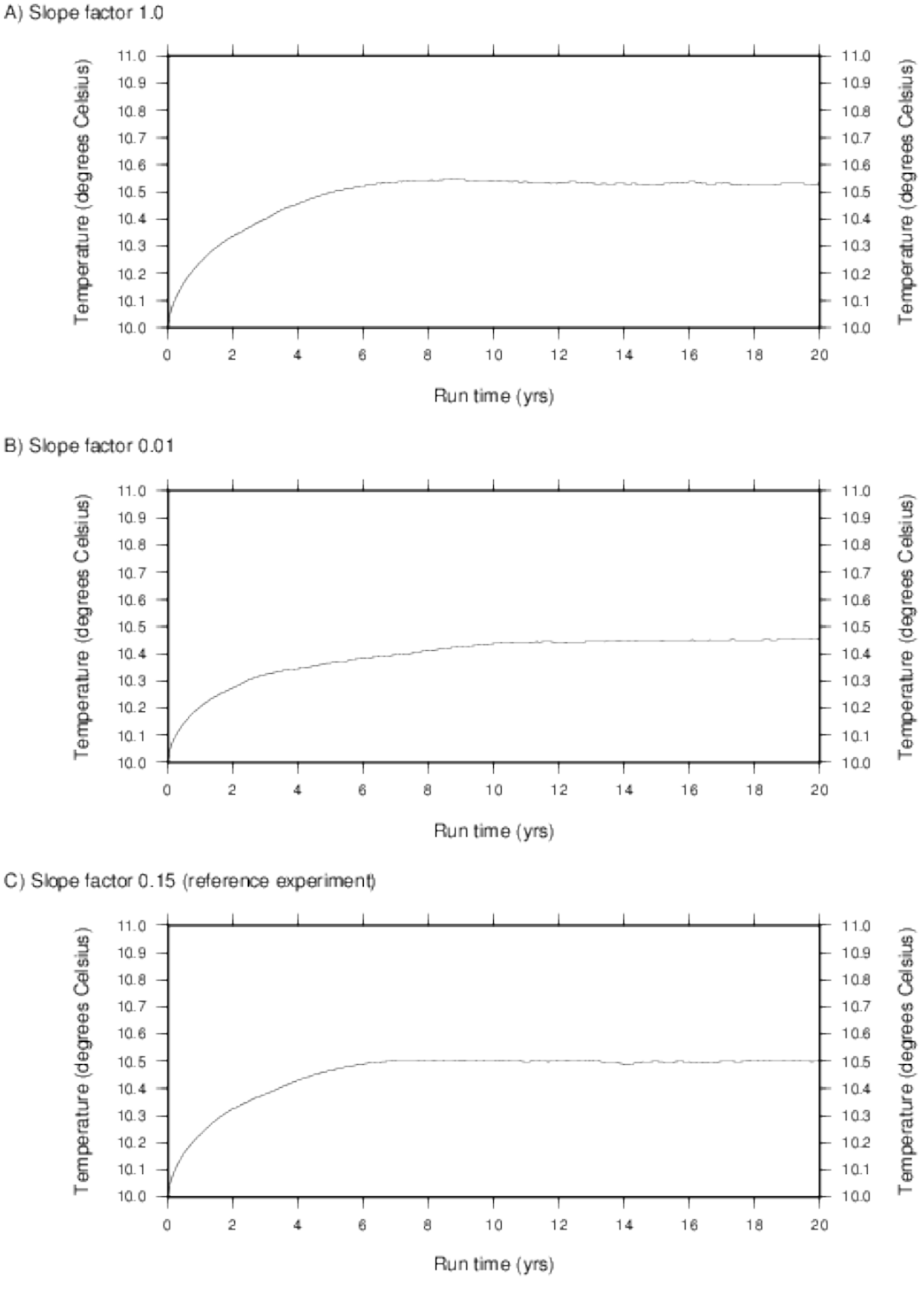

Fig. B12. Evolution of temperature throughout the runs.

Appendix C

Experiment Results: Sealevel changes

- Figure C1 Bathymetry.
- Figure C2: Salinity at a depth of 100m.
- Figure C3: Salinity at a depth of 600m.
- Figure C4: Salinity at a depth of 1200m.
- Figure C5: Salinity at the bottom sigma-layer.
- Figure C6: Salinity profile N-S at 6°15'W.
- Figure C7: Salinity profile N-S at 8°20'W.
- Figure C8: Salinity profile E-W at 35°50'N.
- Figure C9: Graph of evolution of kinetic energy.
- Figure C10: Graph of evolution of sealevel.
- Figure C11: Graph of evolution of salinity.
- Figure C12: Graph of evolution of temperature.

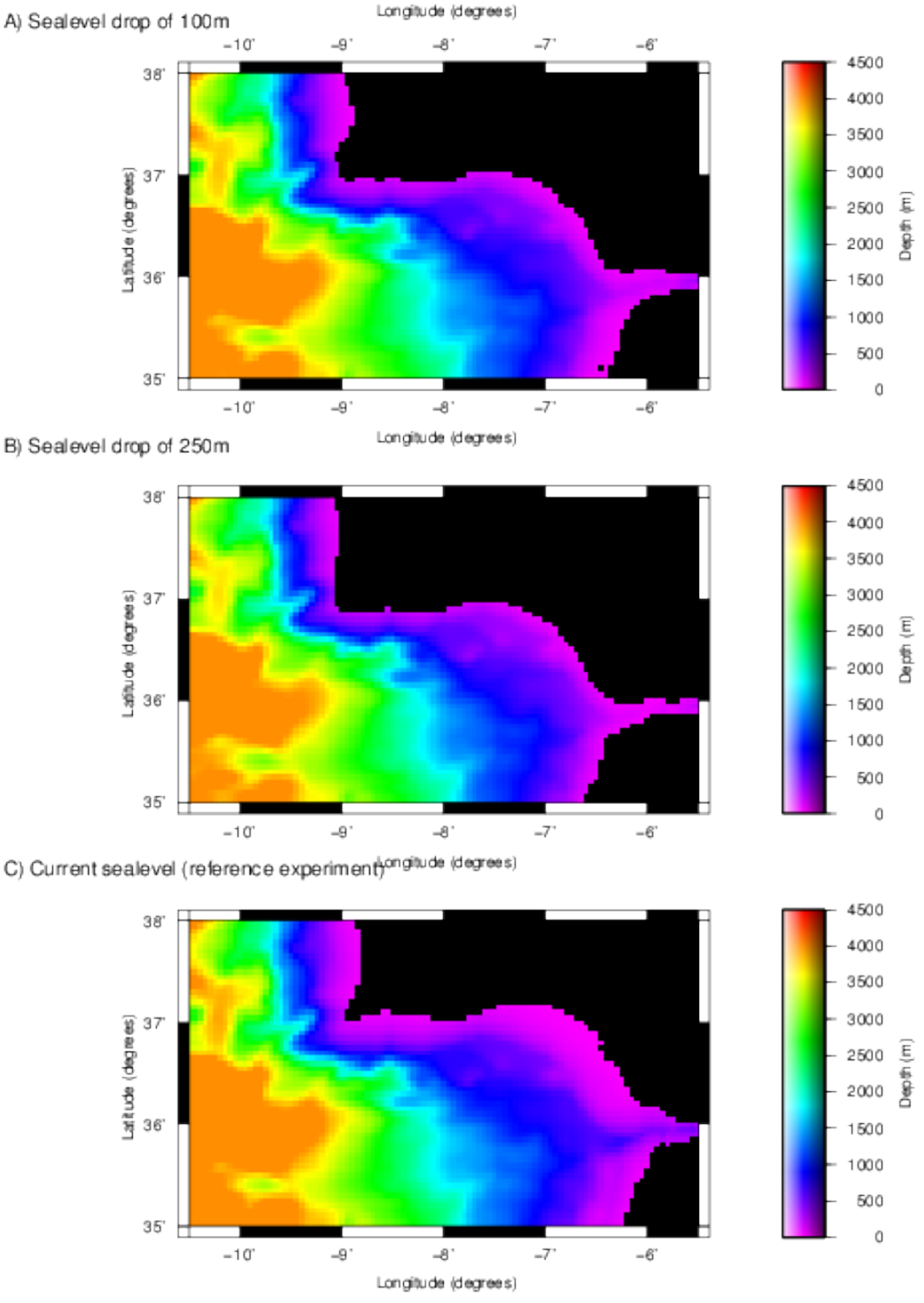

Fig. C1. Bathymetry obtained by using the different slope factors.

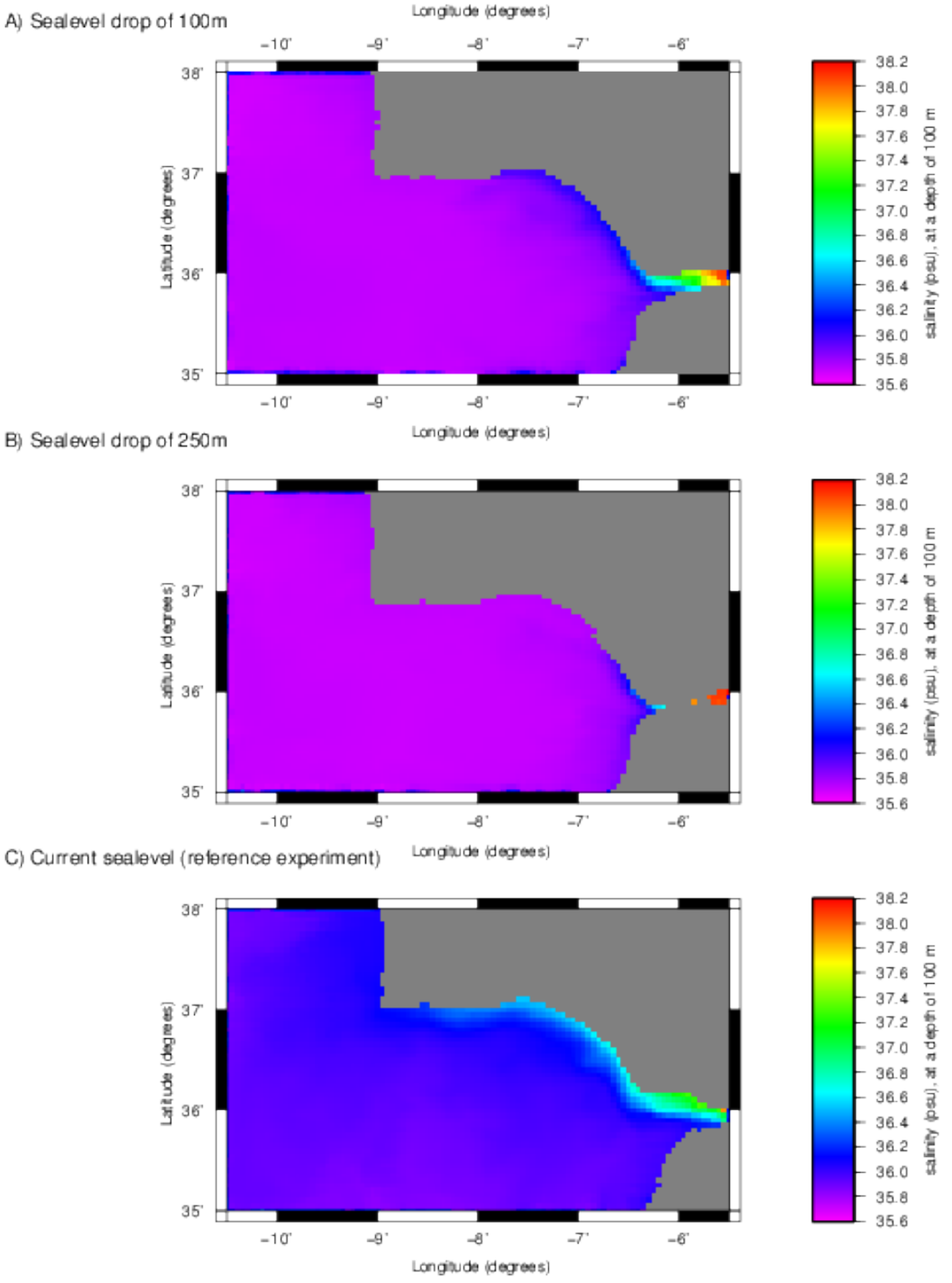

Fig. C2. Salinities at a depth of 100m. Maps taken at t=20 years.

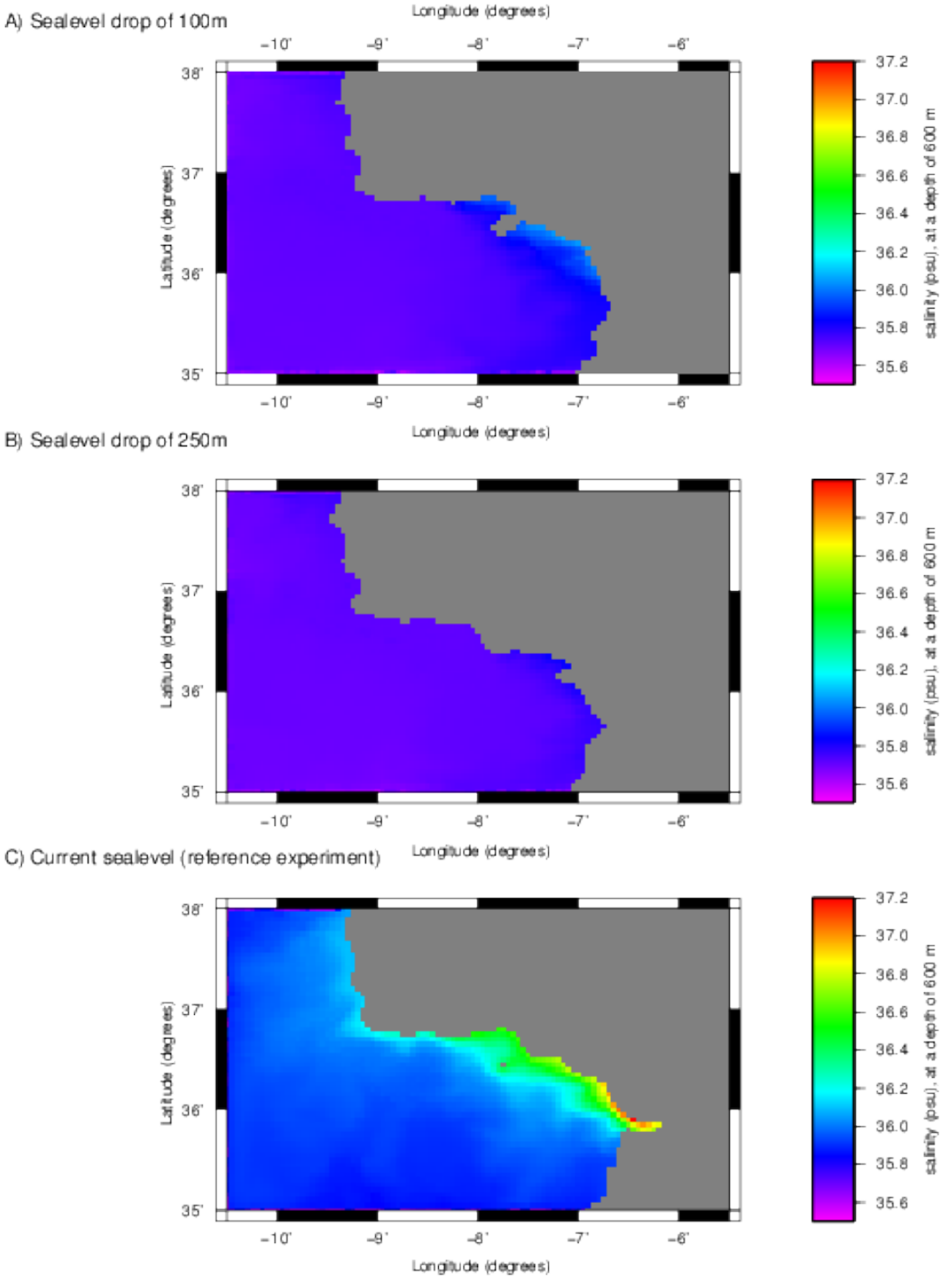

Fig. C3. Salinities at a depth of 600m. Maps taken at t=20 years.

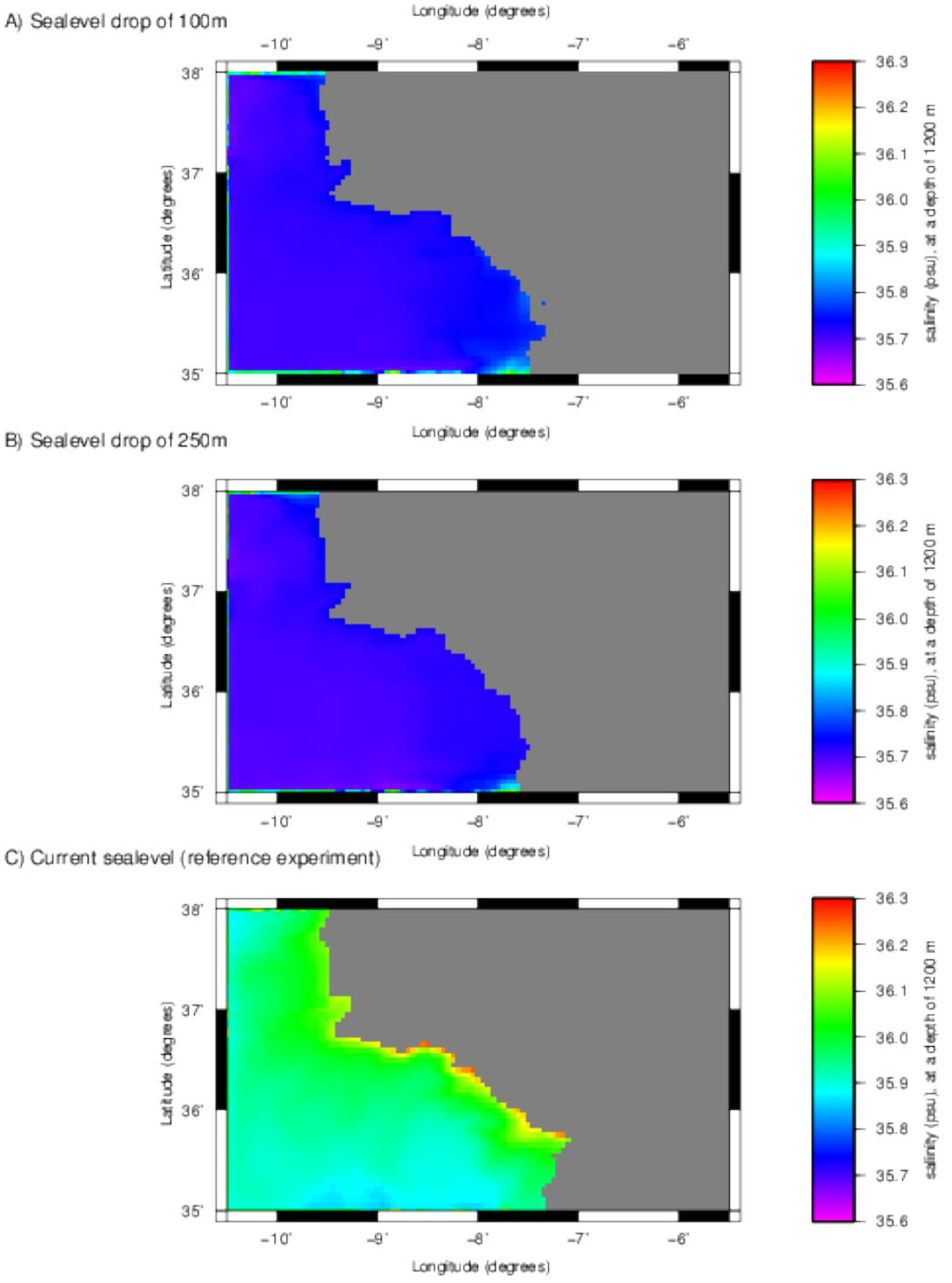

Fig. C4. Salinities at a depth of 1200m. Maps taken at t=20 years.

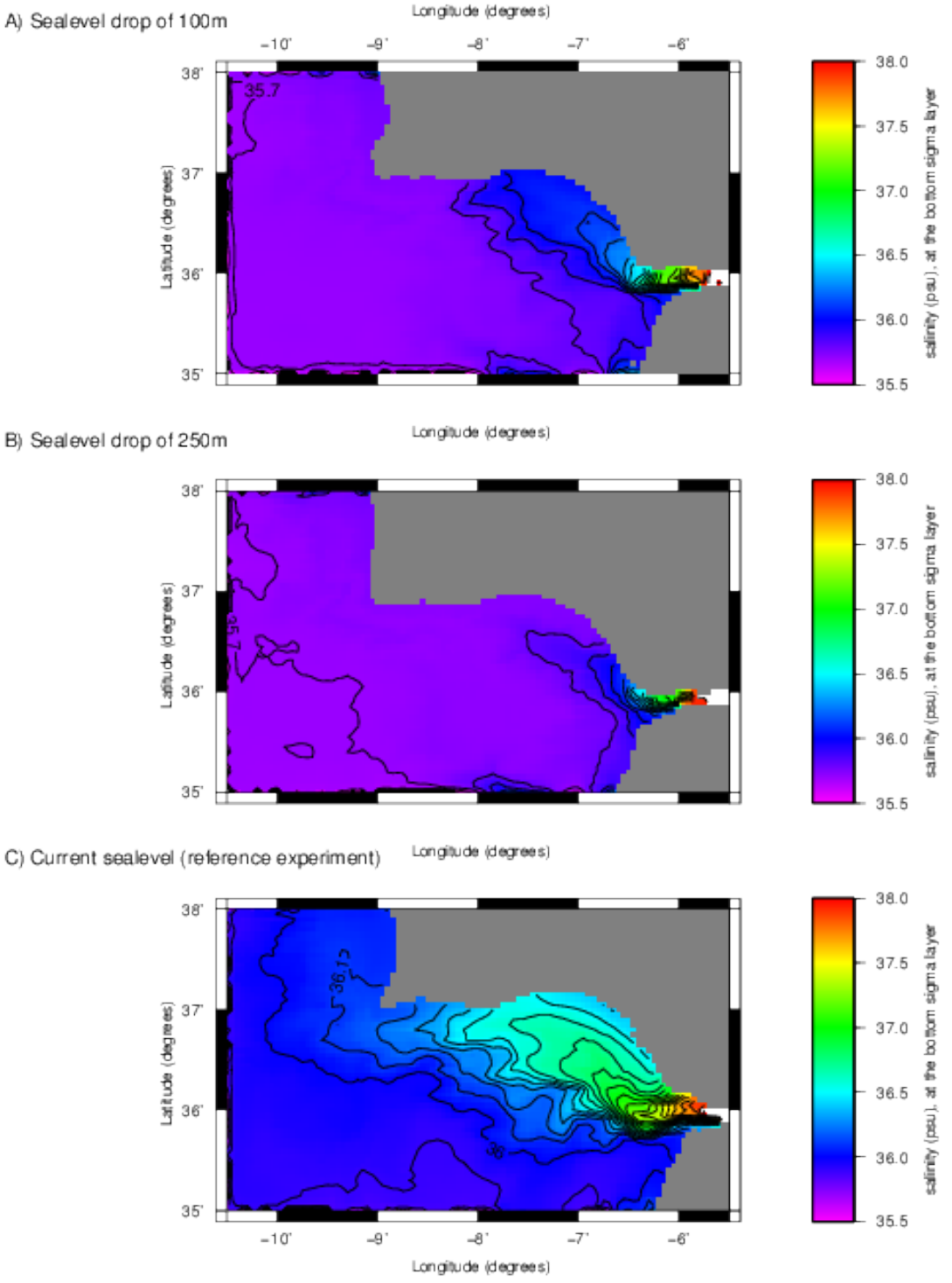

Fig. C5. Salinities at the bottom sigma layer. Maps taken at t=20 years.

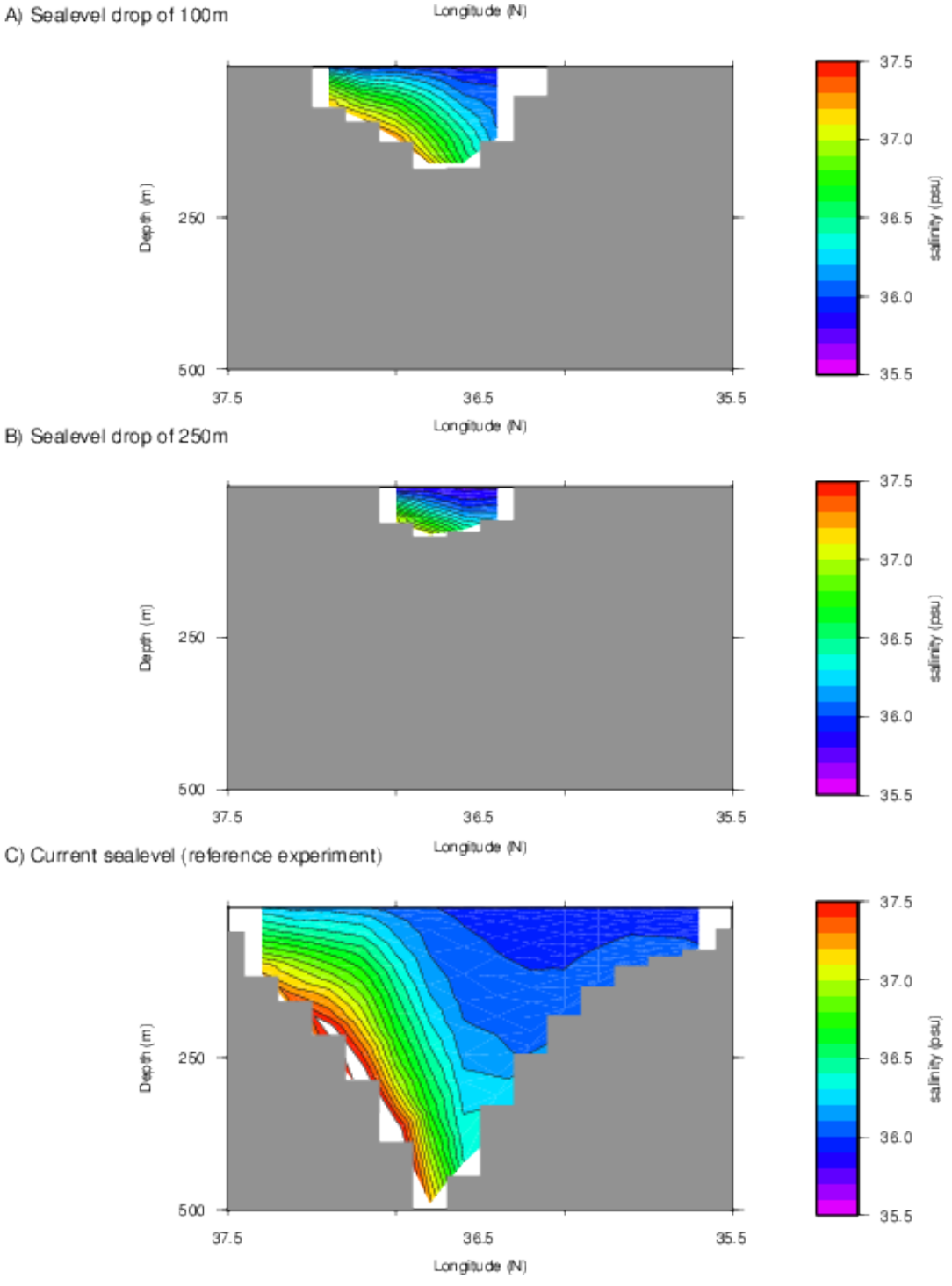

Fig. C6. A north to south salinity profile at 6°15'W. Profiles taken at t=20 years.

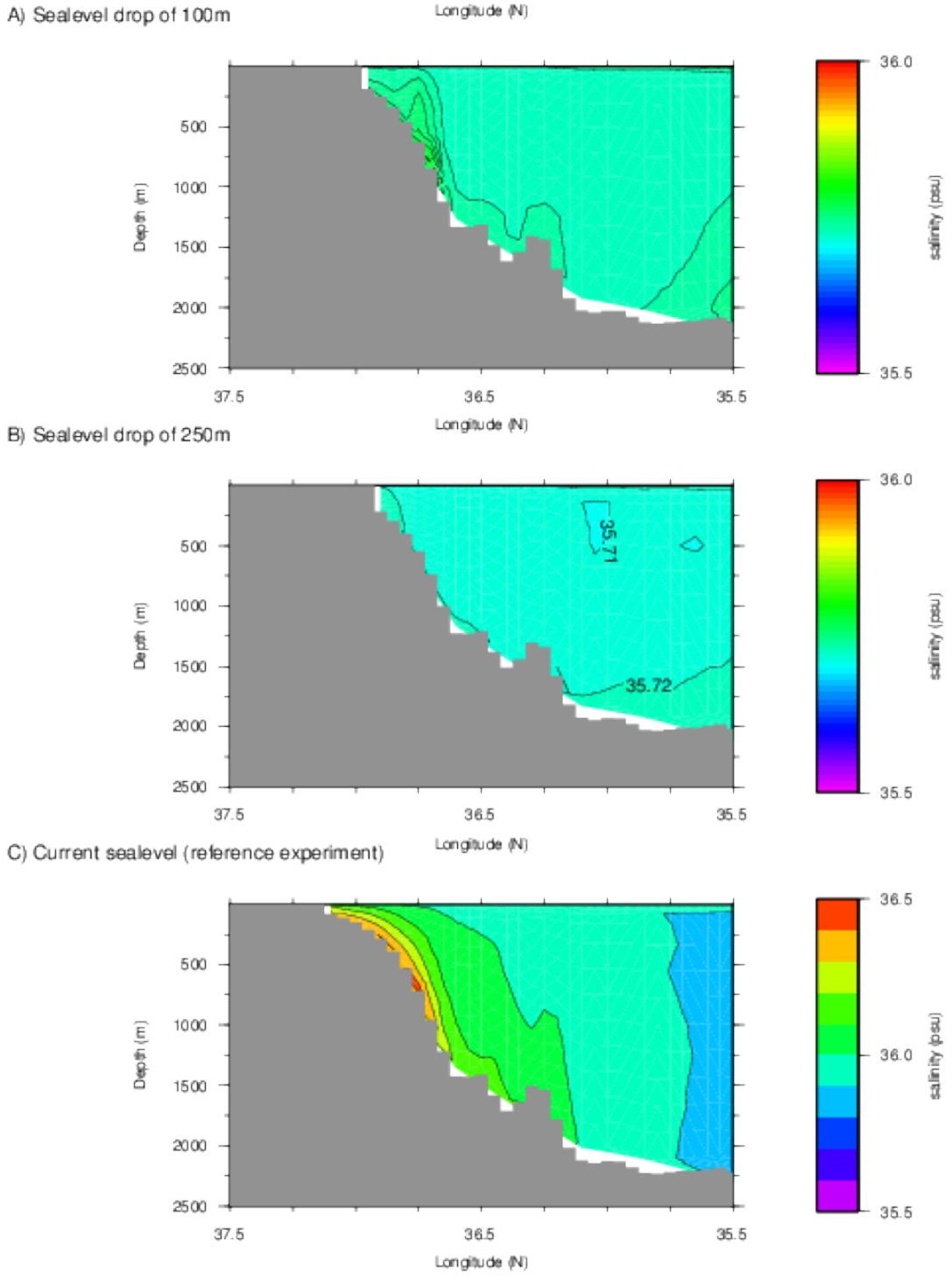

Fig. C7. A north to south salinity profile at 8°20'W. Profiles taken at t=20 years.

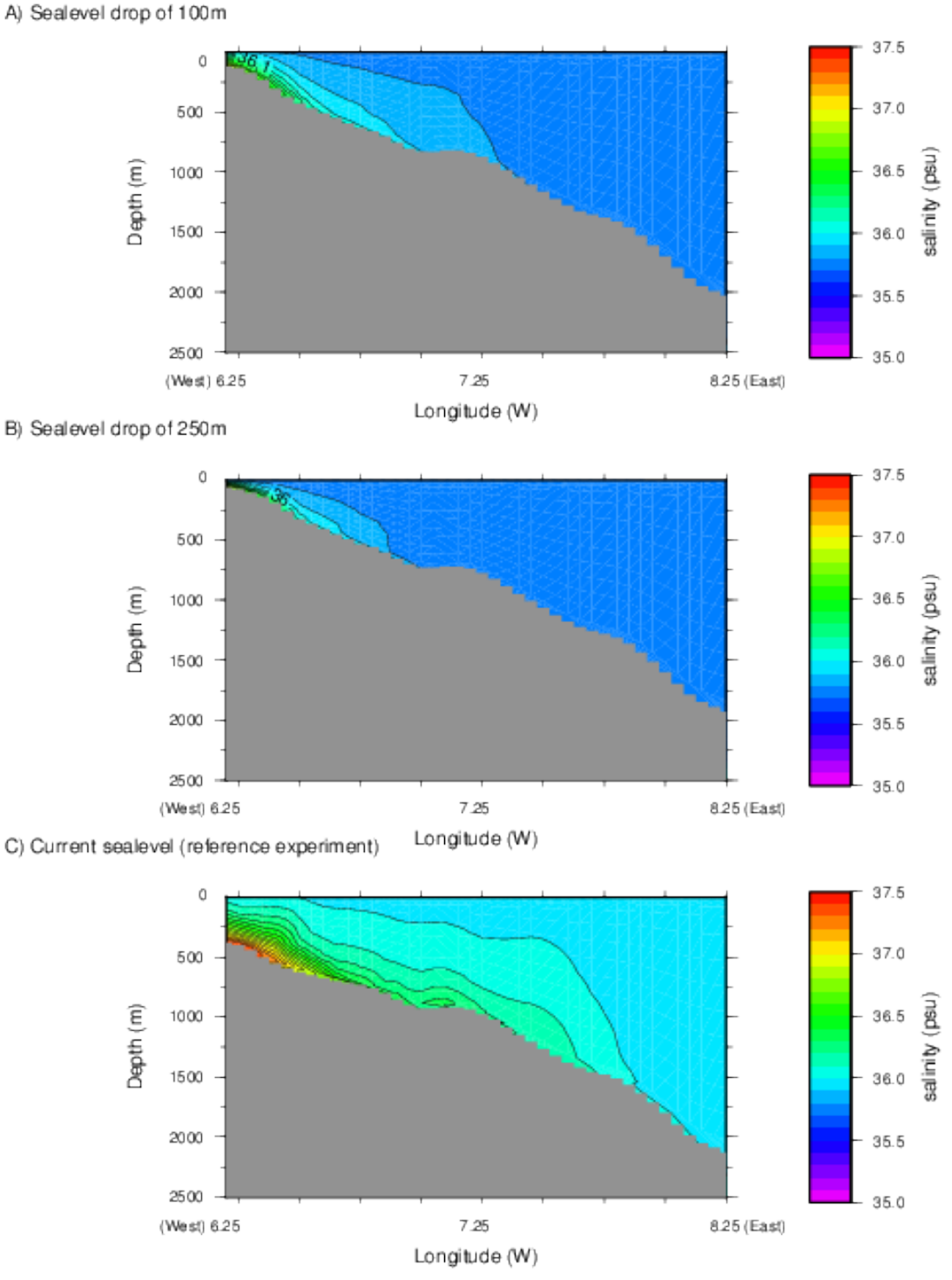

Fig. C8. An east to west salinity profile at 35°50'N, note that east is in the left of the profile. Profiles taken at t=20 years.

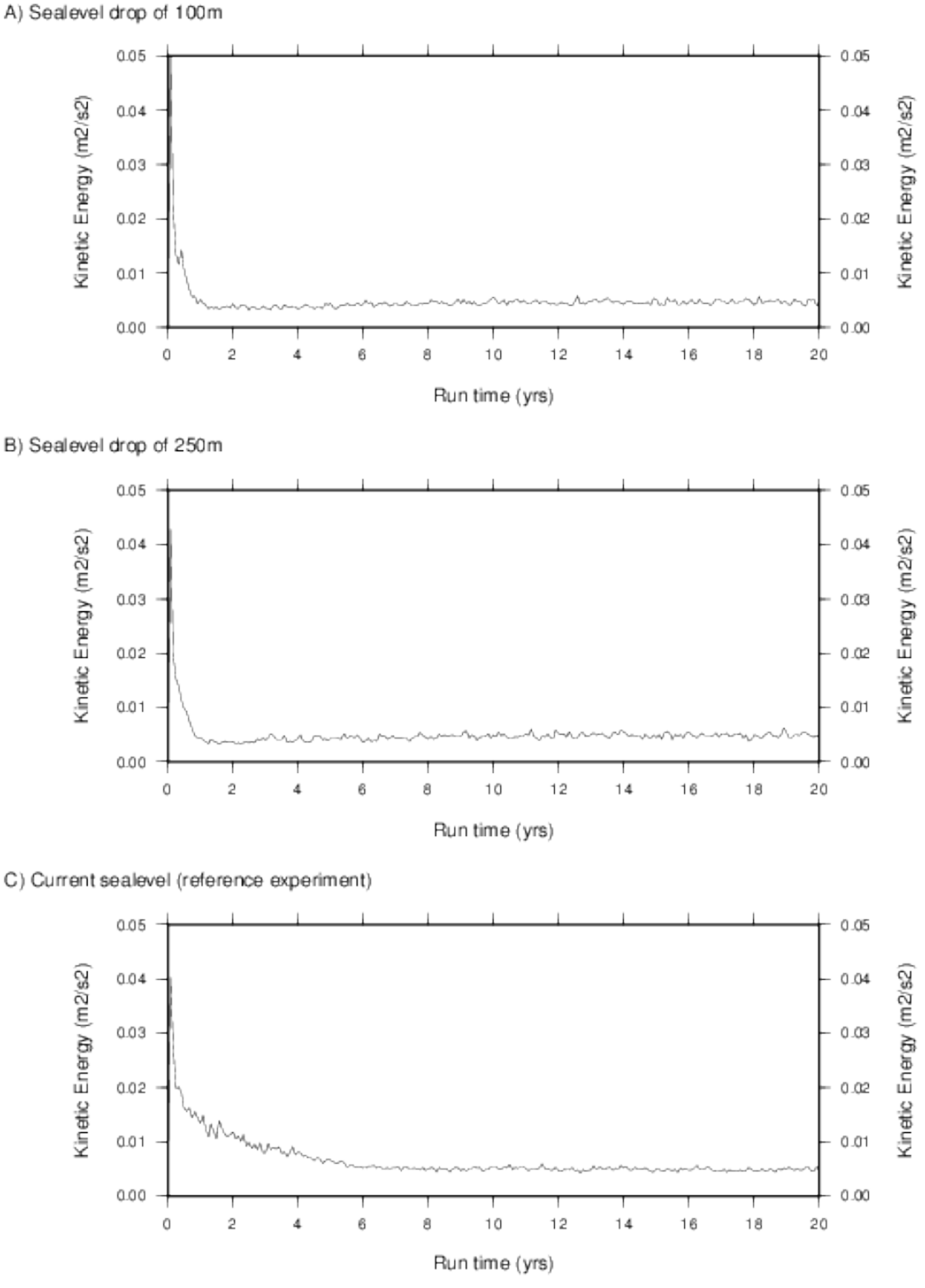

Fig. C9. Evolution of kinetic energy throughout the runs.

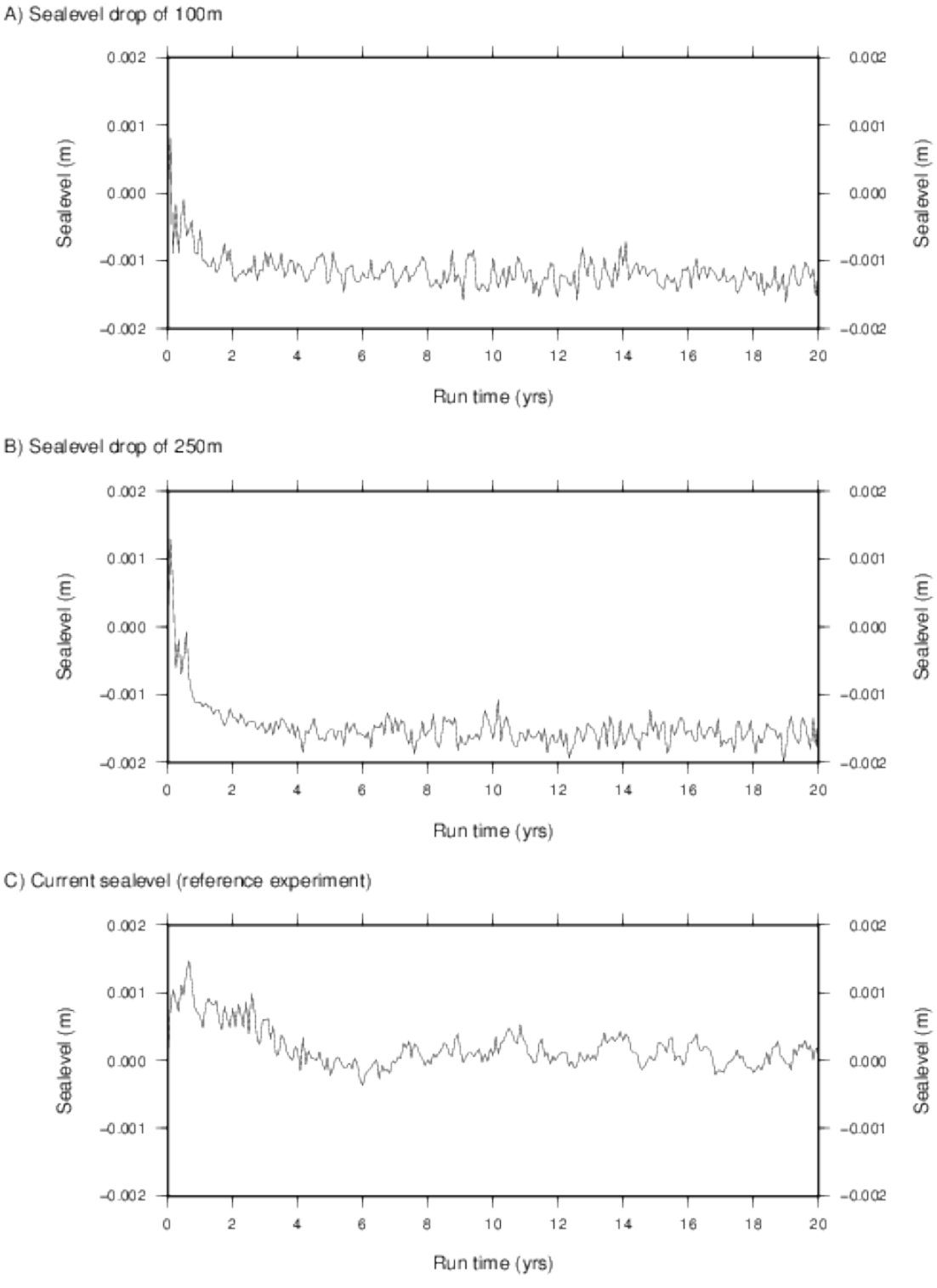

Fig. C10. Evolution of sealevel throughout the runs.

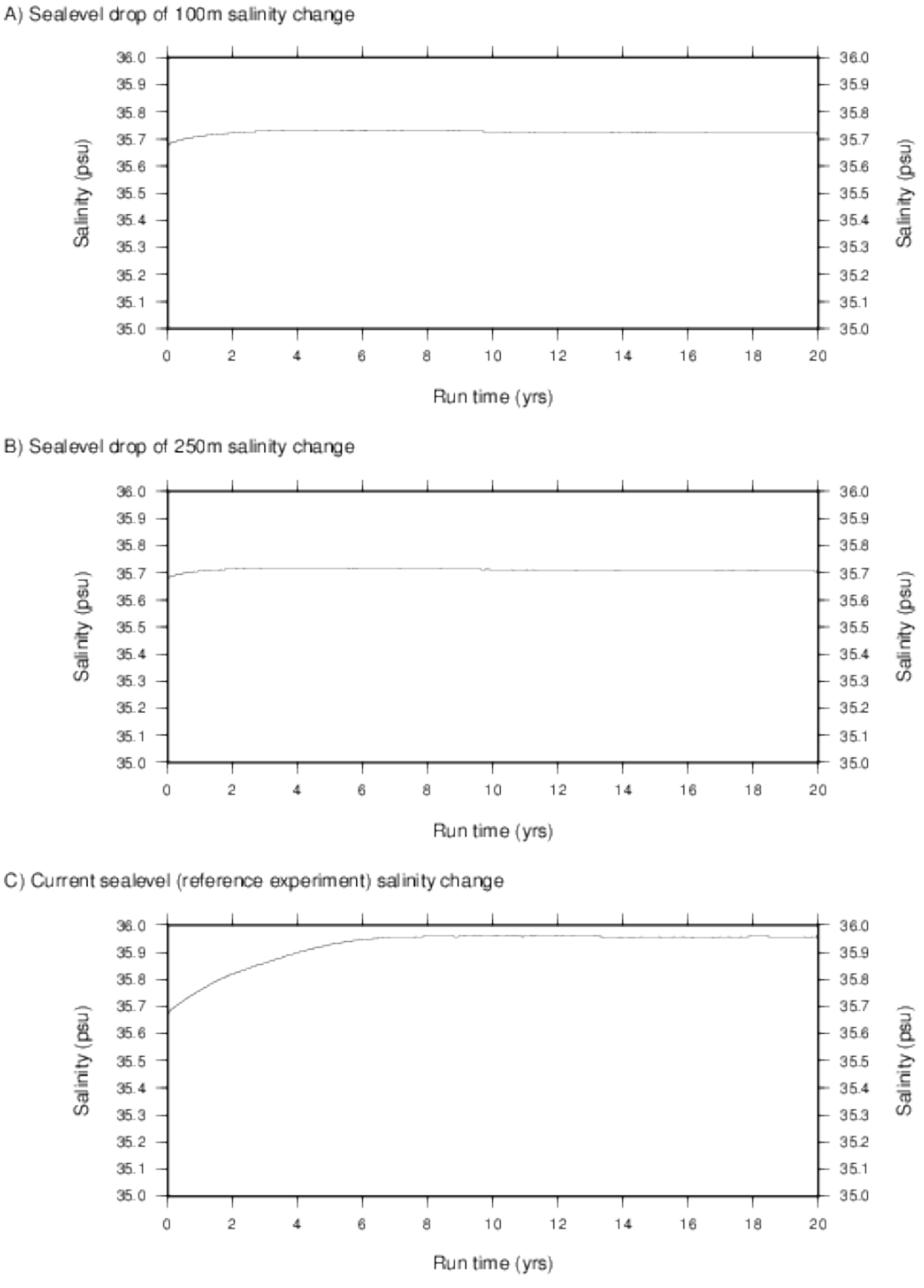

Fig. C11. Evolution of salinity throughout the runs.

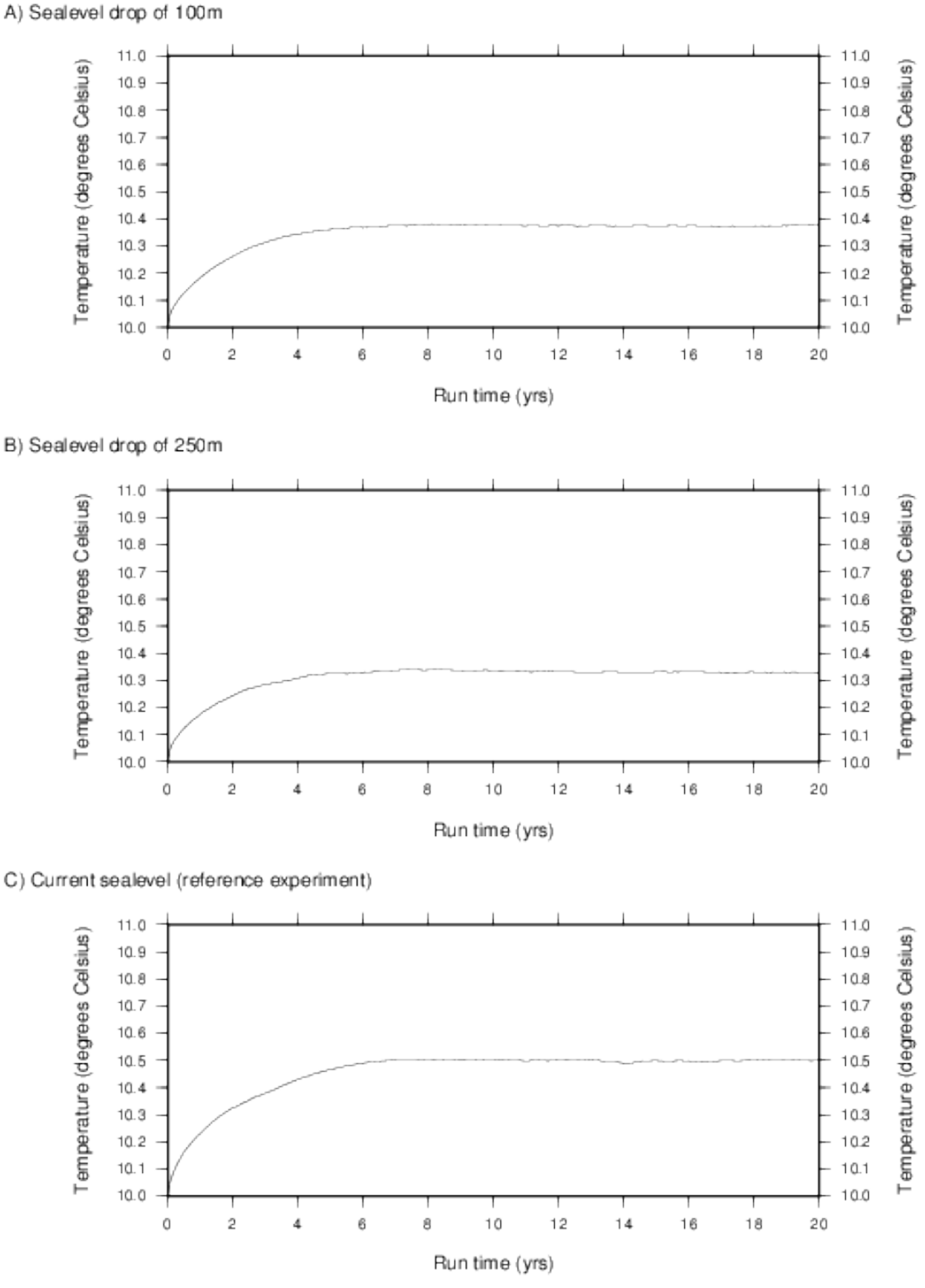

Fig. C12. Evolution of temperature throughout the runs.

Appendix D

Experiment Results: MOW source water conditions

Salinity change of 10 psu.

- Figure D1: Salinity at a depth of 100m.
- Figure D2: Salinity at a depth of 600m.
- Figure D3: Salinity at a depth of 1200m.
- Figure D4: Salinity at the bottom sigma-layer.
- Figure D5: Salinity profile N-S at 6°15'W.
- Figure D6: Salinity profile N-S at 8°20'W.
- Figure D7: Salinity profile E-W at 35°50'N.
- Figure D8: Graph of evolution of kinetic energy.
- Figure D9: Graph of evolution of sealevel.
- Figure D10: Graph of evolution of salinity.
- Figure D11: Graph of evolution of temperature.

Salinity change of 2 psu.

- Figure D12: Salinity at a depth of 100m.
- Figure D13: Salinity at a depth of 600m.
- Figure D14: Salinity at a depth of 1200m.
- Figure D15: Salinity at the bottom sigma-layer.
- Figure D16: Salinity profile N-S at 6°15'W.
- Figure D17: Salinity profile N-S at 8°20'W.
- Figure D18: Salinity profile E-W at 35°50'N.
- Figure D19: Graph of evolution of kinetic energy.
- Figure D20: Graph of evolution of sealevel.
- Figure D21: Graph of evolution of salinity.
- Figure D22: Graph of evolution of temperature.

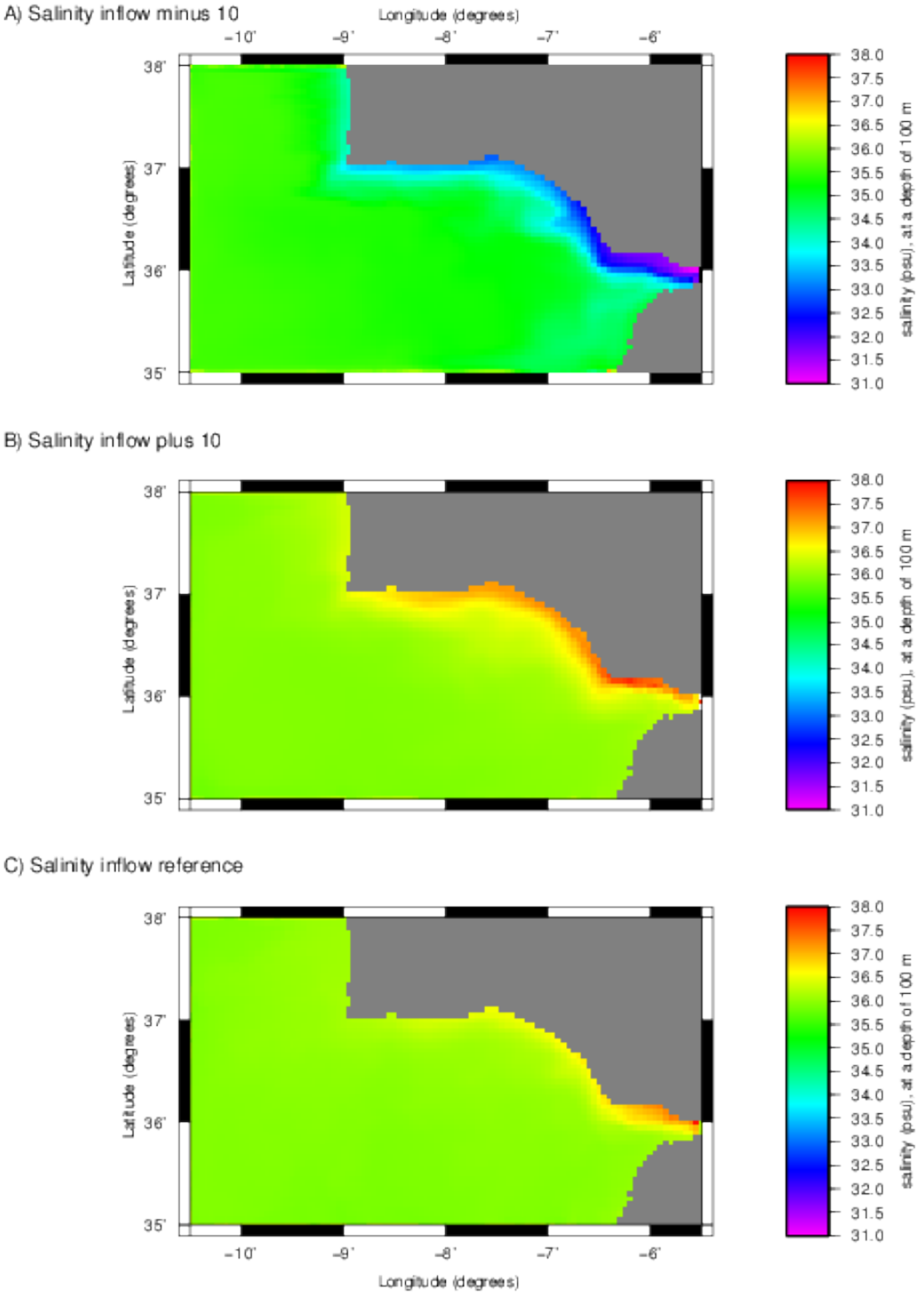

Fig. D1. Salinities at a depth of 100m. Maps taken at t=20 years.

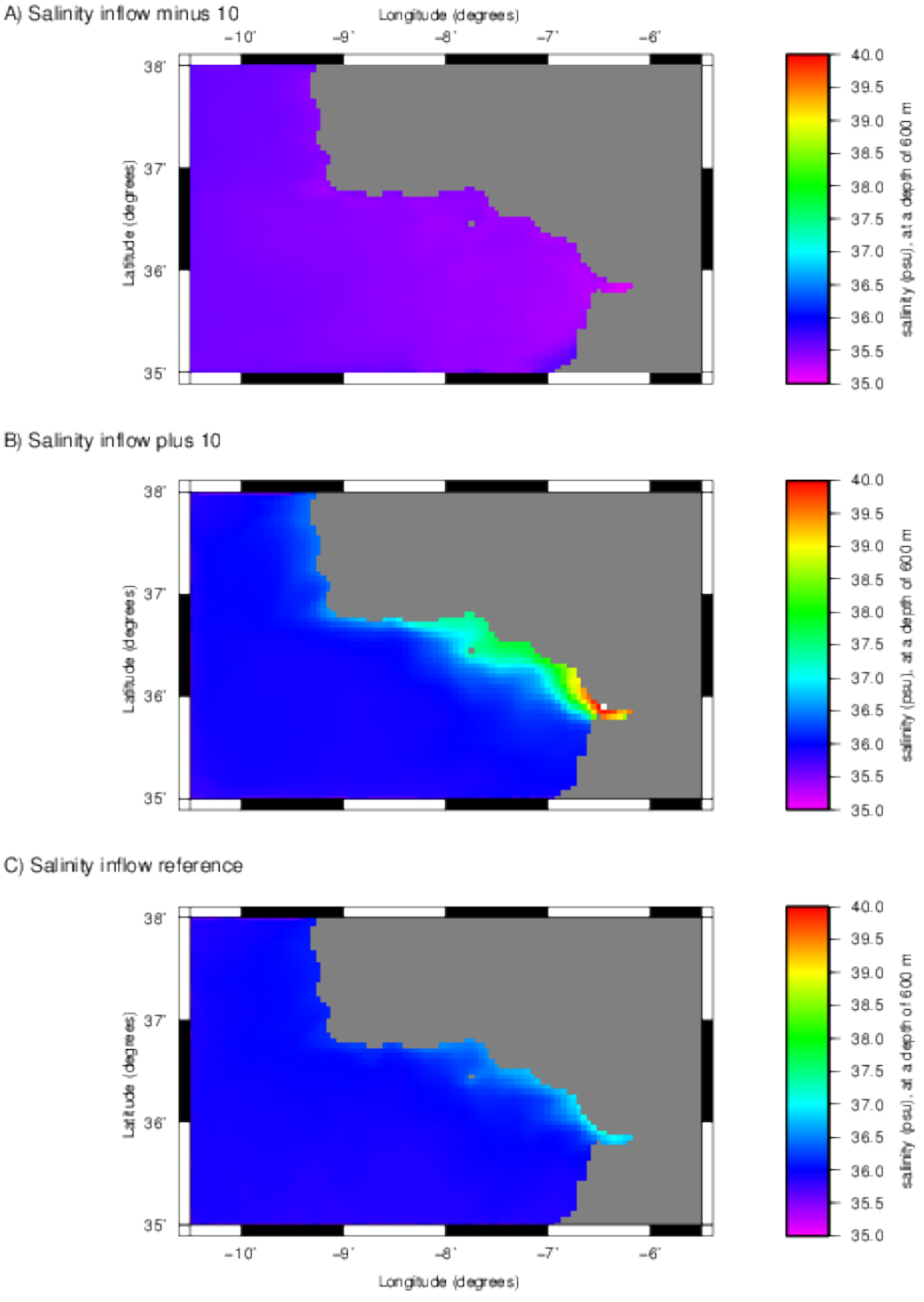

Fig. D2. Salinities at a depth of 600m. Maps taken at t=20 years.

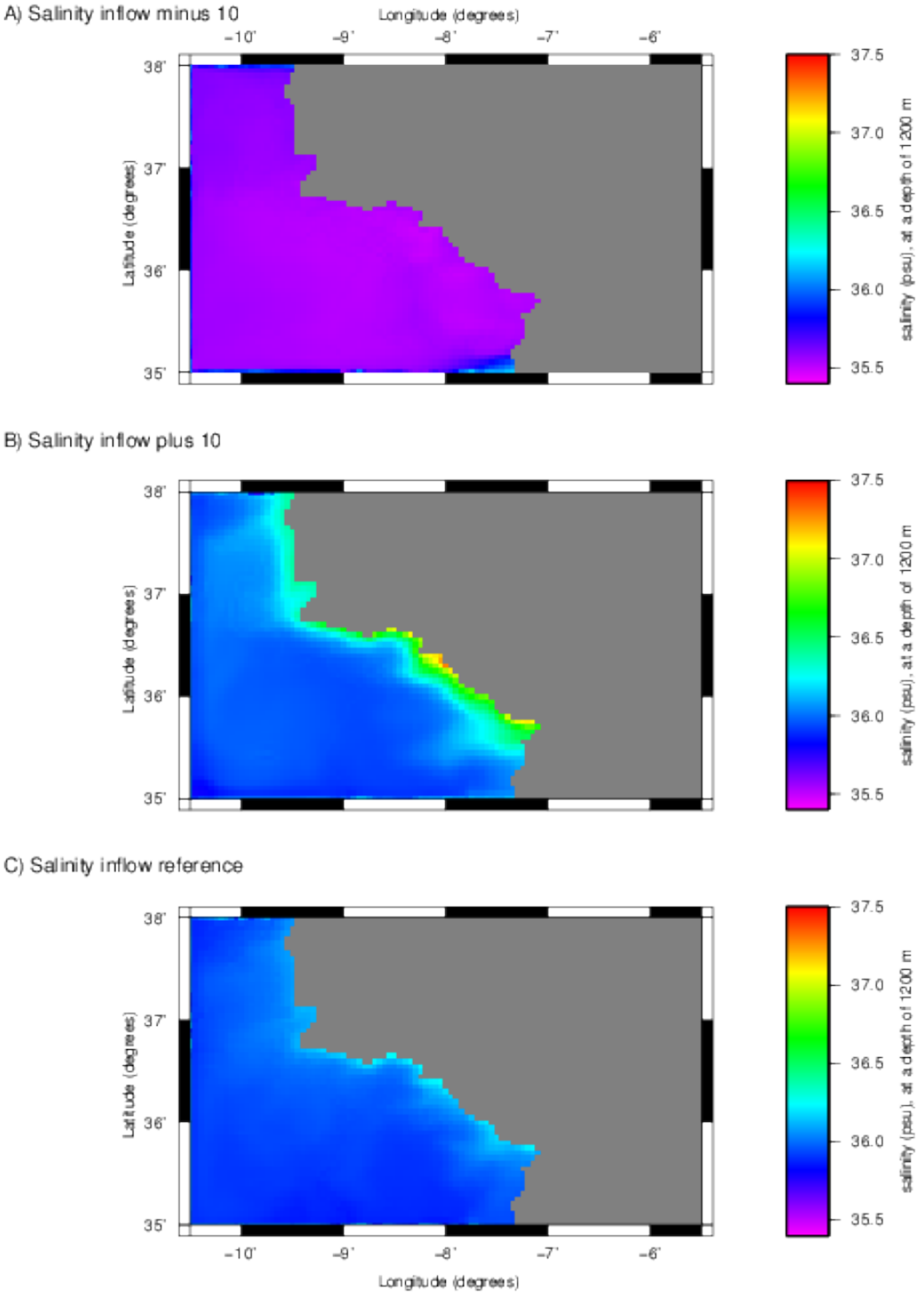

Fig. D3. Salinities at a depth of 1200m. Maps taken at t=20 years.

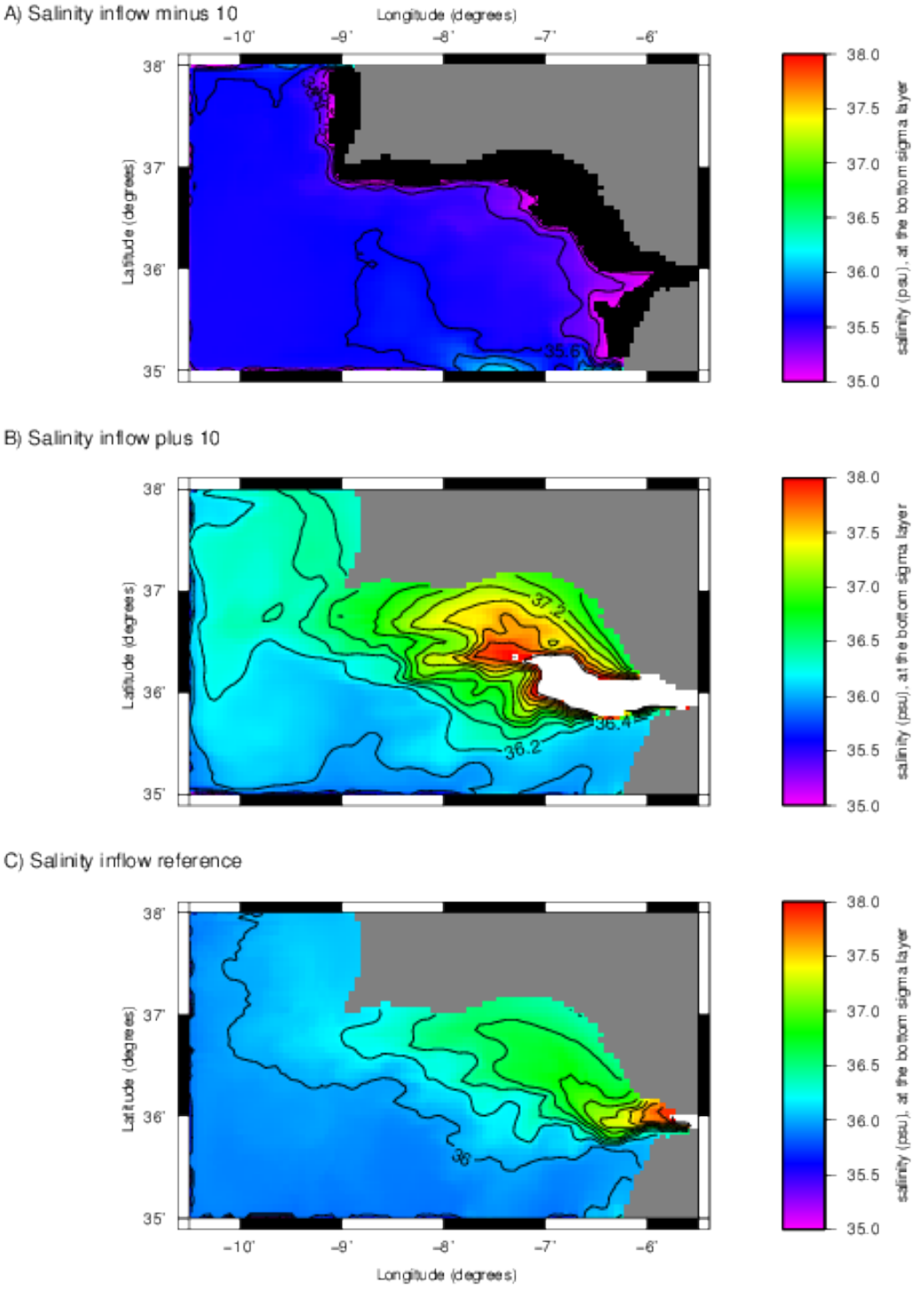

Fig. D4. Salinities at the bottom sigma-layer. Maps taken at t=20 years.

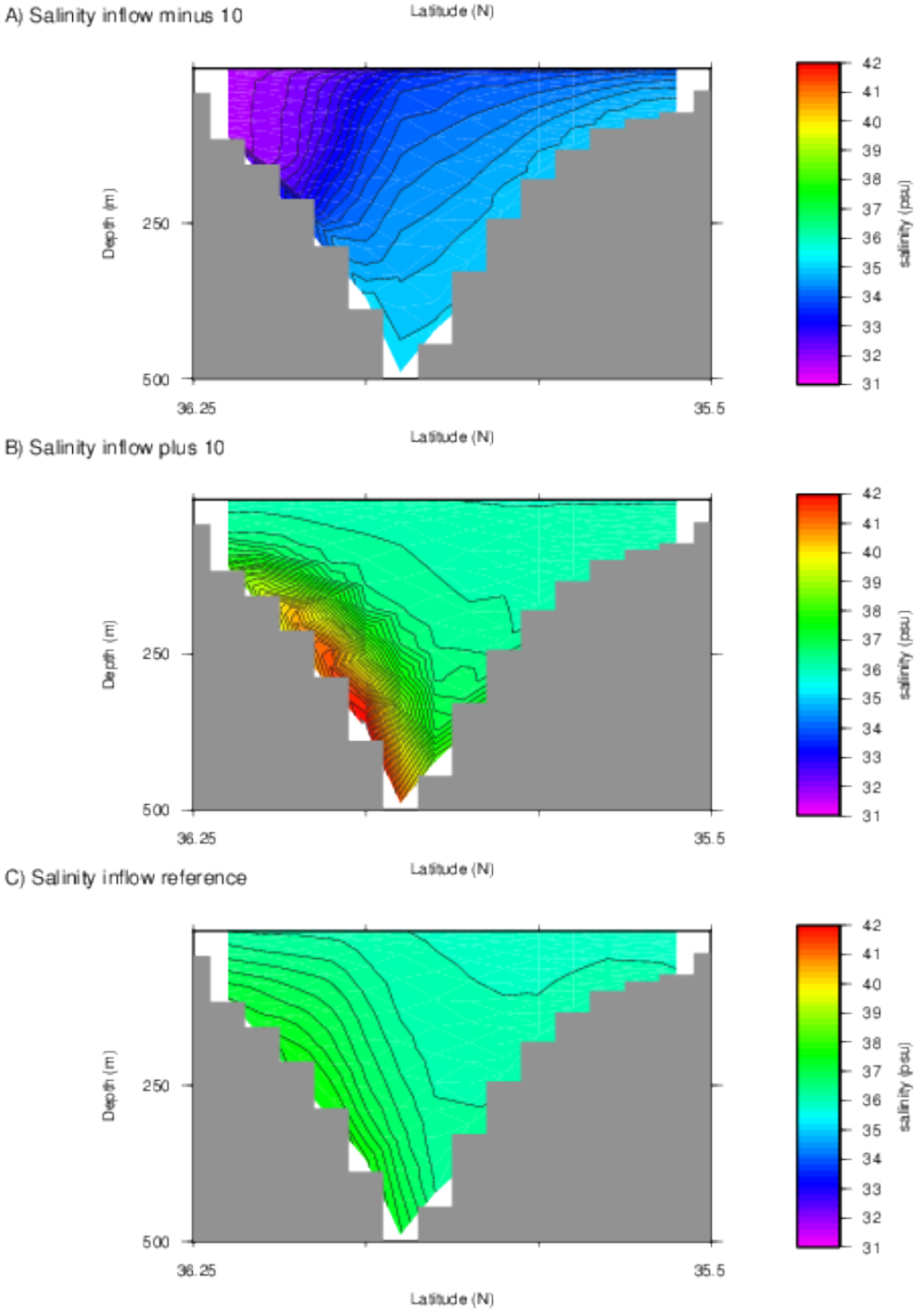

Fig. D5. A north to south salinity profile at 6°15'W. Profiles taken at t=20 years.

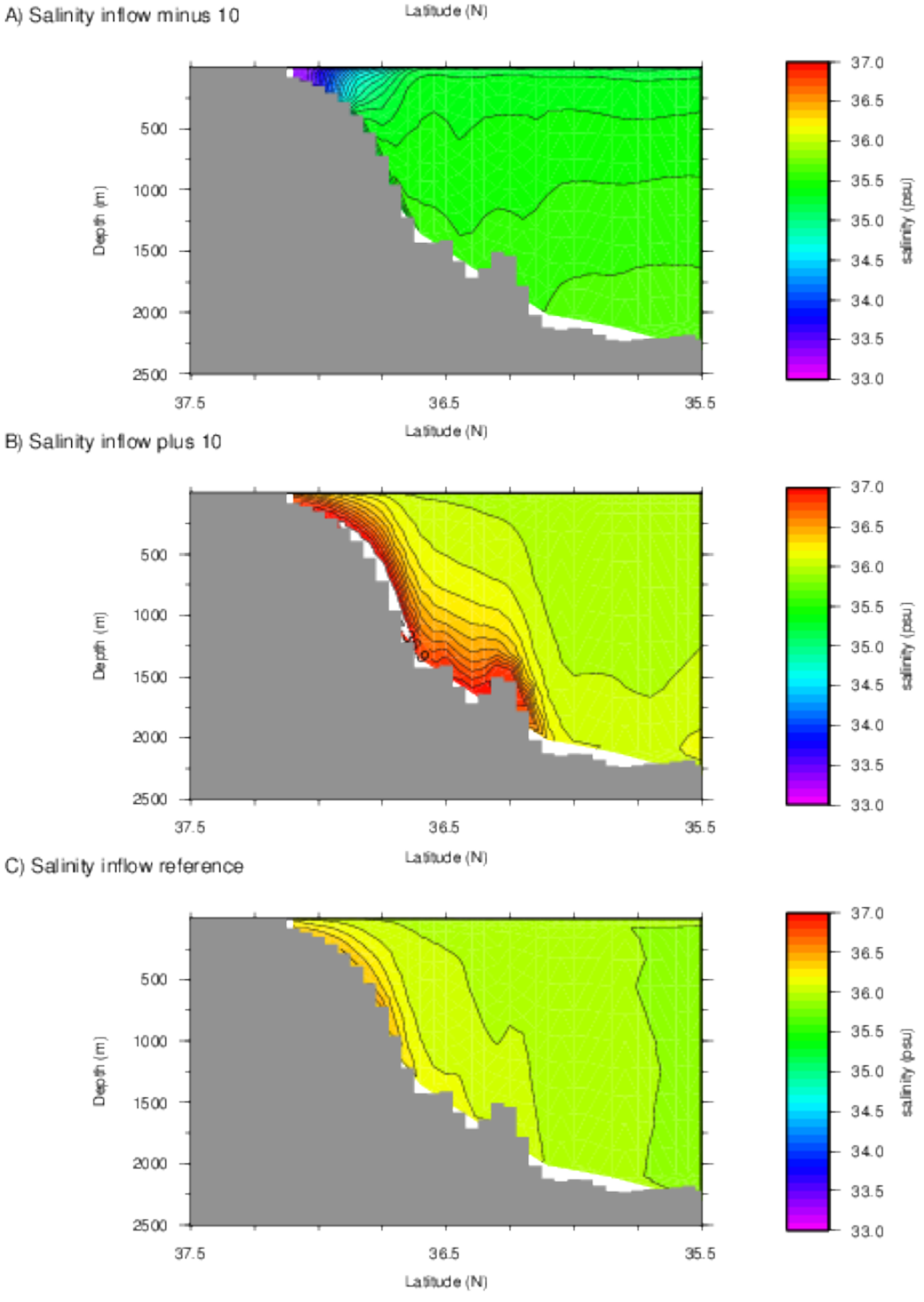

Fig. D6. A north to south salinity profile at 8°20'W. Profiles taken at t=20 years.

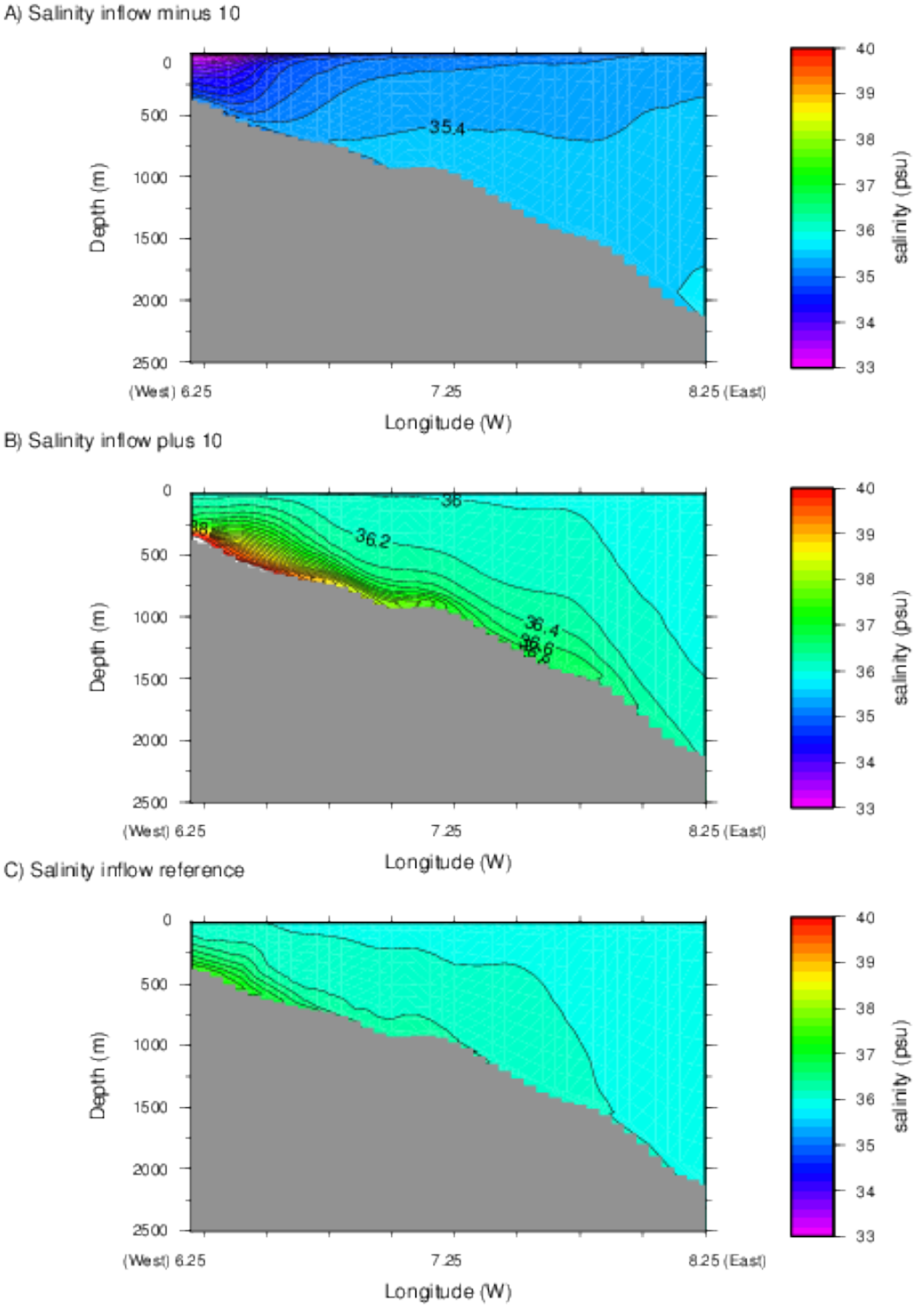

Fig. D7. An east to west salinity profile at 35°50'N, note that east is in the left of the profile. Profiles taken at t=20 years.

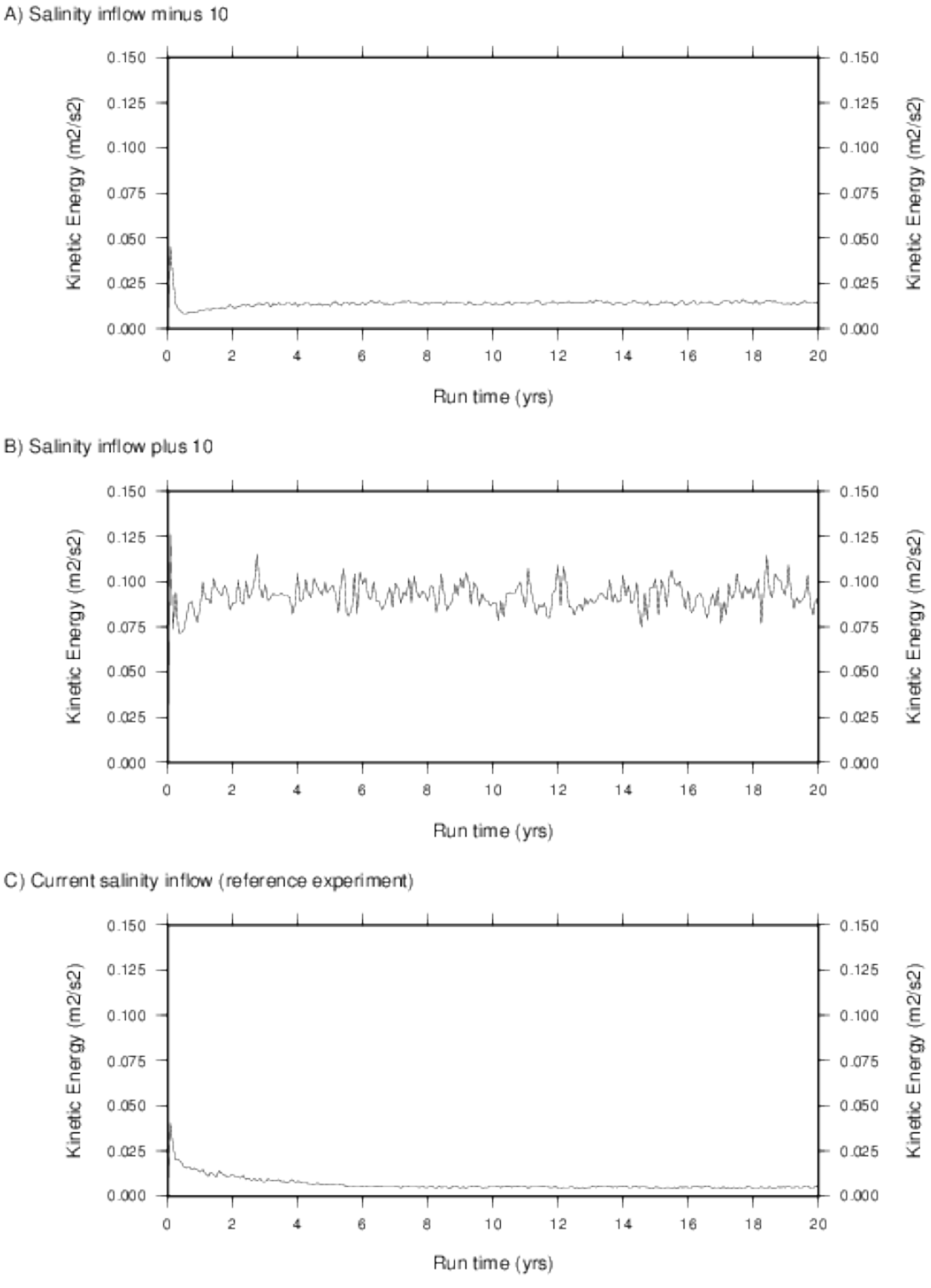

Fig. D8. Evolution of kinetic energy throughout the runs.

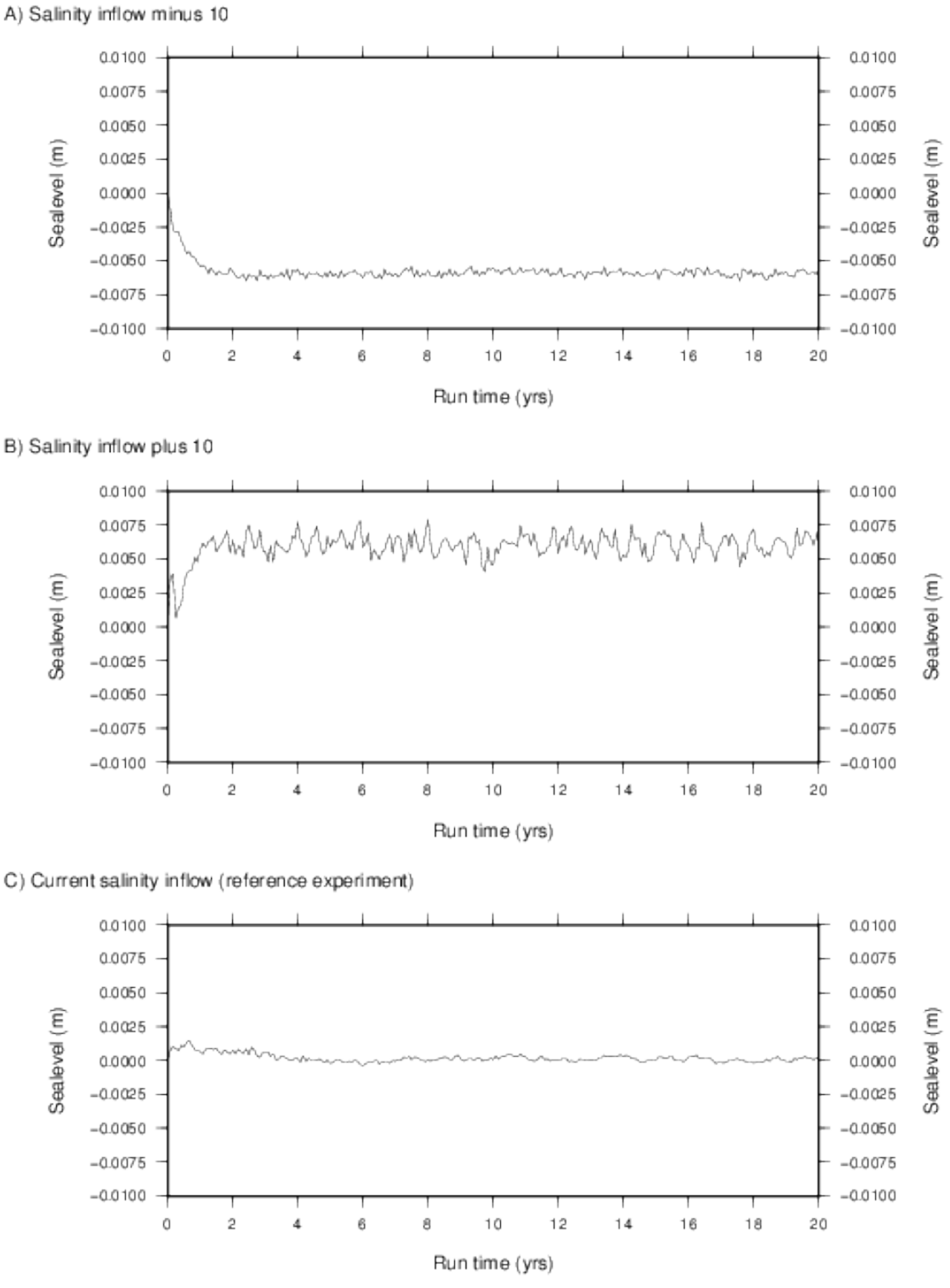

Fig. D9. Evolution of sealevel throughout the runs.

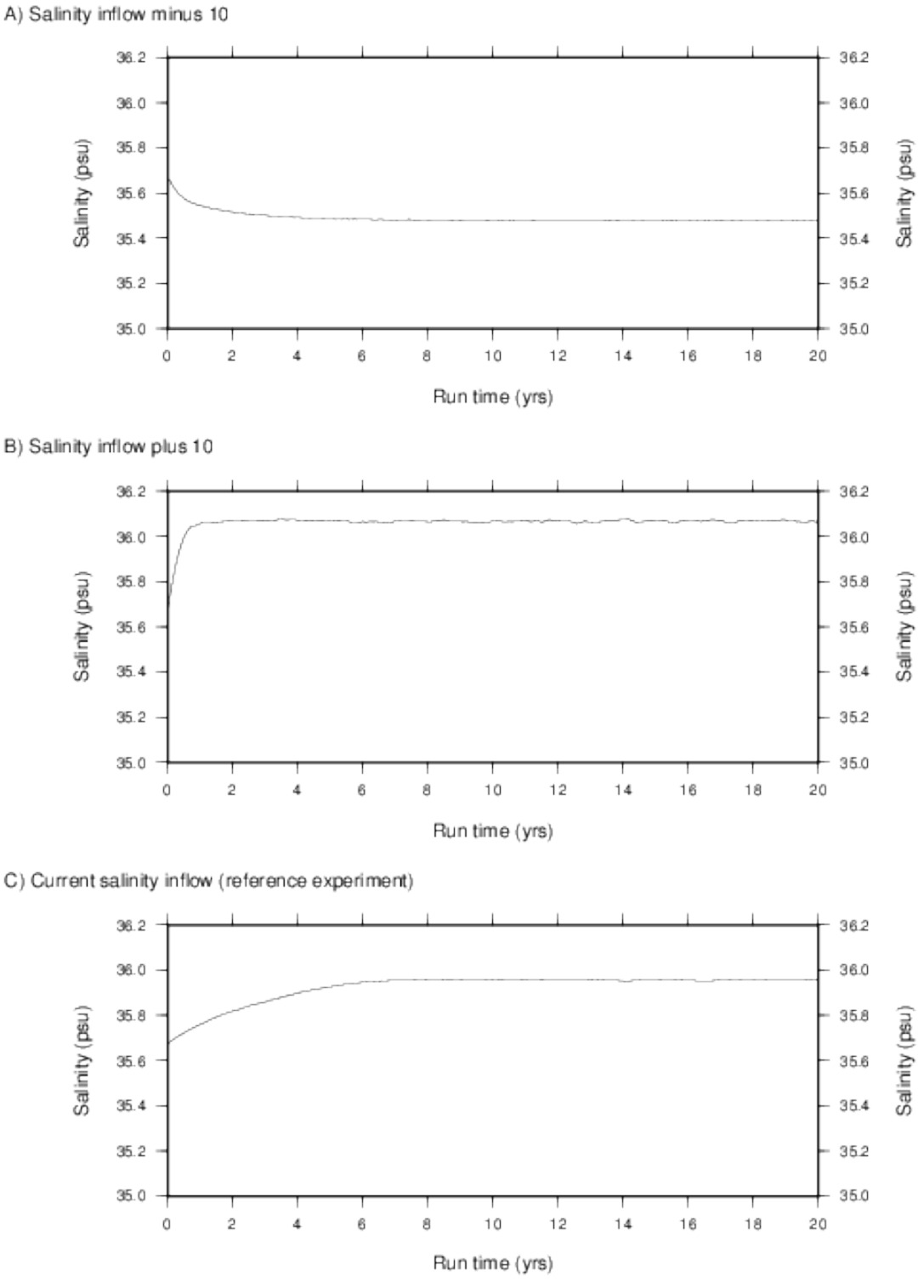

Fig. D10. Evolution of salinity throughout the runs.

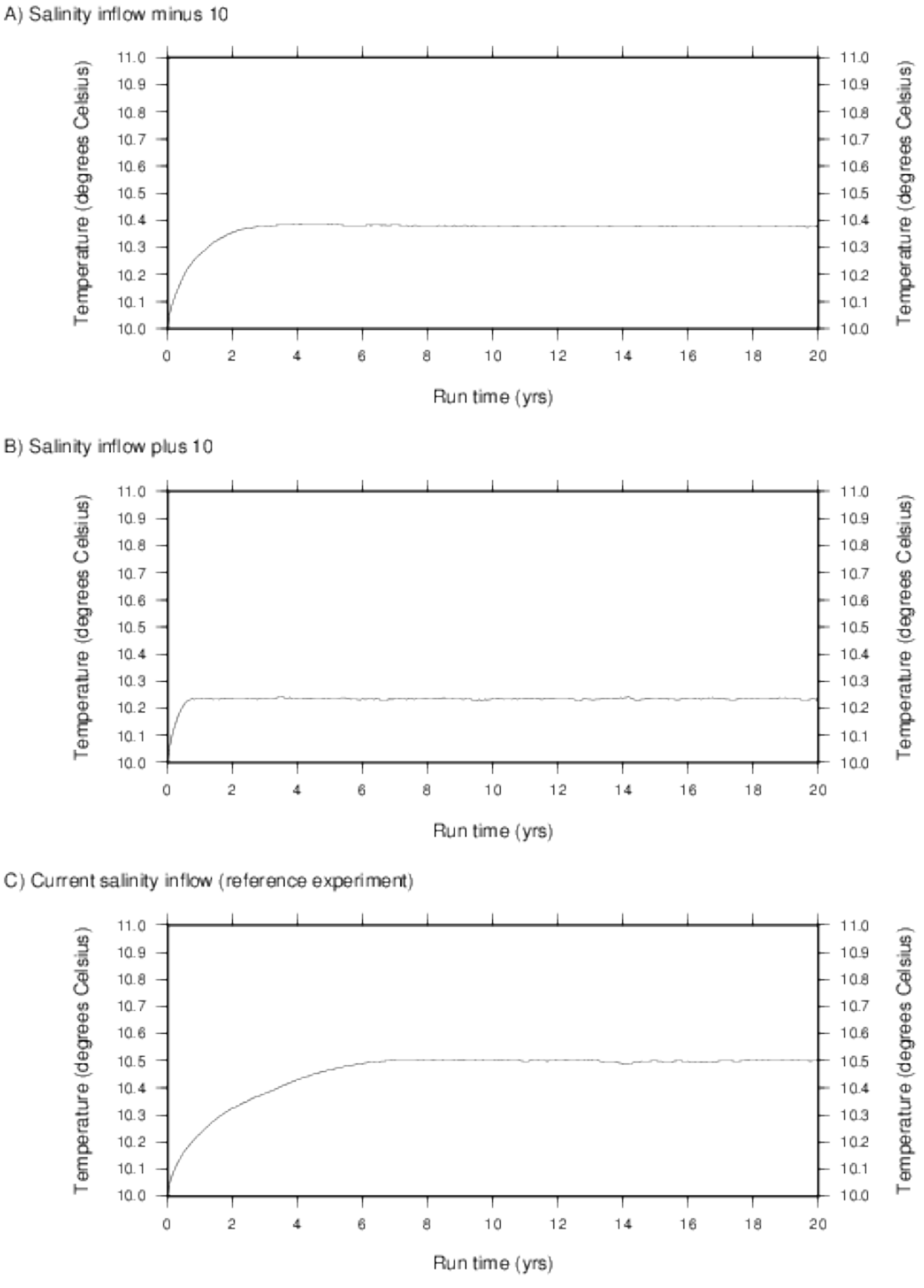

Fig. D11. Evolution of temperature throughout the runs.

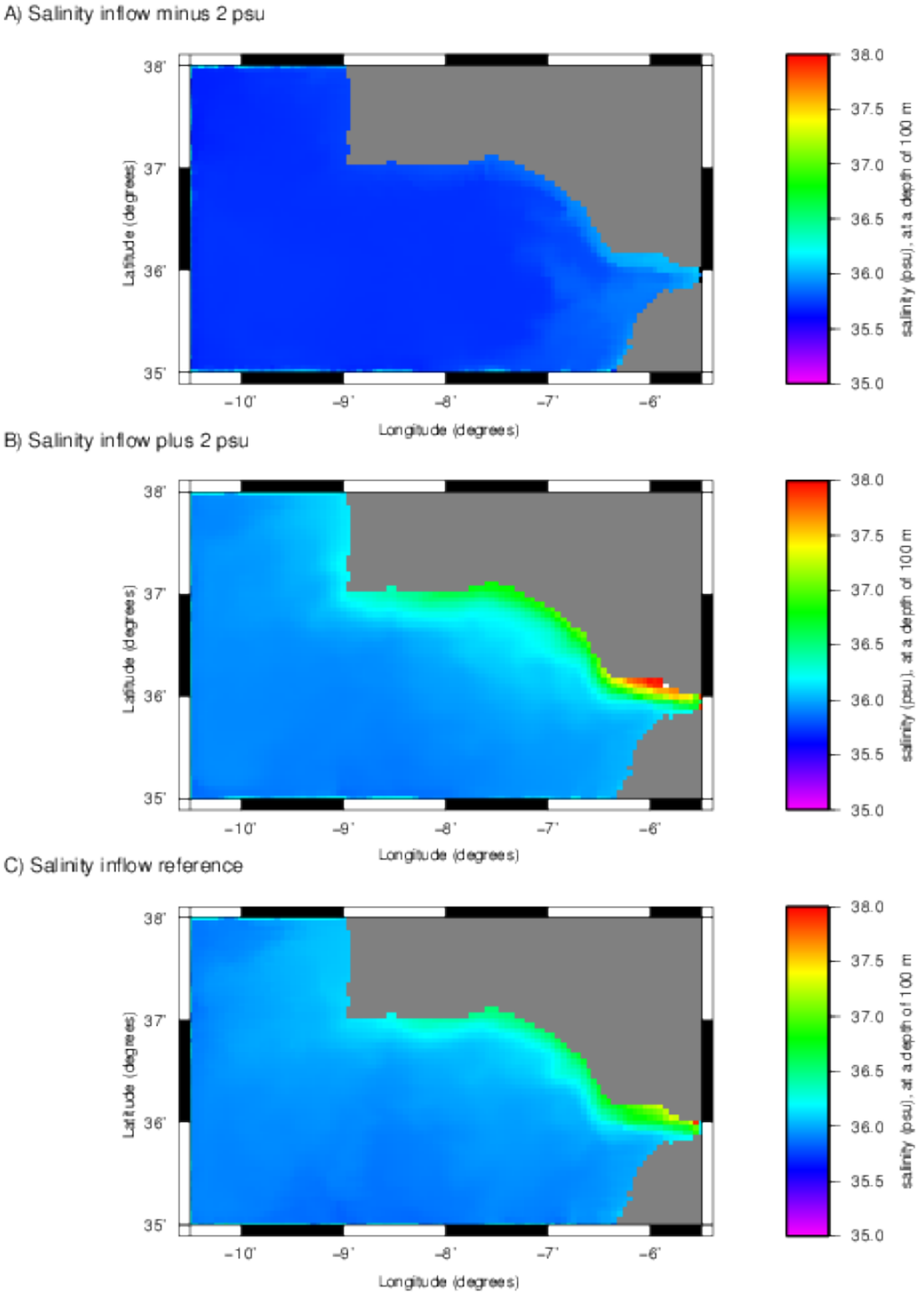

Fig. D12. Salinities at a depth of 100m. Maps taken at t=20 years.

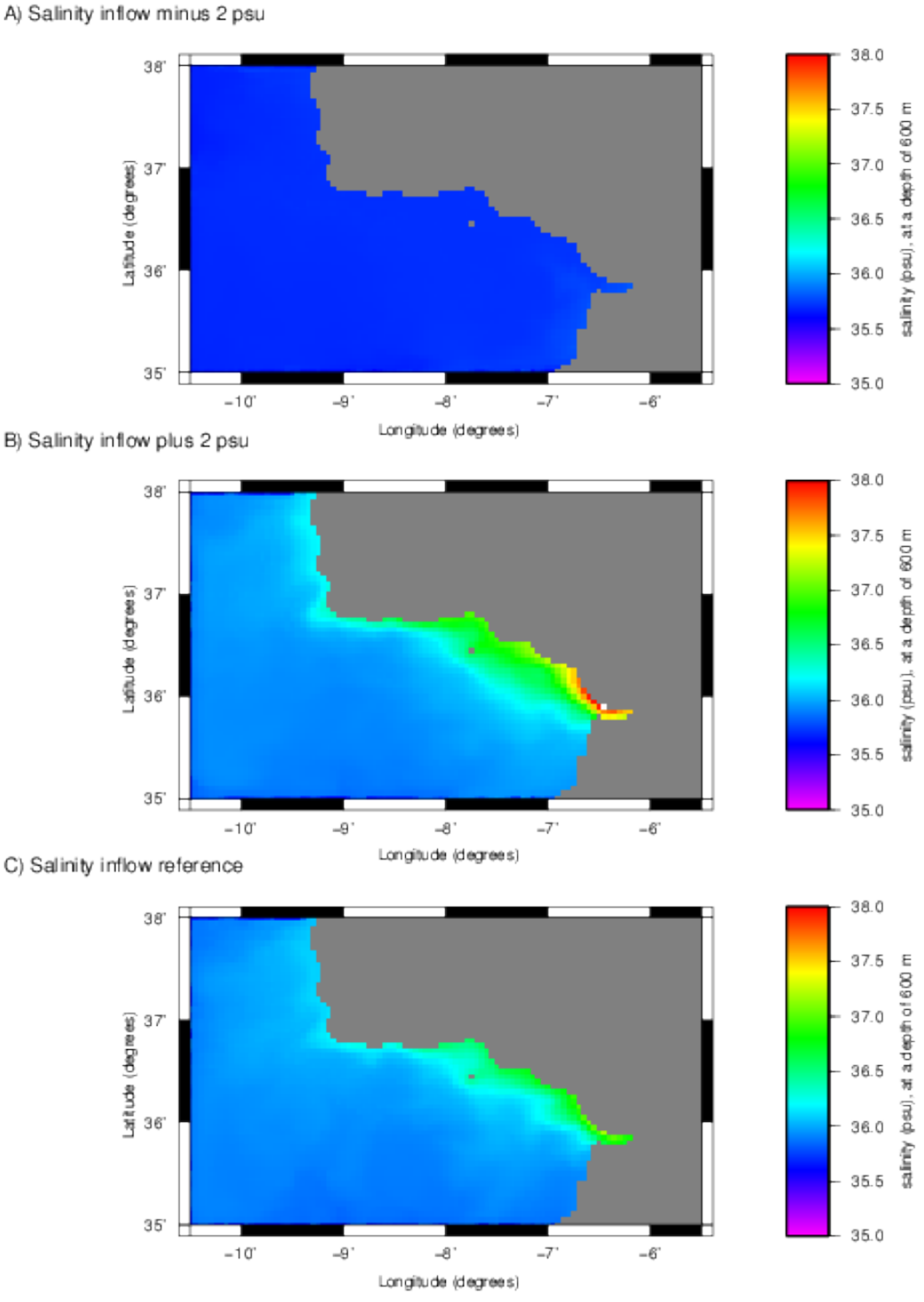

Fig. D13. Salinities at a depth of 600m. Maps taken at t=20 years.

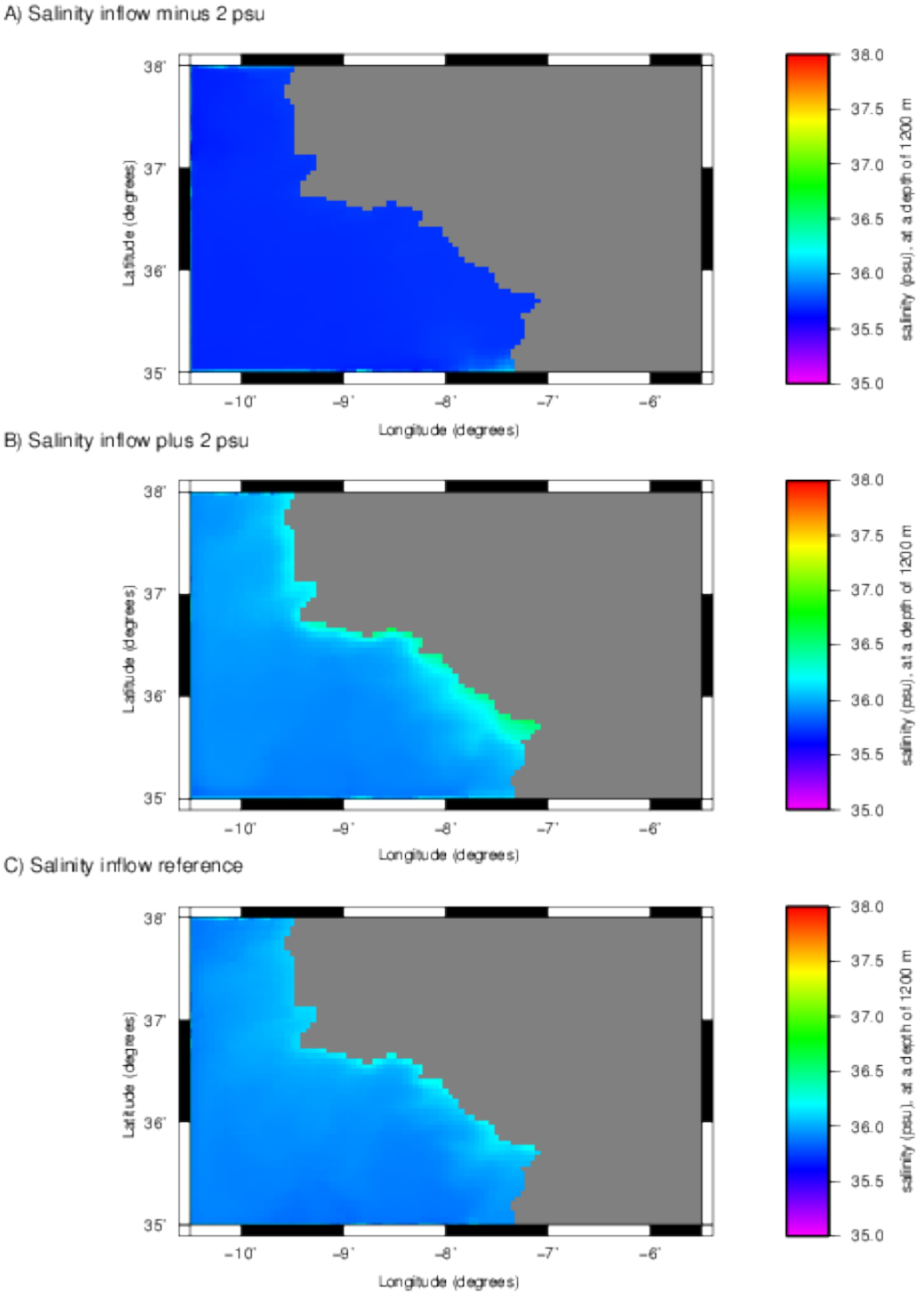

Fig. D14. Salinities at a depth of 1200m. Maps taken at t=20 years.

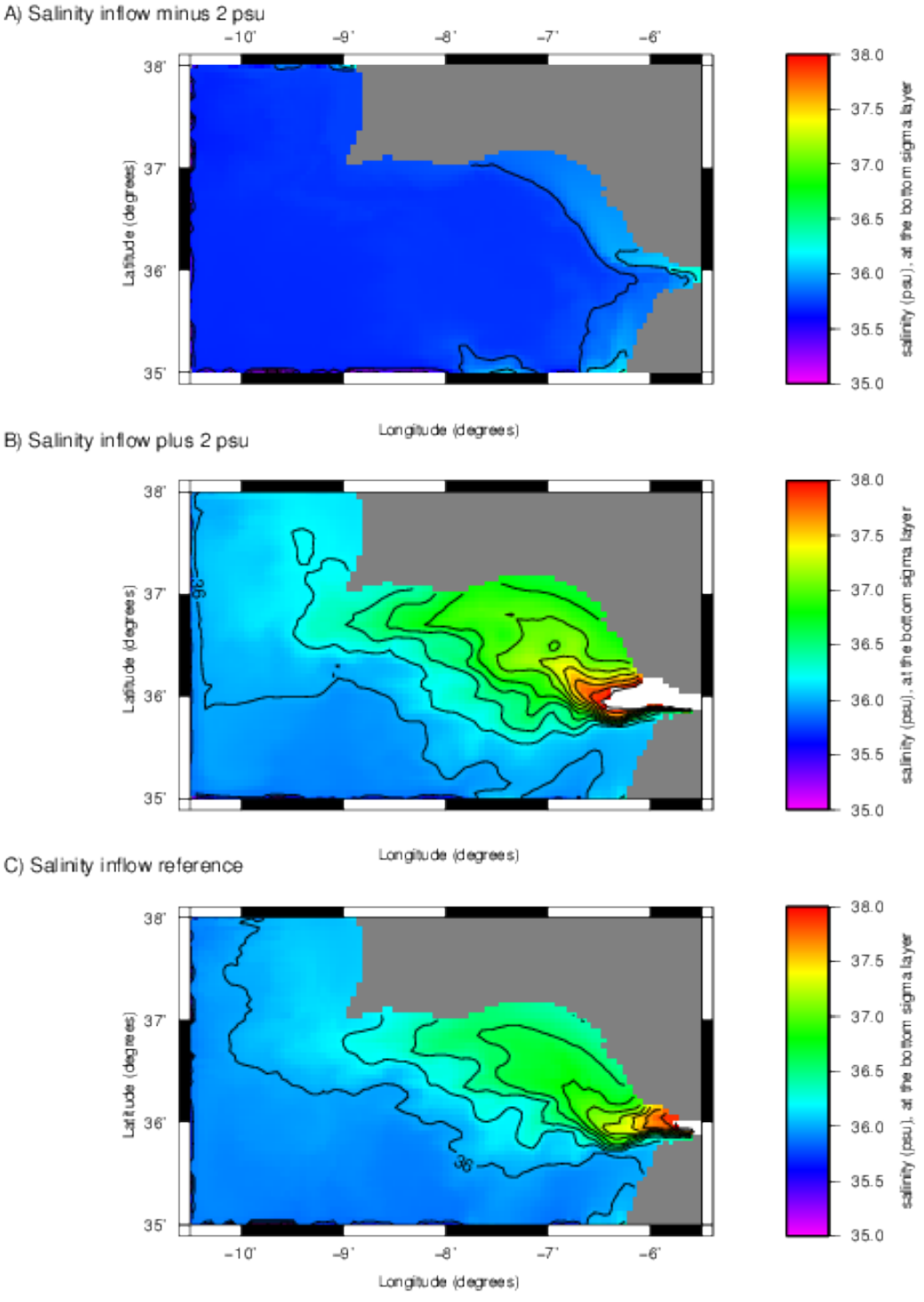

Fig. D15. Salinities at the bottom sigma-layer. Maps taken at t=20 years.

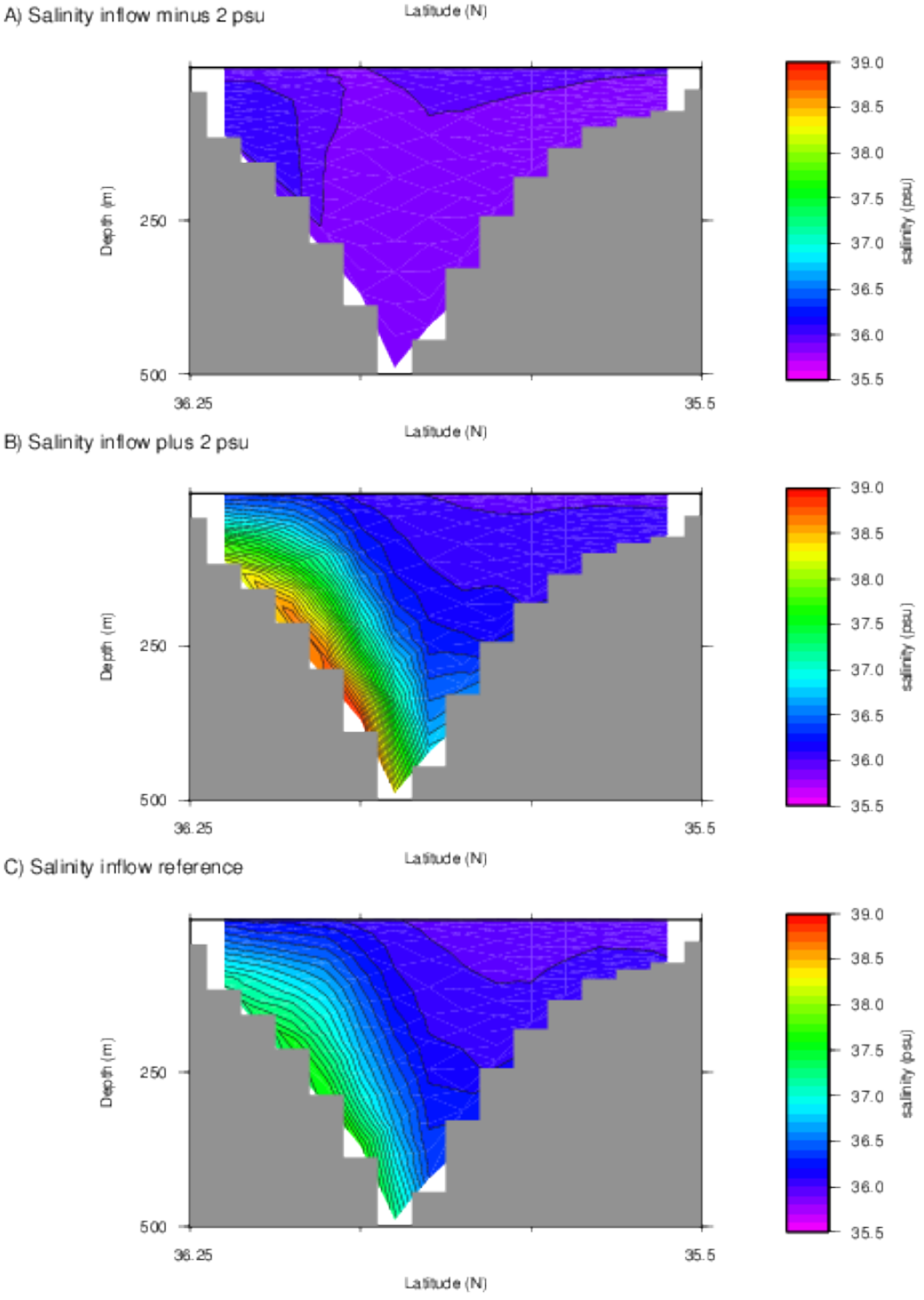

Fig. D16. A north to south salinity profile at 6°15'W. Profiles taken at t=20 years.

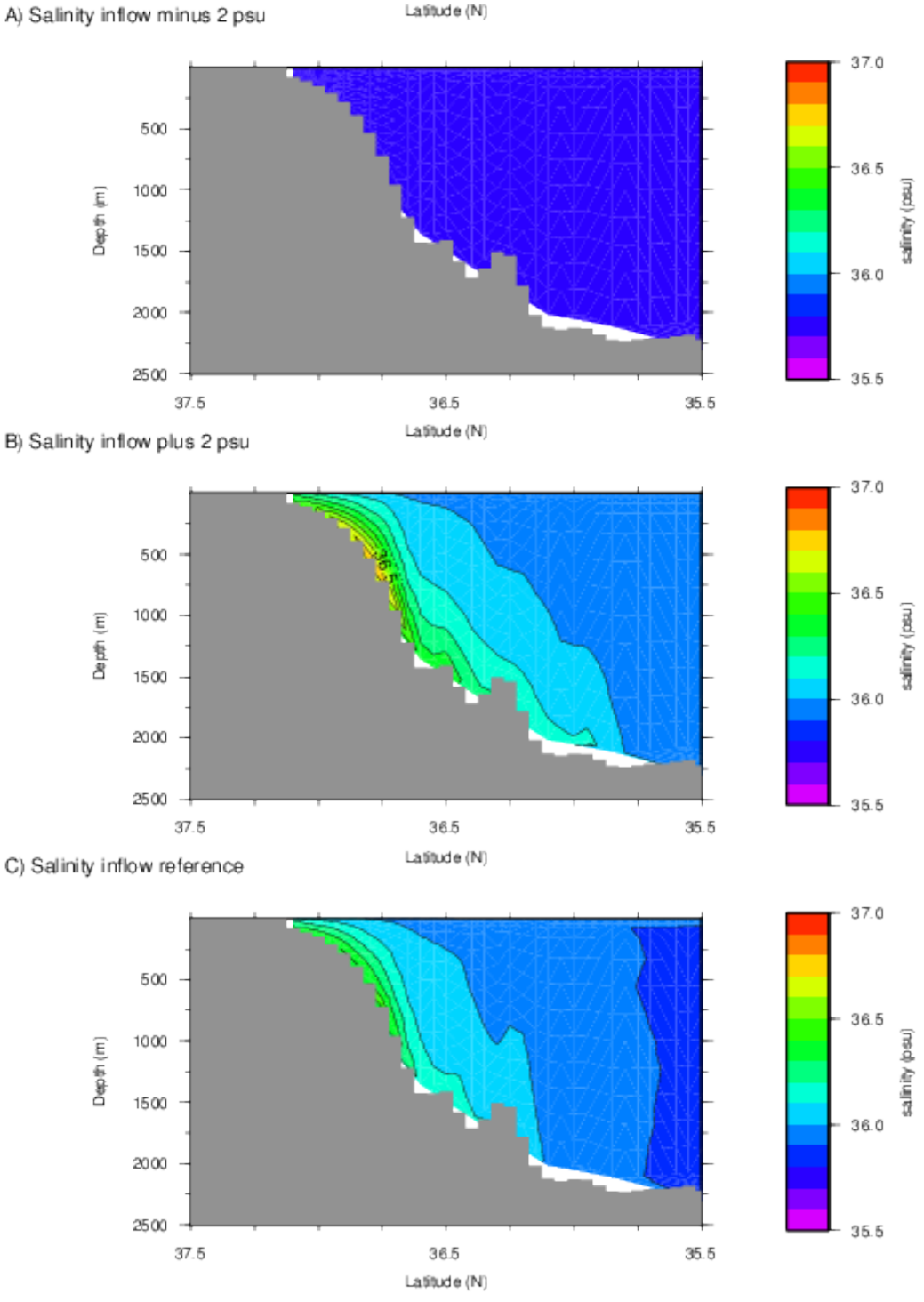

Fig. D17. A north to south salinity profile at 8°20'W. Profiles taken at t=20 years.

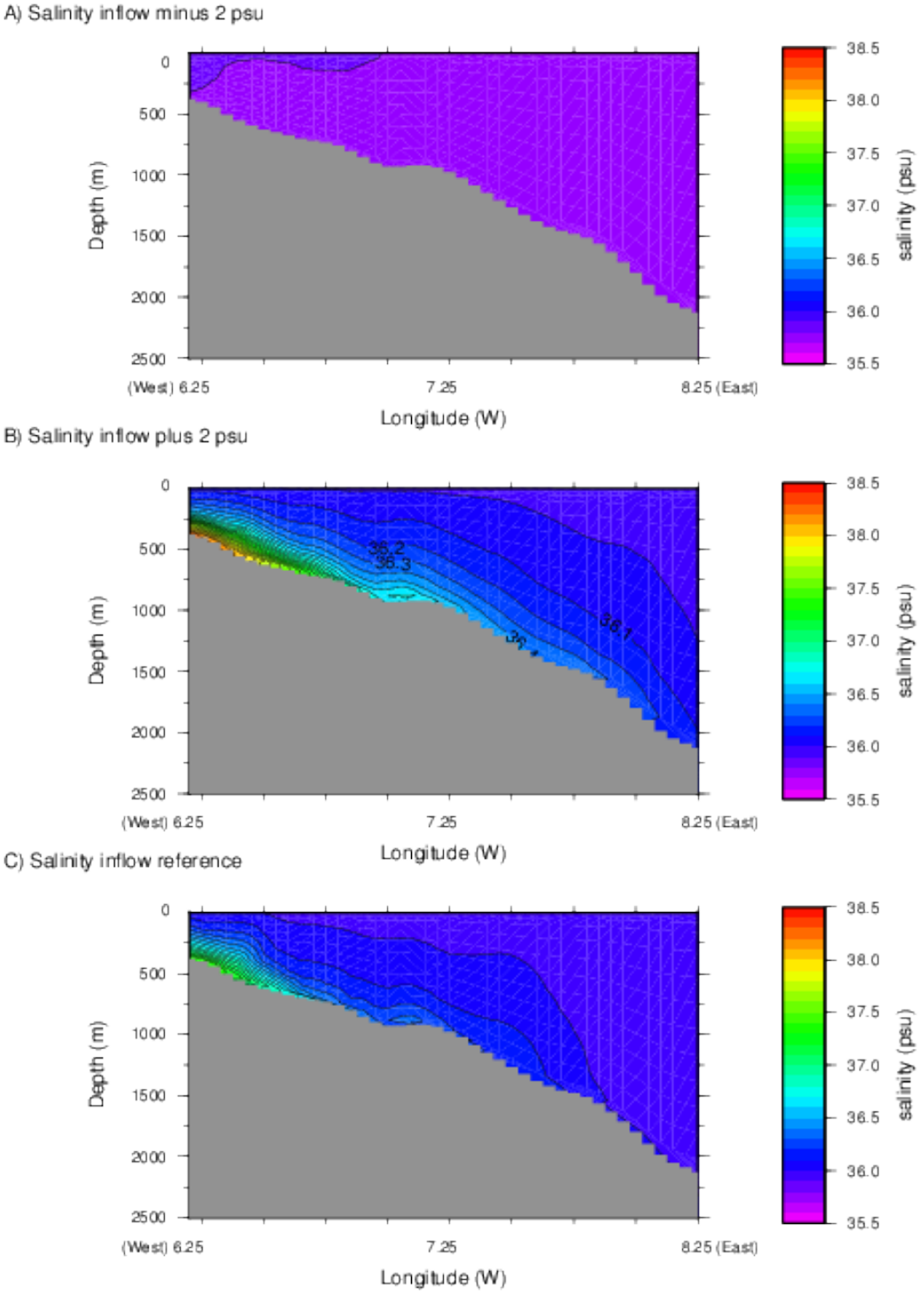

Fig. D18. An east to west salinity profile at 35°50'N, note that east is in the left of the profile. Profiles taken at t=20 years.

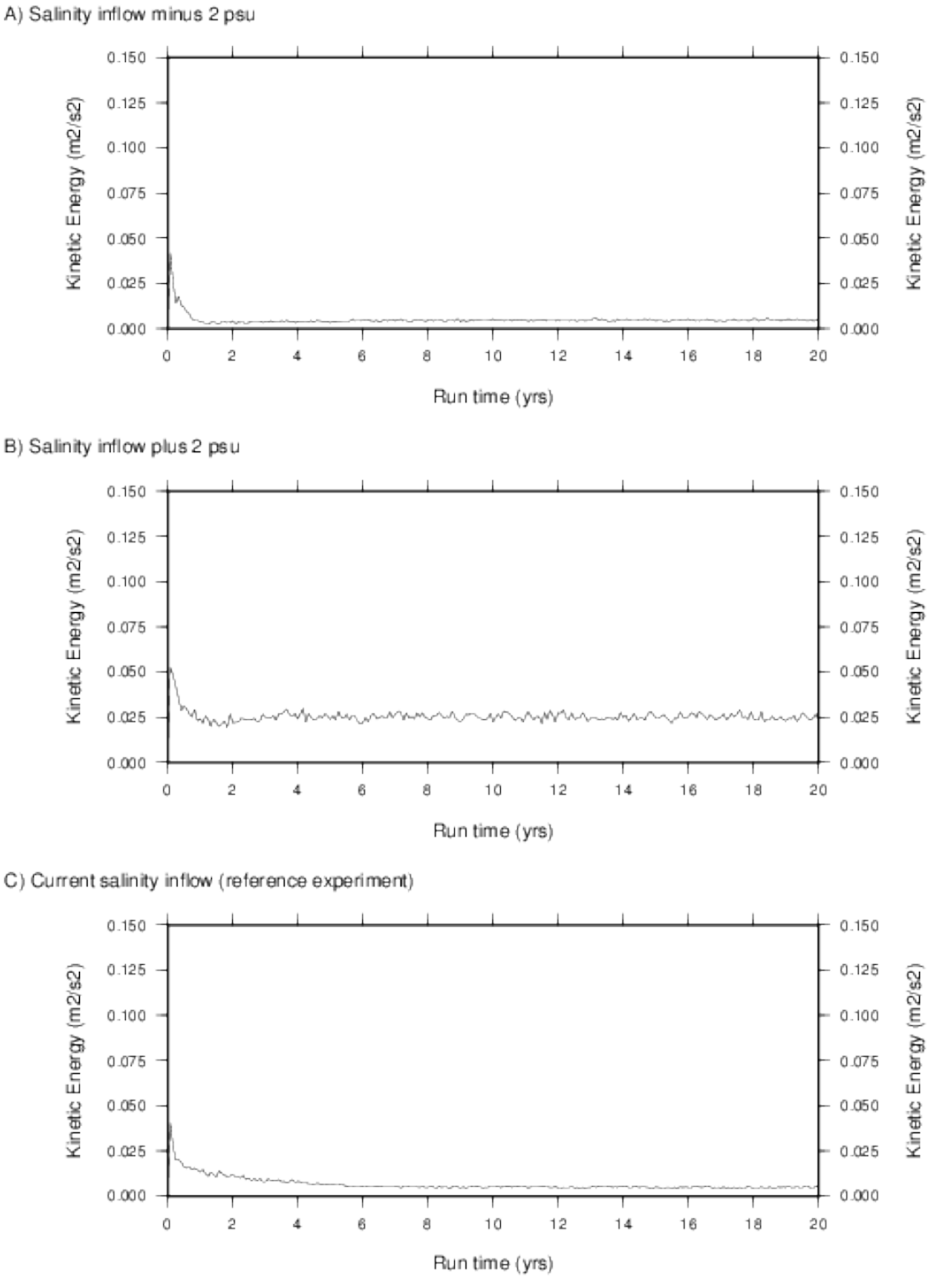

Fig. D19. Evolution of kinetic energy throughout the runs.

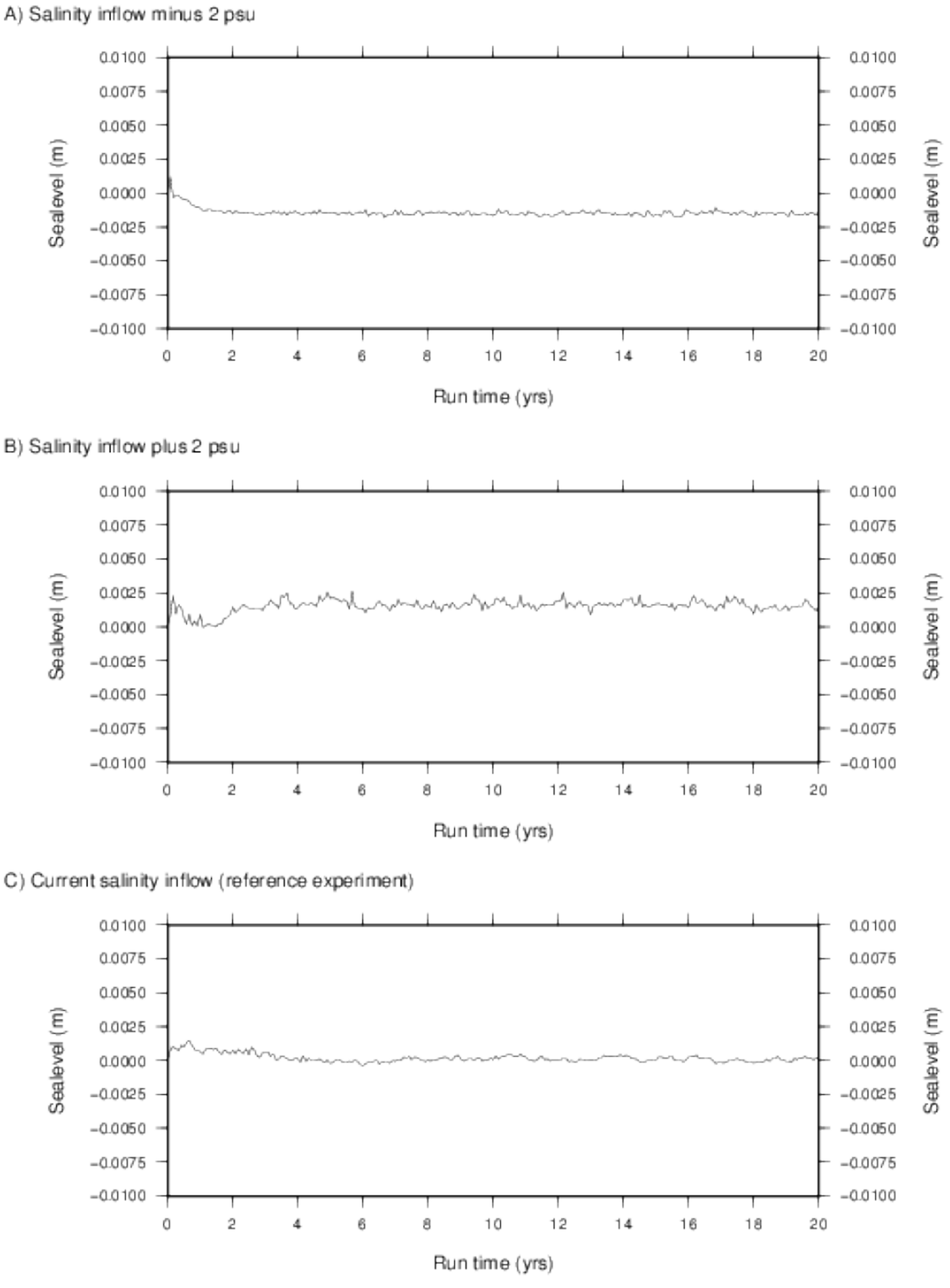

Fig. D20. Evolution of sealevel throughout the runs.

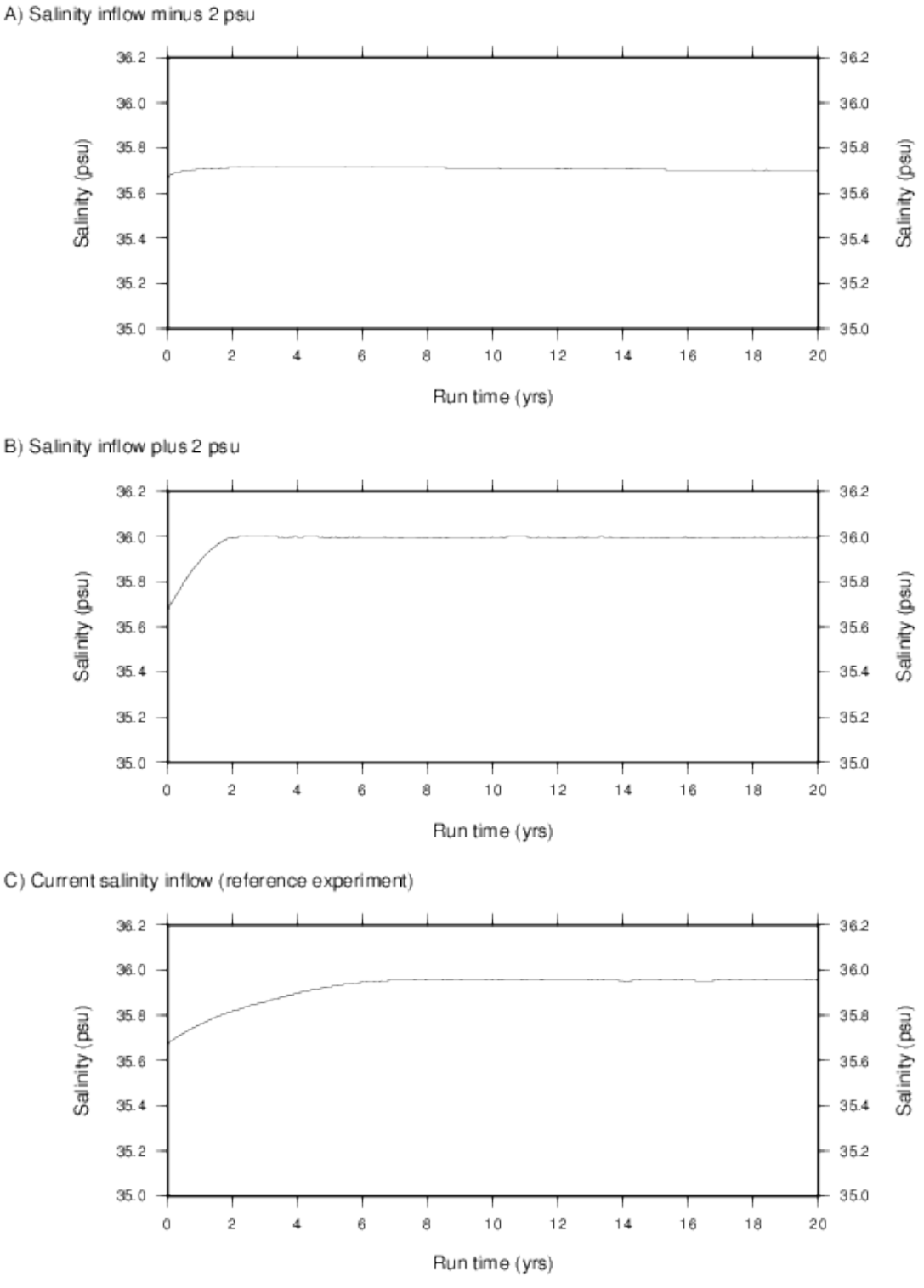

Fig. D21. Evolution of salinity throughout the runs.

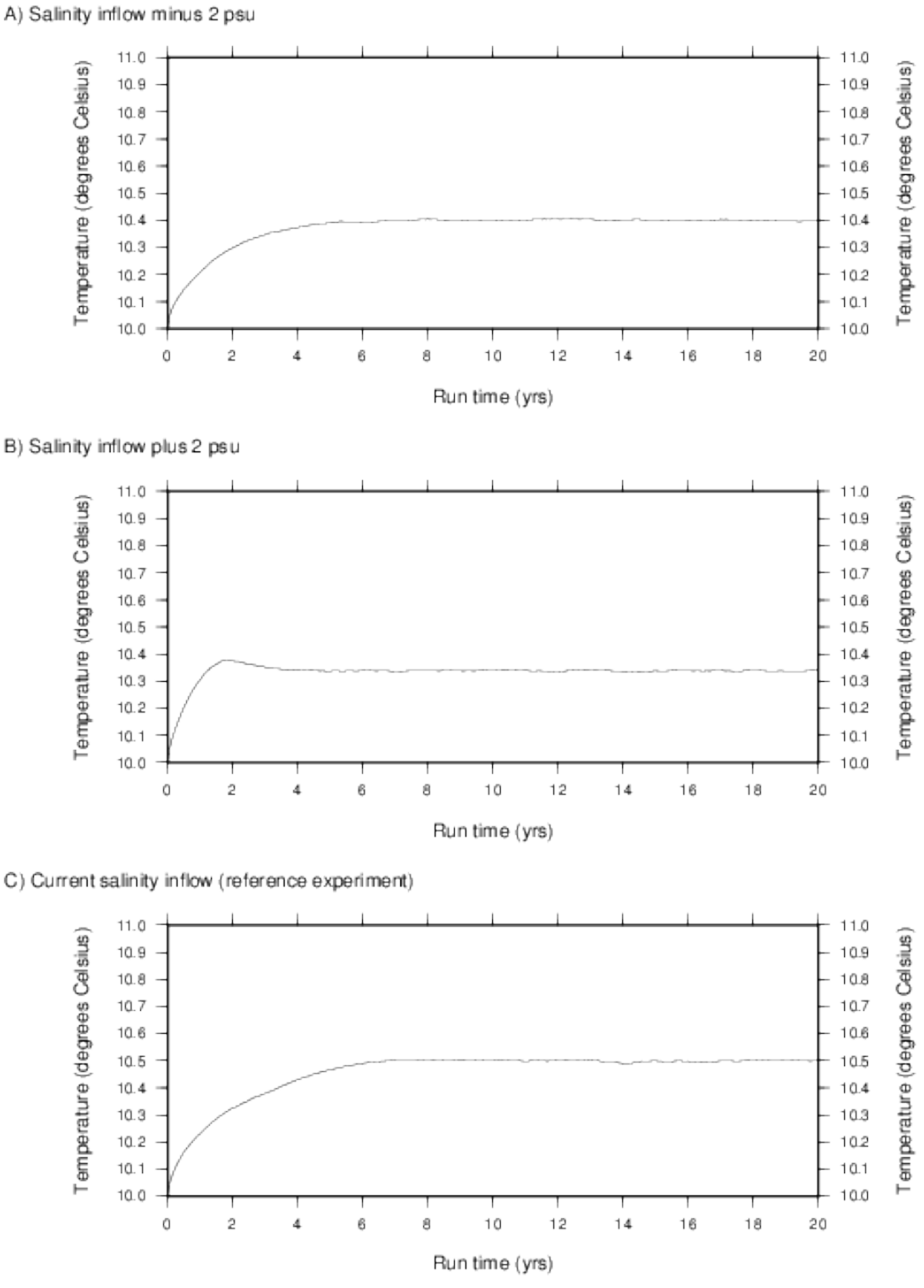

Fig. D22. Evolution of temperature throughout the runs.

Appendix

Appendix E: Experiment Results: MOW entrance speed variations

- Figure 1E: Salinity at a depth of 100m.
- Figure 2E: Salinity at a depth of 600m.
- Figure 3E: Salinity at a depth of 1200m.
- Figure 4E: Salinity profile N-S at 6°15'W.
- Figure 5E: Salinity profile N-S at 8°20'W.
- Figure 6E: Salinity profile E-W at 35°50'N.
- Figure 7E: Graph of evolution of kinetic energy.
- Figure 8E: Graph of evolution of sealevel.
- Figure 9E: Graph of evolution of salinity.
- Figure 10E: Graph of evolution of temperature.

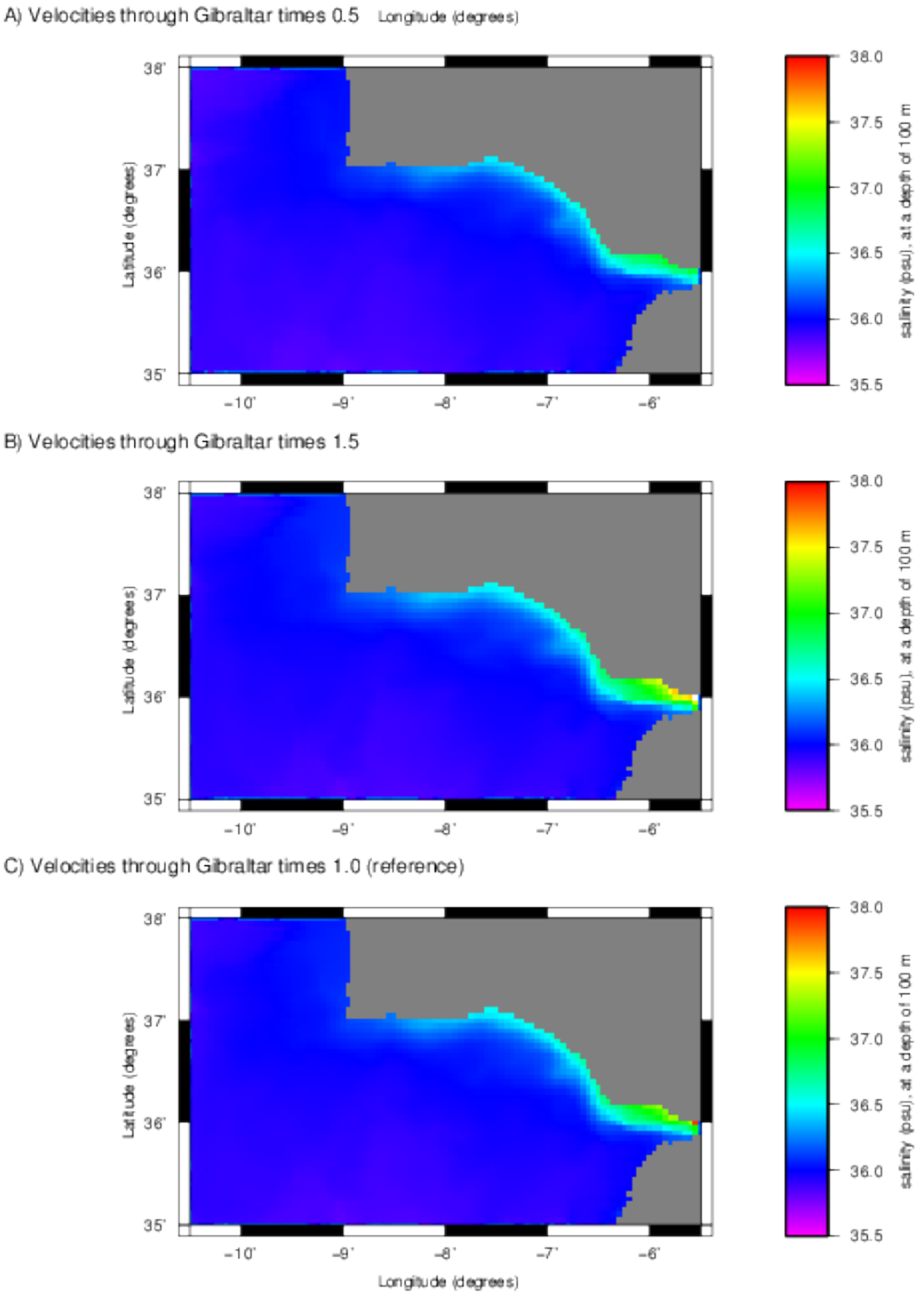

Fig. 1E. Salinities at a depth of 100m. Maps taken at t=20 years.

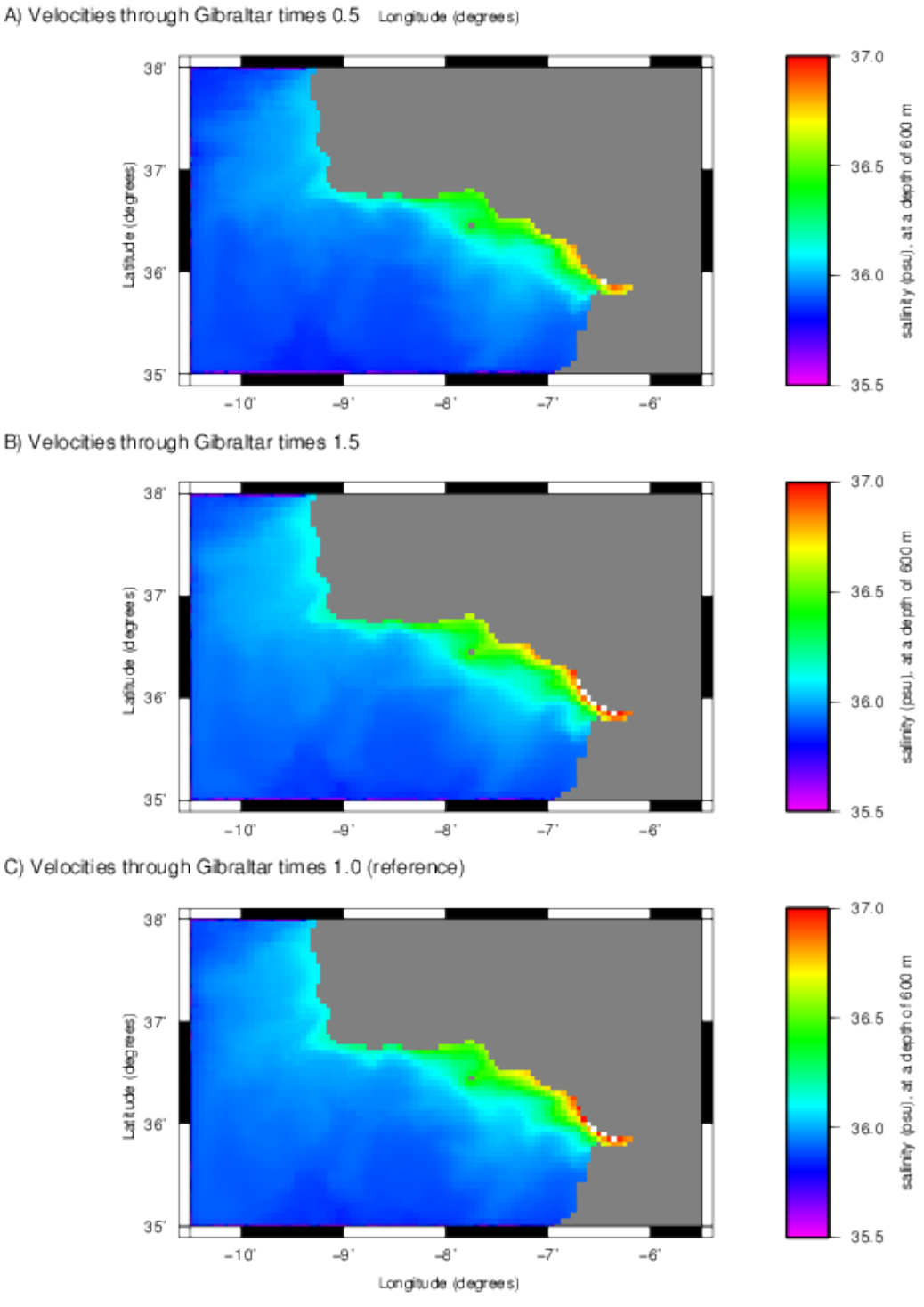

Fig. 2E. Salinities at a depth of 600m. Maps taken at t=20 years.

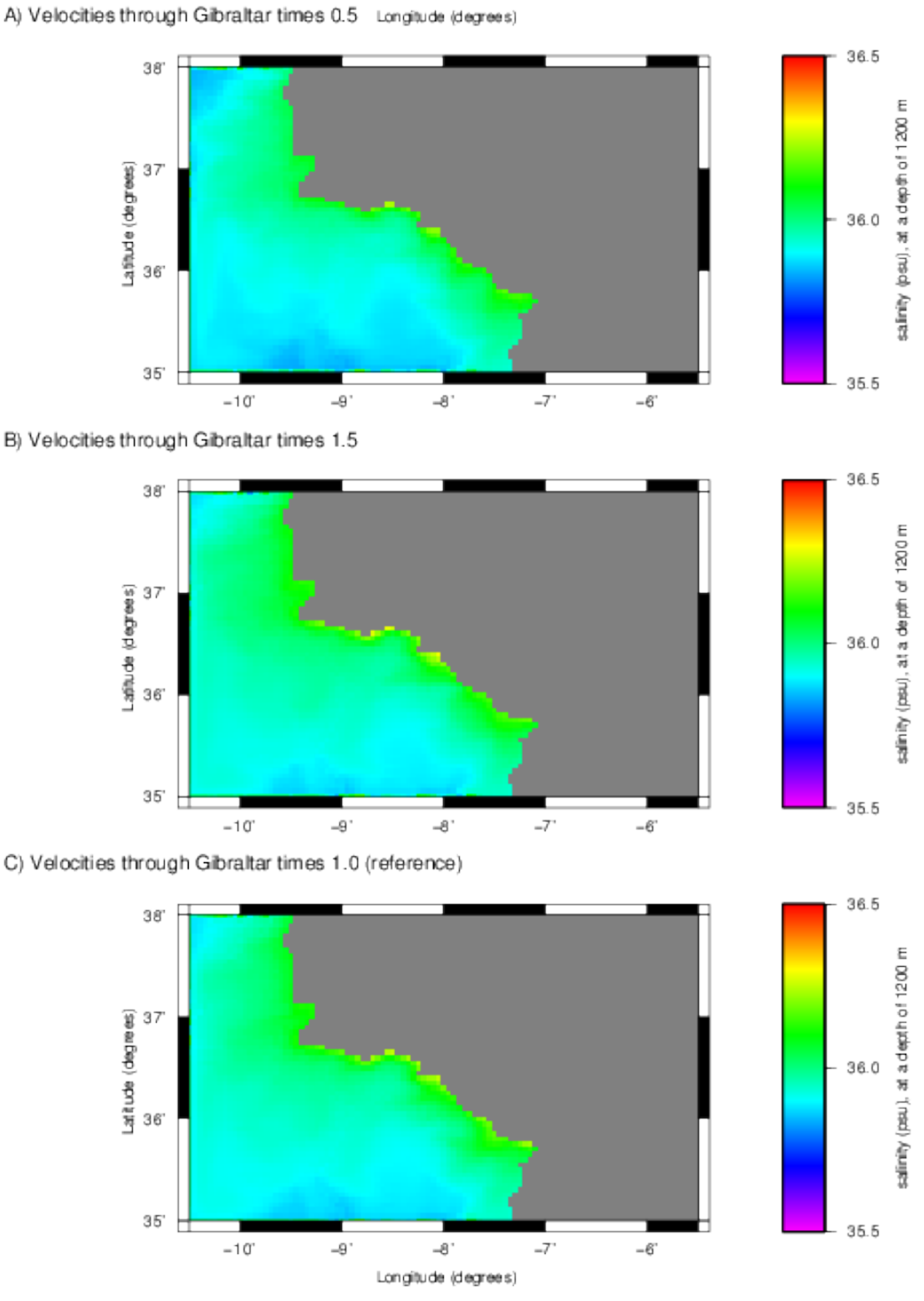

Fig. 3E. Salinities at a depth of 1200m. Maps taken at t=20 years.

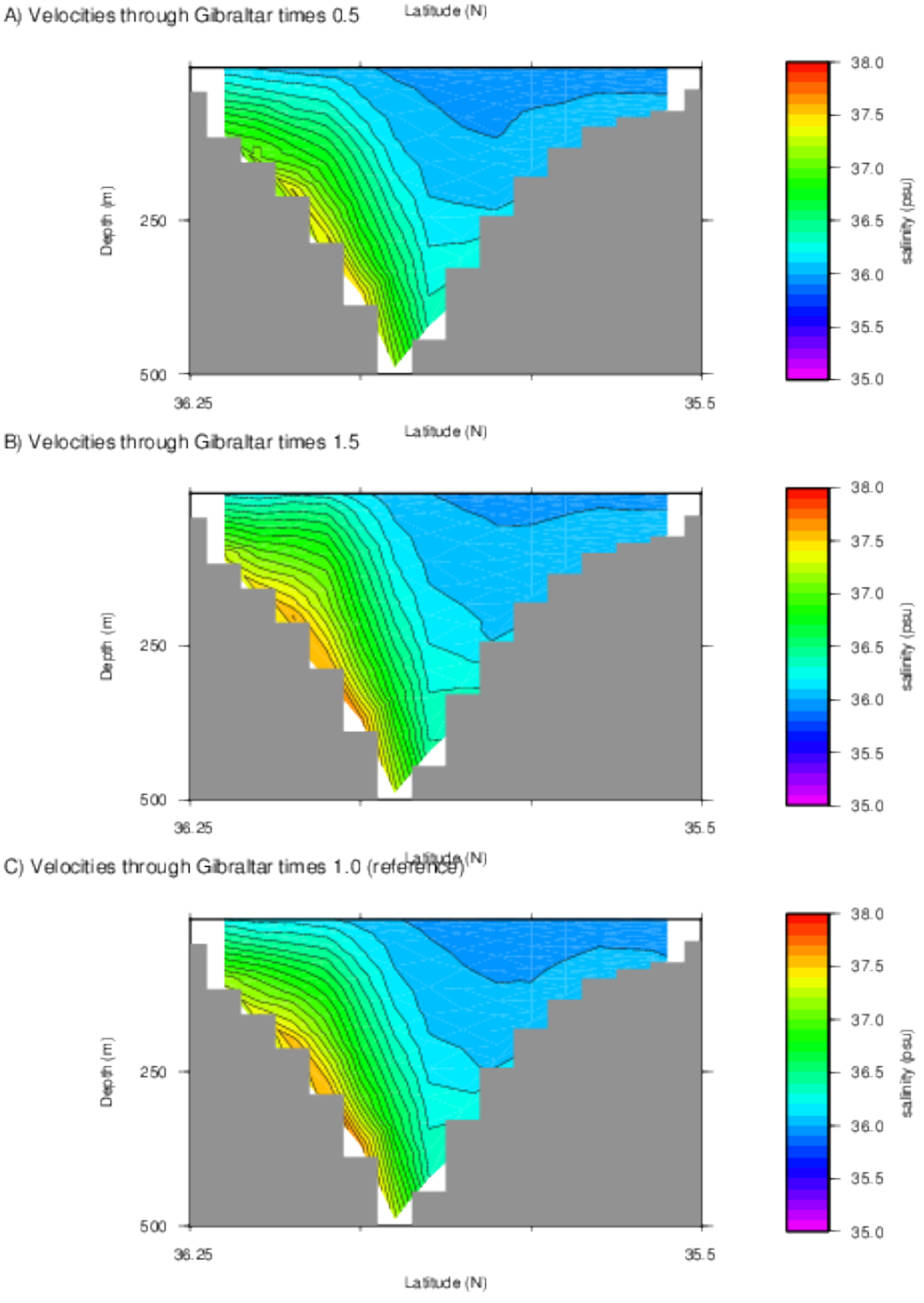

Fig. 4E. A north to south salinity profile at 6°15'W. Profiles taken at t=20 years.

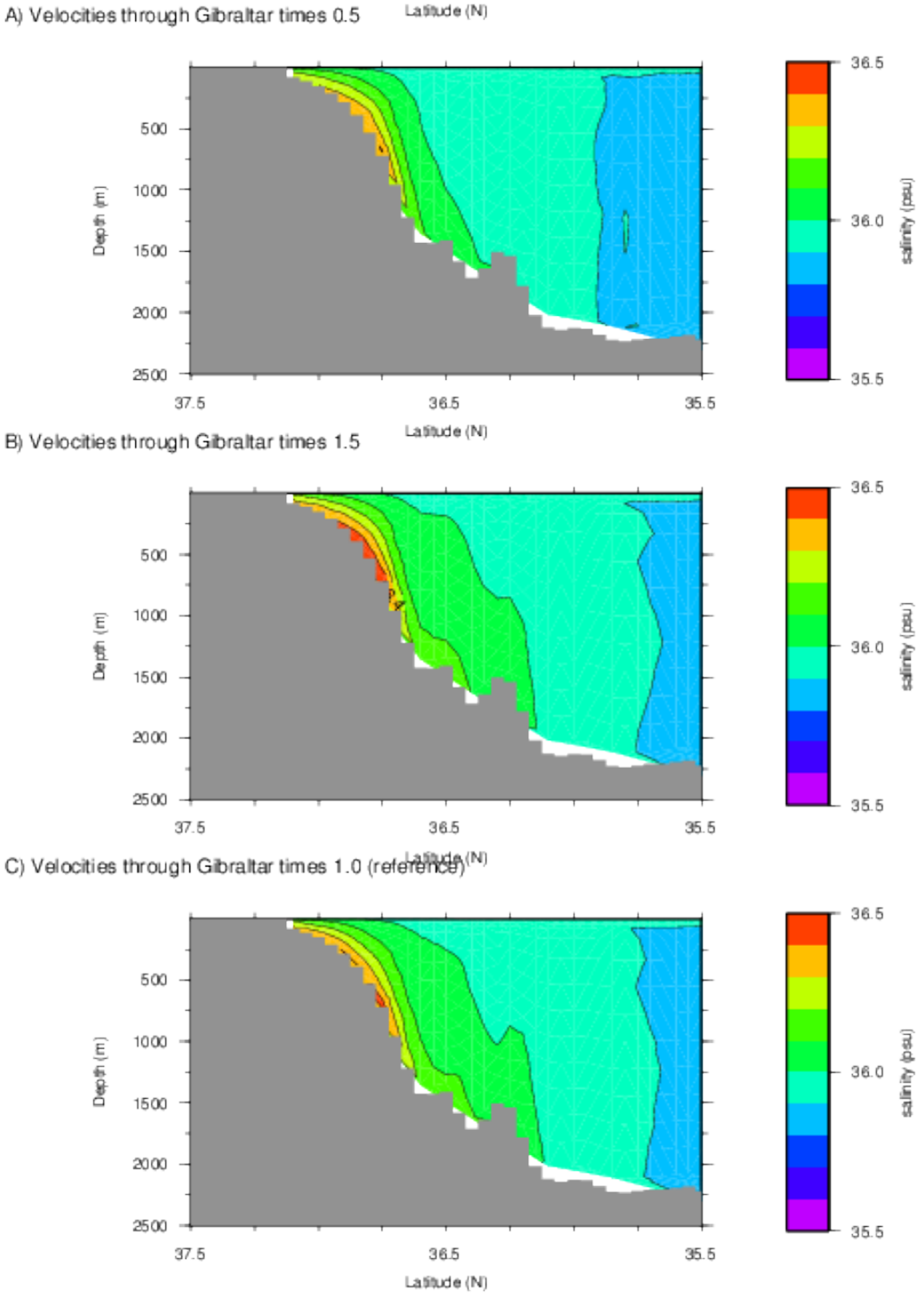

Fig. 5E. A north to south salinity profile at 8°20'W. Profiles taken at t=20 years.

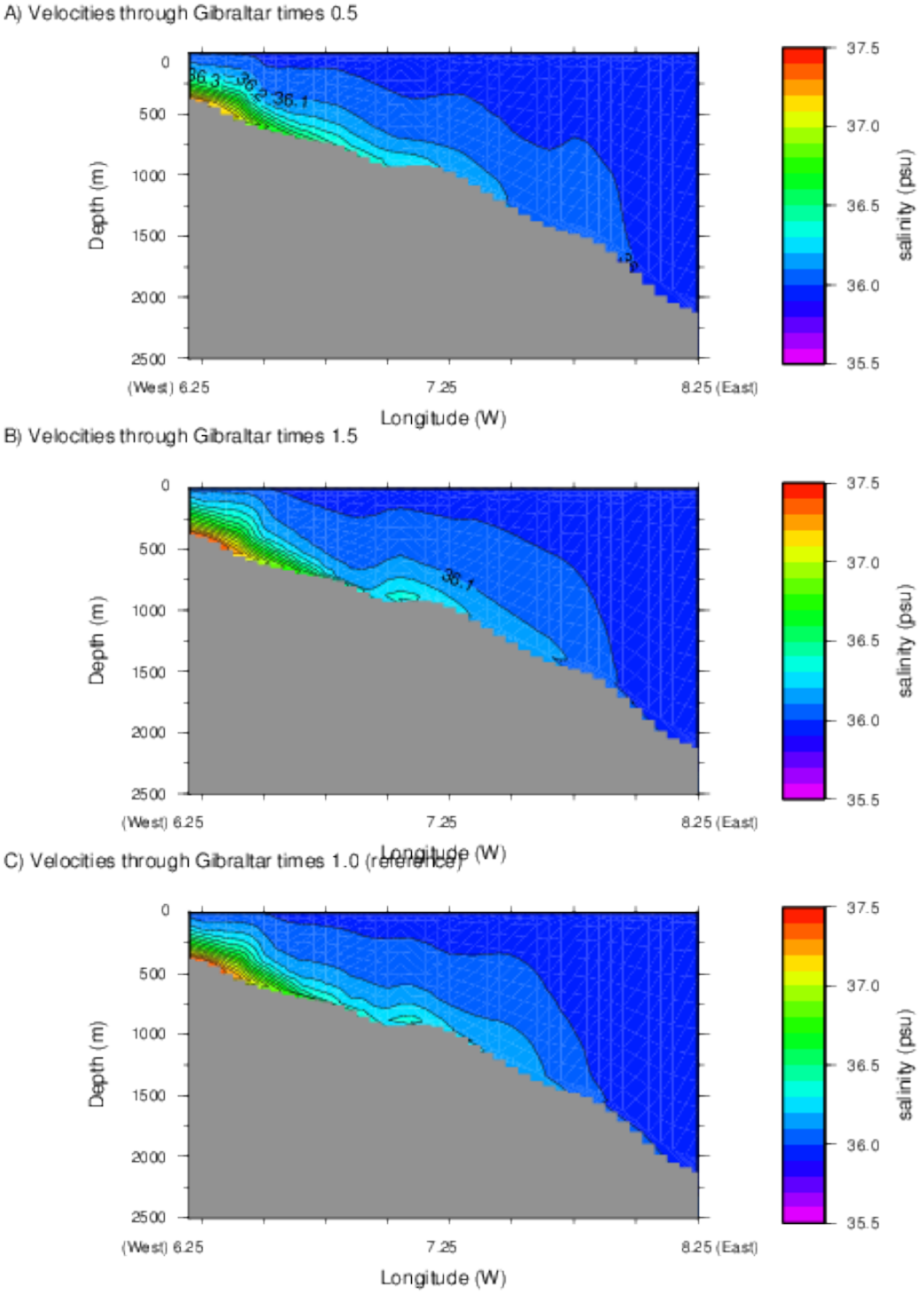

Fig. 6E. An east to west salinity profile at 35°50'N, note that east is in the left of the profile. Profiles taken at t=20 years.

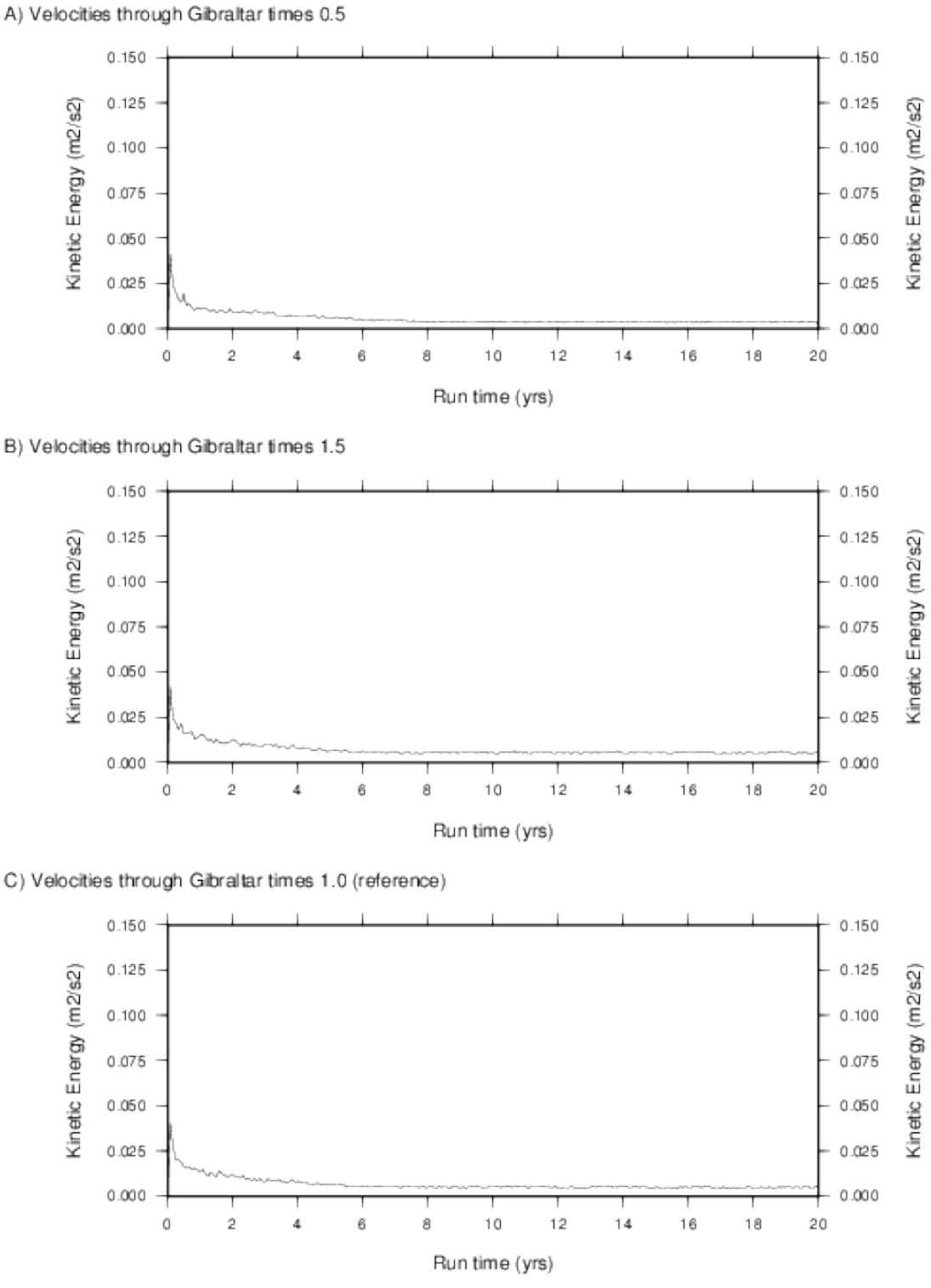

Fig. 7E. Evolution of kinetic energy throughout the runs.

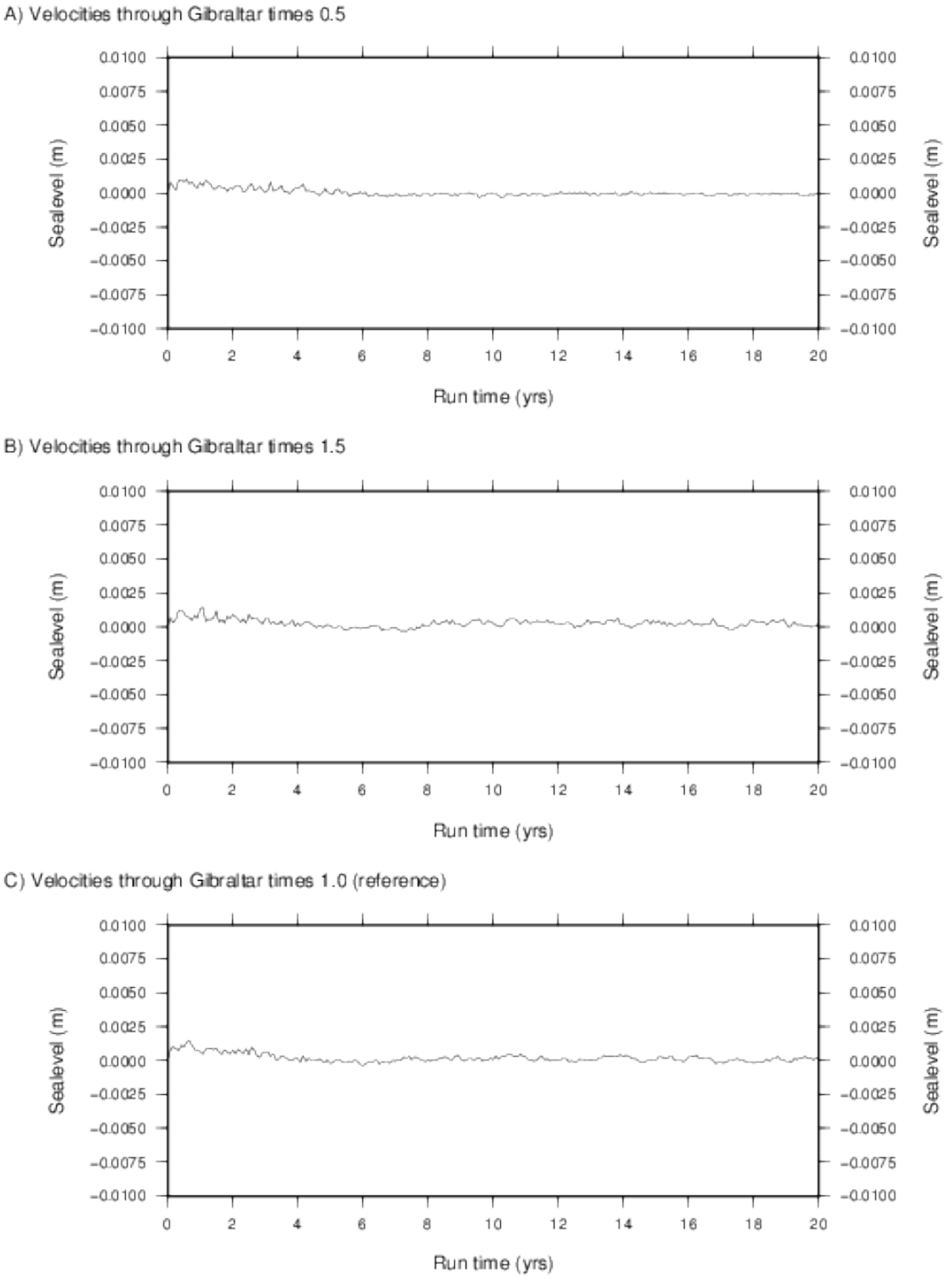

Fig. 8E. Evolution of sealevel throughout the runs.

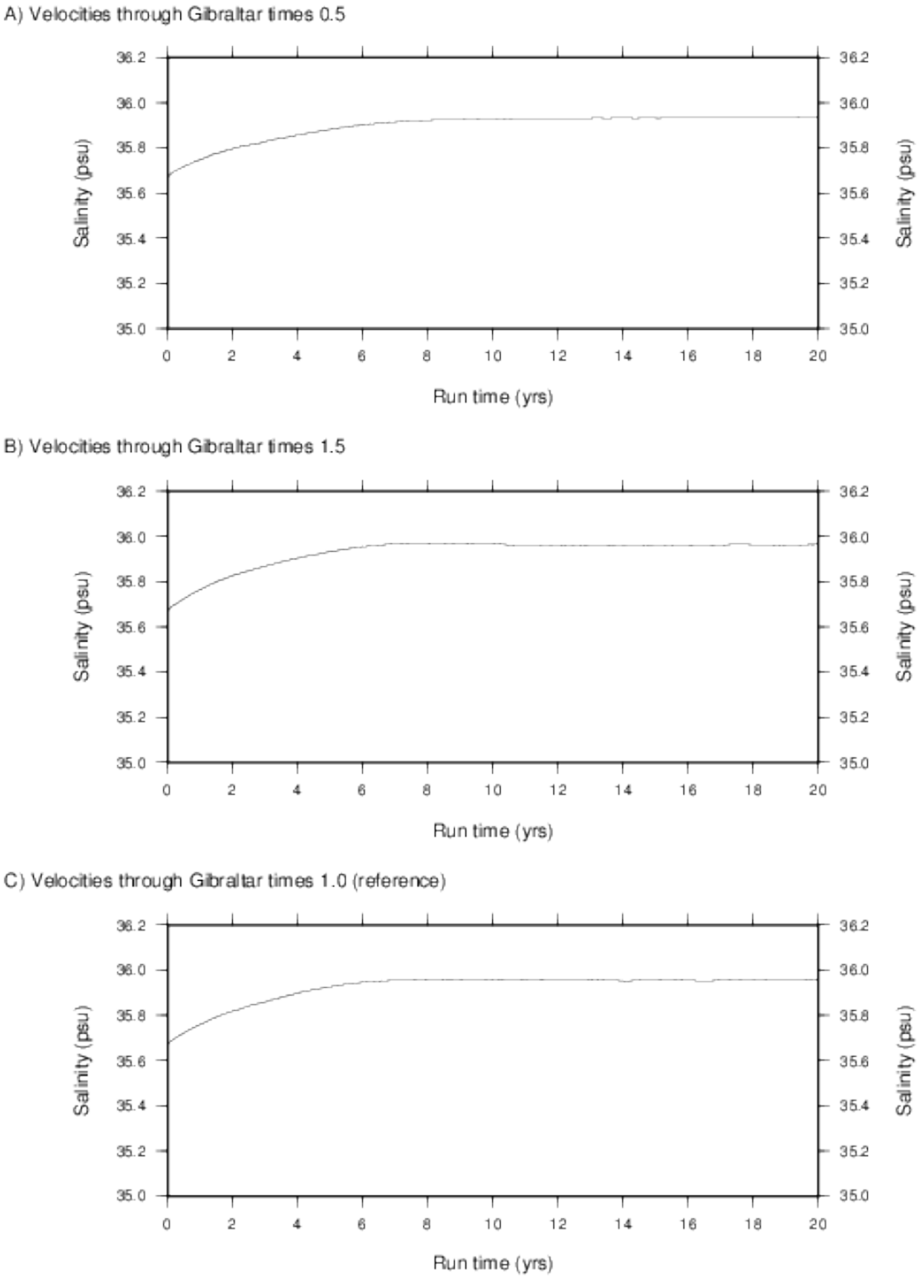

Fig. 9E. Evolution of salinity throughout the runs.

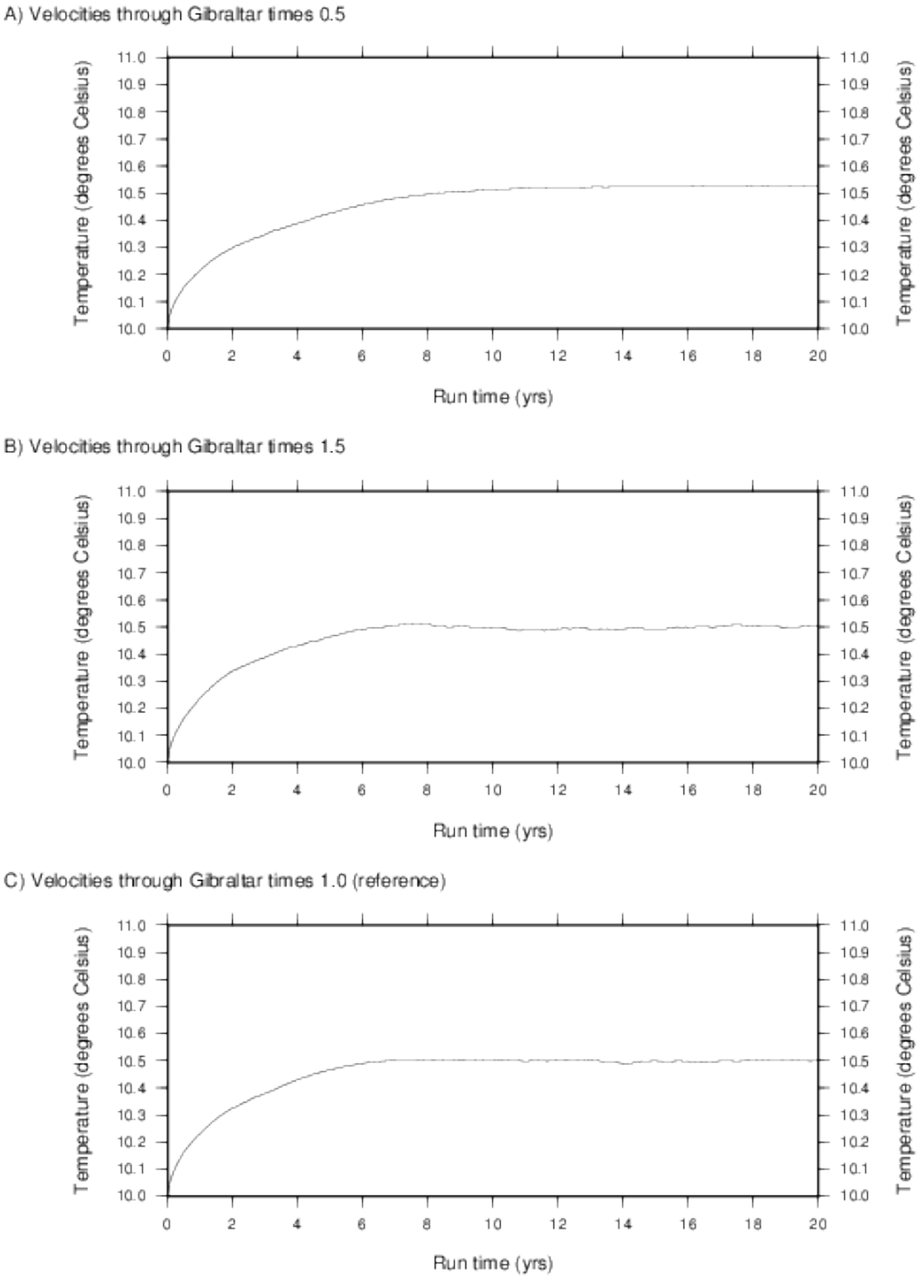

Fig. 10E. Evolution of temperature throughout the runs.